Effect of

Phasor Measurement Unit (PMU)

on the

Network Estimated Variables

A THESIS SUBMITTED IN PARTIAL FULFILLMENT OF THE REQUIREMENTS FOR THE DEGREE OF

MASTER OF TECHNOLOGY
in
POWER SYSTEM

By

Jitender Kumar
(03/PSY/2K10)

Under the Supervision of :
Sh. J. N. Rai

Department of Electrical Engineering
Delhi Technological University
New Delhi
2012

CERTIFICATE

This is to certify that the thesis entitled "**Effect of Phasor Measurement Unit (PMU) on the Network Estimated Variables**" submitted by Jitender Kumar (03/PSY/2K10), in the partial fulfillment of the requirement for the degree of Master in Technology in Power System, Department of Electrical Engineering, Delhi Technological University, New Delhi, is an authentic work carried out by them under my supervision. To the best of my knowledge the matter embodied in the thesis has not been submitted to any other university/institute for the award of any degree or diploma.

Date:

(Sh. Jitendra Nath Rai)
Department of Electrical Engineering,
Delhi Technological University,
New Delhi

ACKNOWLEDGEMENTS

I wish to extend my sincere gratitude to Sh. Jitendra Nath Rai for his help and guidance regarding the work contained in this thesis. I have learned a tremendous amount from him and greatly value the time that we have spent working together.

Also, I would like to thank the faculty of Electrical Engineering Department specially Dr. Narendra Kumar, HOD (EE) and Dr. Suman Bhowmick for creating a positive learning environment for myself and the rest of the students. Because of this I believe that it is not the choice of discipline that defines college experience but the people that you choose surround yourself with. With this said, I would also like to thank my friends and colleagues here at Delhi Technological University, Delhi for their encouragement and companionship.

And finally, I would like to thank my Family for their love, friendship and constant support of my academic pursuits.

JITENDER KUMAR
03/PSY/2K10
M.Tech (PS)

ABSTRACT

The thesis will scrutinize the effect of the Phasor Measurement Units (PMU) on the problem associated in analyzing the state estimation for power system. Initially, the conventional state estimation on a power system bus will be discussed. Then, the significance effect of adding PMU measurements on the solution obtained from state estimation with their accuracy will be studied. Finally, the consequences of PMU system on the accuracy of different bus system will be discussed.

The first objective of the thesis is to develop the linear formulation for the problem associated with the state estimation by using PMUs. The second objective is to formulate the full weighted least square state estimation method when using PMUs and illustrate its performance by using the simulation techniques for power system examples.

TABLE OF CONTENTS

PAGE

CERTIFICATE……...….2

ACKNOWLEDGMENTS……..…..…3

ABSTRACT .....……..….....….4

LIST OF FIGURES……...….7

LIST OF TABLES……..11

CHAPTER

1 INTRODUCTION ……....12

1.1 Introduction……...……12
1.2 System Monitoring by Global Positioning System (GPS)…….....13
1.3 Application……..…..….15
1.4 Challenges…….....…15
1.5 Standards ……..…...…….…..….16

2 LITERATURE REVIEW…….....17

3 FULL WEIGHTED LEAST SQUARE STATE ESTIMATION ….…..……28

3.1 Introduction……28
3.2 WLS State Estimation Algorithm……...……30
3.3 Parameter Measurement and their Modeling…….……33
3.4 PMU Algorithm with State Estimation Technique……...…..……36

4 LINEAR FORMULATION OF STATE ESTIMATION USING PMUs ….…39

4.1 Introduction……..…….……39
4.2 Algorithm for Linear State Estimation……...……40
4.3 Simulation Results……..……42

5 BENEFITS OF USING PMUs……...……47

5.1 PMU improved Variables Accuracy……...……...…47

5.2 Simulation Results……..……48

6 CONCLUSIONS AND FUTURE WORK…….……83

6.1 Conclusions……...……83

6.2 Future Work…….....…84

REFERENCES…….…….……85

APPENDIX A (Park Transform)……...…...……89

APPENDIX B (Specification)…….....……93

LIST OF FIGURES

FIG.	CONTENTS	PAGE
1.1	PHASOR MEASUREMENT UNIT (PMU)	13
1.2	GLOBAL POSITIONING SYSTEM	14
3.1	FLOW-CHART FOR THE WLS STATE ESTIMATION ALGORITHM	32
3.2	EQUIVALENT ‘π’ MODEL OF TWO BUS SYSTEM	33
3.3	SINGLE PMU MEASUREMENT MODEL	36
3.4	TRANSMISSION LINE MODEL	37
4.1	TRANSMISSION LINE MODEL WITH RECTANGULAR FORM	39
4.2	TWO BUS SYSTEMS WITH MEASUREMENTS	41
4.3	IEEE 6 BUS SYSTEM	43
4.4	IEEE 9 BUS SYSTEM	44
4.5	IEEE 14 BUS SYSTEM	45
4.6	IEEE 30 BUS SYSTEM	46
5.1	IEEE 6 BUS SYSTEM	50
5.2	IEEE 9 BUS SYSTEM	50
5.3	IEEE 14 BUS SYSTEM	51
5.4	IEEE 30 BUS SYSTEM	52
5.5	GRAPH BETWEEN MAG OF V (S D) VS BUS NUMBER (IEEE 6 BUS)	53
5.6	GRAPH BETWEEN MAG OF V (S D) VS BUS NUMBER (IEEE 6 BUS)	53
5.7	GRAPH BETWEEN MAG OF V (S D) VS BUS NUMBER (IEEE 9 BUS)	53
5.8	GRAPH BETWEEN MAG OF V (S D) VS BUS NUMBER (IEEE 9 BUS)	54
5.9	GRAPH BETWEEN MAG OF V (S D) VS BUS NUMBER (IEEE 14 BUS)	54
5.10	GRAPH BETWEEN MAG OF V (S D) VS BUS NUMBER (IEEE 14 BUS)	54
5.11	GRAPH BETWEEN MAG OF V (S D) VS BUS NUMBER (IEEE 30 BUS)	55
5.12	GRAPH BETWEEN MAG OF V (S D) VS BUS NUMBER (IEEE 30 BUS)	55
5.13	GRAPH BETWEEN MAG OF ANGLE (S D) VS BUS NUMBER (IEEE 6 BUS)	55
5.14	GRAPH BETWEEN MAG OF ANGLE (S D) VS BUS NUMBER (IEEE 6 BUS)	56

FIG.	CONTENTS	PAGE
5.15	GRAPH BETWEEN MAG OF ANGLE (S D) VS BUS NUMBER (IEEE 9 BUS)	56
5.16	GRAPH BETWEEN MAG OF ANGLE (S D) VS BUS NUMBER (IEEE 9 BUS)	56
5.17	GRAPH BETWEEN MAG OF ANGLE (S D) VS BUS NUMBER (IEEE 14 BUS)	57
5.18	GRAPH BETWEEN MAG OF ANGLE (S D) VS BUS NUMBER (IEEE 14 BUS)	57
5.19	GRAPH BETWEEN MAG OF ANGLE (S D) VS BUS NUMBER (IEEE 30 BUS)	57
5.20	GRAPH BETWEEN MAG OF ANGLE (S D) VS BUS NUMBER (IEEE 30 BUS)	58
5.21	GRAPH BETWEEN I (S D) VS BUS NUMBER (IEEE 6 BUS)	58
5.22	GRAPH BETWEEN I (S D) VS BUS NUMBER (IEEE 6 BUS)	58
5.23	GRAPH BETWEEN I (S D) VS BUS NUMBER (IEEE 9 BUS)	59
5.24	GRAPH BETWEEN I (S D) VS BUS NUMBER (IEEE 9 BUS)	59
5.25	GRAPH BETWEEN I (S D) VS BUS NUMBER (IEEE 14 BUS)	59
5.26	GRAPH BETWEEN I (S D) VS BUS NUMBER (IEEE 14 BUS)	60
5.27	GRAPH BETWEEN I (S D) VS BUS NUMBER (IEEE 30 BUS)	60
5.28	GRAPH BETWEEN I (S D) VS BUS NUMBER (IEEE 30 BUS)	60
5.29	GRAPH BETWEEN P (S D) VS BUS NUMBER (IEEE 6 BUS)	61
5.30	GRAPH BETWEEN P (S D) VS BUS NUMBER (IEEE 6 BUS)	61
5.31	GRAPH BETWEEN P (S D) VS BUS NUMBER (IEEE 9 BUS)	61
5.32	GRAPH BETWEEN P (S D) VS BUS NUMBER (IEEE 9 BUS)	62
5.33	GRAPH BETWEEN P (S D) VS BUS NUMBER (IEEE 14 BUS)	62
5.34	GRAPH BETWEEN P (S D) VS BUS NUMBER (IEEE 14 BUS)	62
5.35	GRAPH BETWEEN P (S D) VS BUS NUMBER (IEEE 30 BUS)	63
5.36	GRAPH BETWEEN P (S D) VS BUS NUMBER (IEEE 30 BUS)	63
5.37	GRAPH BETWEEN Q (S D) VS BUS NUMBER (IEEE 6 BUS)	63
5.38	GRAPH BETWEEN Q (S D) VS BUS NUMBER (IEEE 6 BUS)	64
5.39	GRAPH BETWEEN Q (S D) VS BUS NUMBER (IEEE 9 BUS)	64
5.40	GRAPH BETWEEN Q (S D) VS BUS NUMBER (IEEE 9 BUS)	64
5.41	GRAPH BETWEEN Q (S D) VS BUS NUMBER (IEEE 14 BUS)	65
5.42	GRAPH BETWEEN Q (S D) VS BUS NUMBER (IEEE 14 BUS)	65
5.43	GRAPH BETWEEN Q (S D) VS BUS NUMBER (IEEE 30 BUS)	65
5.44	GRAPH BETWEEN Q (S D) VS BUS NUMBER (IEEE 30 BUS)	66

FIG.	CONTENTS	PAGE
5.45	AVERAGE VOLTAGE STANDARD DEVIATION (IEEE 6 BUS)	66
5.46	AVERAGE VOLTAGE STANDARD DEVIATION (IEEE 6 BUS)	67
5.47	AVERAGE VOLTAGE STANDARD DEVIATION (IEEE 9 BUS)	67
5.48	AVERAGE VOLTAGE STANDARD DEVIATION (IEEE 9 BUS)	67
5.49	AVERAGE VOLTAGE STANDARD DEVIATION (IEEE 14 BUS)	68
5.50	AVERAGE VOLTAGE STANDARD DEVIATION (IEEE 14 BUS)	68
5.51	AVERAGE VOLTAGE STANDARD DEVIATION (IEEE 30 BUS)	68
5.52	AVERAGE VOLTAGE STANDARD DEVIATION (IEEE 30 BUS)	69
5.53	AVERAGE VOLTAGE ANGLE STANDARD DEVIATION (IEEE 6 BUS)	69
5.54	AVERAGE VOLTAGE ANGLE STANDARD DEVIATION (IEEE 6 BUS)	69
5.55	AVERAGE VOLTAGE ANGLE STANDARD DEVIATION (IEEE 9 BUS)	70
5.56	AVERAGE VOLTAGE ANGLE STANDARD DEVIATION (IEEE 9 BUS)	70
5.57	AVERAGE VOLTAGE ANGLE STANDARD DEVIATION (IEEE 14 BUS)	70
5.58	AVERAGE VOLTAGE ANGLE STANDARD DEVIATION (IEEE 14 BUS)	71
5.59	AVERAGE VOLTAGE ANGLE STANDARD DEVIATION (IEEE 30 BUS)	71
5.60	AVERAGE VOLTAGE ANGLE STANDARD DEVIATION (IEEE 30 BUS)	71
5.61	AVERAGE CURRENT STANDARD DEVIATION (IEEE 6 BUS)	72
5.62	AVERAGE CURRENT STANDARD DEVIATION (IEEE 6 BUS)	72
5.63	AVERAGE CURRENT STANDARD DEVIATION (IEEE 9 BUS)	72
5.64	AVERAGE CURRENT STANDARD DEVIATION (IEEE 9 BUS)	73
5.65	AVERAGE CURRENT STANDARD DEVIATION (IEEE 14 BUS)	73
5.66	AVERAGE CURRENT STANDARD DEVIATION (IEEE 14 BUS)	73
5.67	AVERAGE CURRENT STANDARD DEVIATION (IEEE 30 BUS)	74
5.68	AVERAGE CURRENT STANDARD DEVIATION (IEEE 30 BUS)	74
5.69	AVERAGE P STANDARD DEVIATION (IEEE 6 BUS)	74
5.70	AVERAGE P STANDARD DEVIATION (IEEE 6 BUS)	75
5.71	AVERAGE P STANDARD DEVIATION (IEEE 9 BUS)	75
5.72	AVERAGE P STANDARD DEVIATION (IEEE 9 BUS)	75
5.73	AVERAGE P STANDARD DEVIATION (IEEE 14 BUS)	76
5.74	AVERAGE P STANDARD DEVIATION (IEEE 14 BUS)	76

FIG.	CONTENTS	PAGE
5.75	AVERAGE P STANDARD DEVIATION (IEEE 30 BUS)	76
5.76	AVERAGE P STANDARD DEVIATION (IEEE 30 BUS)	77
5.77	AVERAGE Q STANDARD DEVIATION (IEEE 6 BUS)	77
5.78	AVERAGE Q STANDARD DEVIATION (IEEE 6 BUS)	77
5.79	AVERAGE Q STANDARD DEVIATION (IEEE 9 BUS)	78
5.80	AVERAGE Q STANDARD DEVIATION (IEEE 9 BUS)	78
5.81	AVERAGE Q STANDARD DEVIATION (IEEE 14 BUS)	78
5.82	AVERAGE Q STANDARD DEVIATION (IEEE 14 BUS)	79
5.83	AVERAGE Q STANDARD DEVIATION (IEEE 30 BUS)	79
5.84	AVERAGE Q STANDARD DEVIATION (IEEE 30 BUS)	79

LIST OF TABLES

TABLE	CONTENTS	PAGE
4.1	Measurements with their PMU Cases	42
4.2	PMU Locations for Each Bus System	43
5.1	Type of Variables and Measurement	48
5.2	Standard Deviations of the Measurements for the Test	49
5.3	Average Standard Deviations of the Estimated Variables	80
B1	Generator Data IEEE – 6 Bus System	93
B2	Bus Data of IEEE – 6 Bus Test System	93
B3	Line Data of IEEE – 6 Bus Test System	93
B4	Generator Data IEEE – 9 Bus System	94
B5	Bus Data of IEEE – 9 Bus Test System	94
B6	Line Data of IEEE – 9 Bus Test System	94
B7	Generator Data IEEE – 14 Bus System	95
B8	Bus Data of IEEE – 14 Bus Test System	95
B9	Line Data of IEEE – 14 Bus Test System	96
B10	Generator Data IEEE – 30 Bus System	97
B11	Bus Data of IEEE – 30 Bus Test System	97
B12	Line Data of IEEE – 30 Bus Test System	98

CHAPTER - 1

INTRODUCTION

1.1 Introduction

A **Phasor Measurement Unit** (PMU) dealing with the electrical waves on an electricity grid to measure the health of the system. A phasor is a multifarious number of electricity that represents both the magnitude and phase angle of the sine waves. Phasor measurements that occur at the same time are called "Synchrophasor", as are the PMU devices that allow their measurement. In power engineering, traditionally we use number of devices such as Circuit Breaker, Relay, CT & PT, Voltmeter, Wattmeter, Ammeter, Synchro-scope, Isolator, Compensator devices, etc. for measurement purposes on every substation. The recently developed PMU will help in deciding to stall such devices at proper location for:-

- More accurate and comprehensive planning.
- Better congestion tracking,
- Visualization and advanced warning systems,
- Information sharing over a wide region,
- Improvements of System Integrity Protection Schemes (SIPS),
- Grid restorations,
- More reliable,
- Efficient,
- Cost effective grid operation, resulting from better information and the ability to manage the grid dynamically, as opposed to reactive management in the face of unusual, and potentially catastrophic, events.

According to Klump *et al* [2005] as shown in fig.1.1, PMU is a useful device that will help as

- Substations parameter measurement
- Sent data in real time to Phasor Data Concentrator(PDC)
- PDC sent data to applications, stores disturbance data, manages measurement system

- Application includes monitors, recorders, alarms, and control.

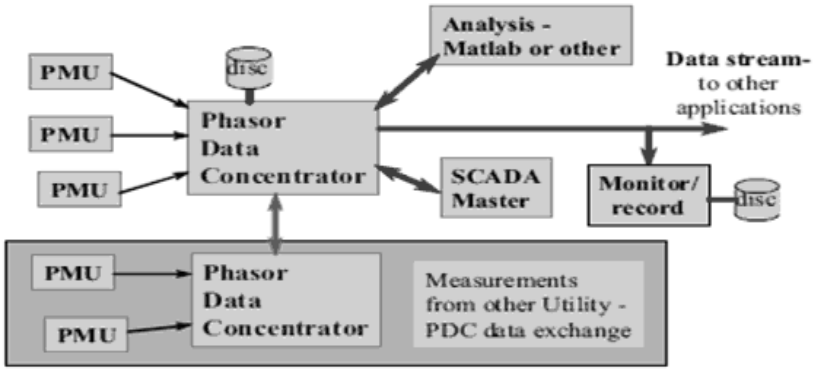

Fig. 1.1: Phasor Measurement Unit (PMU) [Ref.: Klump *et al* [2005]

Such device is also referred to as Synchro-phasor and is considered one of the most important measuring devices in the near future of power systems as in Smart Grid. A PMU can be a enthusiastic device, or the PMU function can be integrated with a protective relay or other device. The sensor [Kamwa and Grondin [2002]] responses to the bus voltage magnitude, the angle and frequency coherency indexes, which are estimated by means of a statistical sampling of power system response signals from a transient-stability program. Through the "successive addition" scheme, one of these algorithms easily incorporates mandatory locations such as tie-line busses and large generator step-up transformers.

1.2 System Monitoring by Global Positioning System (GPS)

In typical applications phasor measurement units are sampled from widely dispersed locations in the power system network and synchronized from the common time source of a global positioning system (GPS) radio clock. Synchro-phasor technology provides a tool for system operators and planners to measure the state of the electrical system and manage power quality. Synchro-phasor measure voltages and currents at diverse locations on a power grid [Rahman K. A. *et al* [2001]] and provide output accurately in time-stamped voltage and current phasors. Because these phasors are truly synchronized, so that the synchronized comparison of two quantities is possible, in real time, [Phadke *et al* [2009]] as shown in the fig.1.2

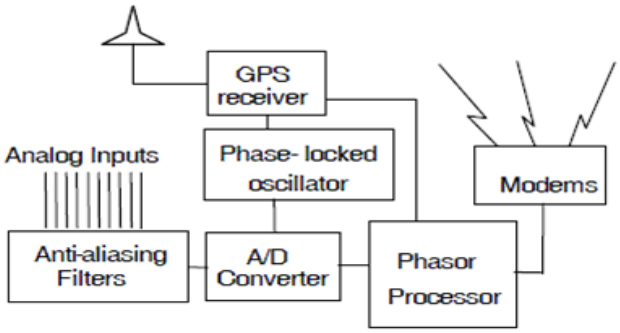

Fig 1.2: Global Positioning System [Ref.: Klump *et al* [2005]]

Such comparisons may be used to assess system conditions. The technology has the potential to change the economics of power delivery by allowing increased power flow over existing lines. Synchro-phasor data could be used to allow power flow up to a line's dynamic limit instead of to its worst-case limit [Rakpenthai C.et al [2004]].

State estimation is a key element of the online security analysis function in modern power system energy control centers. The purpose of state estimation is to practice a set of redundant measurements to obtain the best estimation of the current state of a power system [Zhao L. and Abur A [2005]]. State estimation is traditionally solved by the weighted least square algorithm with conventional measurements such as voltage magnitude, real and reactive power injection, Real and Reactive power flow. Recently developed synchronized phasor measurement techniques based on a time signal of the GPS (Global Positioning System) in the field of power systems. A PMU, when placed at a bus, can measure the voltage phasor at the bus, as well as the current phasors through the lines incident to the bus. It illustrates the ac voltage and current waveforms while synchronizing the sampling instants with a GPS clock. The computed values of voltage and current phasors are then time stamped and transmitted by the PMUs to the local or remote receiver. The traditional state estimation is by nature a nonlinear problem. The most commonly used approach is Weighted Least Squares [Cheng *et al* [2008], Madtharad *et al* [2003], Xu and Abur [2004]], which converts the nonlinear equations into the normal equations by using first-order Taylor series. However, the state estimation equations for PMU measurements are inherently linear equations. Some research has been conducted to try to formulate the mixed set of traditional and PMU measurements. The natural approach is to treat PMU measurements as additional measurements to be appended to traditional measurements, which causes the additional computation burden

of calculation. Another approach is to use the distributed scheme for the mixed state estimation. The problem of finding optimal PMU locations for power system state estimation is well investigated in various literatures [Zhou M et al [2006]].

1.3 Application

- Power system automation, as in smart grids
- Load shedding and other load control techniques such as demand response mechanisms to manage a power system. (i.e. Directing power where it is needed in real-time)
- Increase the reliability of the power grid by detecting faults early, allowing for isolation of operative system, and the prevention of power outages.
- Enhance the quality of power by precise analysis and automated correction of sources of system degradation.
- Over Wide Area measurement and control of a Power System, e.g. in very wide area super grids, regional transmission networks, and local distribution grids.

1.4 Challenges

Typical challenges while installing PMUs on you power system can be summarized [Weekes M.A. et al [2007]]:

- Establishing a project leader and coordinating the various groups needed.
- Assessing risks either during commissioning or after installation including cyber-security issues.
- Finding a suitable location that meets the needs of the unit and is easily accessible.
- During testing and commissioning of bench
- The operational understanding like performance tests and difficulties with managing excessively large data files. It was concluded that before proper accuracy could be obtained from the steady-state frequency tests, angle data must be obtained from both the site where the tests are performed and the reference bus used otherwise errors are introduced when the reference bus is off-nominal.
- Development of a business case and their road map for plan a future integration of devices.

1.5 Standards

The IEEE 1344 standard for Synchro-phasor was accomplished in 1995, and reaffirmed in 2001. In 2005, it was reinstate by IEEE Standard C37.118-2005, which was a comprehensive revision and dealt with issues in regard of PMUs in electric power systems. The specification describes for standard measurement, the method of quantifying the measurements, testing & certification requirements for verifying accuracy, and data transmission format and protocol for real-time data communication. The comprehensive standards are not yet address all factors that PMUs can detect in power system dynamic activity.

Other standards used with PMU interfacing:

- **OPC-DA / OPC-HDA** - A Microsoft Windows based interface protocol that is currently being generalized to use XML and run on non Windows computers.
- **IEC 61850** a standard for electrical substation automation
- **BPA PDC Stream** - a variant of IEEE 1344 used by the Bonneville Power Administration (BPA) PDCs and user interface software.

CHAPTER - 2

LITERATURE REVIEW

In this chapter some selected research papers related to economical placement of Phasor Measurement Unit (PMU) are reviewed as:-

Bretas, N.G. and London, J.B.A. Jr. [2001] presents a method for designing or upgrading measurement placement plans for state estimation purposes. The method allows obtaining a measurement placement plan that besides to make the associated system observable, maintain the observability against loss of one or two measurements. In order to do that, the redundancy level of the available measurements are evaluated and, if necessary, increased. The redundancy level of the measurements is identified from the relationship between the measurements and the equivalent states, which are obtained from a convenient exchange of basis in the state space. One numerical example illustrating the proposed method is given. The method is successfully tested in several measurement configurations, considering the IEEE-14-bus and a system of 121 buses of the ELETROSUL, a Brazilian utility.

Chakrabarti, S. *et al* [2007] proposes a method for optimal placement of phasor measurement units (PMUs) for measuring the states of a power system. A method to compute the measurement uncertainty associated with the estimated states is also illustrated in the paper. The PMU placement strategy ensures complete observability of the power system states for normal operating conditions, as well as under the loss of a single transmission line or even a single measurement unit. An integer quadratic programming approach is used to minimize the total number of PMUs required to make the system completely observable, and to maximize the measurement redundancy at the power system busses. The goal of the research is to take into account the measurement uncertainty while determining the optimal number and locations of the PMUs for state estimation. Simulation results on the IEEE 14-bus test system are presented in this paper.

Chakrabarti, S. *et al* [2008] proposes a method for optimal placement of phasor measurement units (PMUs) for complete observability of a power system for normal operating conditions, as well as for single branch outages. A binary search algorithm is used to determine the minimum number of PMUs needed to make the system observable.

In case of more than one solution, a strategy is proposed to select the solution resulting in the most preferred pattern of measurement redundancy. The proposed method is used to benchmark the optimal PMU placement solutions for the IEEE 14-bus, IEEE 24-bus, IEEE 30-bus and New England 39-bus test systems. The proposed method is applied on a 298-bus system to determine the optimal placement of PMUs when conventional measurements are available.

Cheng, Y. *et al* [2008] proposed most commonly used WLS state estimator in power industry is non-linear and formulated by using conventional measurements such as line flow and injection measurements. The computational burden becomes a concern for the existing WLS state estimation when integrating PMU measurements. Distributed state estimators, which can solve this problem of integrating, have been proposed for this reason. However, the discrepancy between distributed state estimator and the integrated state estimator exists. This paper proposes an approach to formulate the state estimation in a new manner that is able to formulate together the traditional measurements as well as PMU measurements easily and efficiently. The proposed estimator is tested on IEEE 118-bus system and ERCOT 5514- bus system.

Ebrahimian, R. and Baldick, R. [2000] presents an application of a parallel algorithm to Power Systems State Estimation. We apply the Auxiliary Problem Principle to develop a distributed state estimator, demonstrating performance on the Electric Reliability Council of Texas (ERCOT) and the Southwest Power Pool (SPP) systems.

Ebrahimpour, R. *et al* [2011] illustrated the very importance behind recent blackouts in different countries and vital need of more frequent and thorough power system stability. Therefore transient stability investigation on power system have became in focus of many researchers in the field. We have tried to introduce a new model for transient stability prediction of a power system to add a contribution to the subject. For this reason we applied so called, Committee Neural Networks (CNNs) methods as tools for Transient Stability Assessment (TSA) of power system. We use the "Mixture of Experts" (ME) in which, the problem space is divided into several subspaces for the experts, and then the outputs of experts are combined by a gating network to form the final output. In this paper Mixture of the Experts (ME) is used to assess the transient stability of power system after faults occur on transmission lines. Simulations were carried out on the IEEE 9-bus and IEEE 14- bus tests systems considering three phase faults on the systems. The

data collected from the time domain simulations are then used as inputs to the ME in which is used as a classifier to determine whether the power systems are stable or unstable.

Filho, M. B. D. C. *et al* [2001] presents data redundancy an important prerequisite for state estimation. During system operation, critical redundancy levels can be reached, creating adverse conditions for the state estimation process, especially regarding data validation. In this paper a numerical algorithm for the identification of critical measurements and sets is proposed. Results covering its application to typical power system networks are presented and discussed.

Fitiwi, D. Z. and Rao, K.S. R. [2009] focuses on methods to discriminate a temporary fault from a permanent one, and accurately determine fault extinction time in an extra high voltage (EHV) transmission line in a bid to develop a self-adaptive automatic reclosing scheme. Consequently, improper reclosing of the line onto a fault is avoided. The fault identification prior to reclosing is based on optimized artificial neural network associated with three different training algorithms. In addition, Taguchi's methodology is employed in optimizing parameters that significantly influence during and post-training performance of the neural network. A comparison of overall performance of the three algorithms, developed and coded in MATLABTM software environment, is also presented. To validate the work, the developed technique in a single machine infinite bus (SMIB) model has been tested by data obtained from benchmark IEEE 14-bus system model simulations. The results show the efficacy of the developed adaptive automatic reclosing method.

Gou, B. [2008] presents a simple optimal placement algorithm of phasor measurement units (PMU) by using integer linear programming. Cases with and without conventional power flow and injection measurements are considered. The measurement placement problems under those cases are formulated as an integer linear programming which saves the CPU computation time greatly. Simulation results show that the proposed algorithm can be used in practice.

Huang, G. M. and Lei, J. [2002] introduced power market deregulation companies cooperate to share one whole grid system and try to achieve their own economic goals. They focuses on how to improve the state estimation result of member companies or ISO

by exchanging raw or estimated data with neighboring member companies/ISO. The concept of Bus Redundancy Descriptor (BRD) is developed based on critical measurement set. BRD and leverage points are used as criteria to evaluate the quality of measurement systems. Accordingly, based on BRD a heuristic algorithm for measurement design under distributed multi-utility operation is presented to search for possible beneficial data exchange schemes. Numerical results verify that every member companies including ISO benefit from mutual data exchange when some principles of design are carefully applied.

Iyambo, P.K. and Tzoneva, R. [2007] presented that transient stability is an important aspect in designing and upgrading electric power system. They cover the modeling and the transient stability analysis of the IEEE 14 test bus system using Matlab Power System Toolbox (PST) package. A three-phase fault is located at two different locations, to analyze the effect of fault location and critical clearing time on the system stability. In order to protect overhead transmission line, conductors and insulators, it is suggested that the faulted part to be isolated rapidly from the rest of the system so as to increase stability margin and hence decrease damage.

Jiang, W. and Vittal, V. [2006] presents a phasor measurements placement algorithm which enhances the accuracy of the state estimation solutions and increases local redundancy. The algorithm developed determines a list of buses with low local redundancy and a list of buses with low sate estimator accuracy. The optimal placement of phasor measurements is determined by a ranking of group of buses which are determined with respect to the characteristics of phasor measurements. Test results on the IEEE 14-bus and 118-bus IEEE Test System are provided.

Jiang, W. *et al* [2007] provide the creation of balancing authorities by the North American Reliability Council that span large portions of the North American interconnection, and stringent requirements for real time monitoring of power system evolution, faster and more accurate state estimation algorithms that can efficiently handle systems of very large sizes are needed in the present environment. This paper presents a distributed state estimation algorithm suitable for large-scale power systems. Synchronized phasor measurements are applied to aggregate the voltage phase angles of each decomposed subsystem in the distributed state estimation solution. The aggregated state estimation solution is obtained from the distributed solution using a sensitivity

analysis based update at chosen boundary buses. Placement of synchronized phasor measurements in the decomposed subsystems is also investigated. Test results on the IEEE 118-bus test bed are provided.

Kamwa,I. and Grondin, R. [2002] says effective assessment of the dynamic performance of the power system requires wide-area information from properly distributed phasor measurement units (PMUs). However, to maximize the information content of the captured signals, the sensors need to be located appropriately, with due account given to the structural properties underlying the given system. In this paper, two numerical algorithms are proposed to achieve this goal. They aim to maximize the overall sensor response while minimizing the correlation among sensor outputs so as to minimize the redundant information provided by multiple sensors. The sensor responses of interest are the bus voltage magnitude, and the angle and frequency coherency indexes, which are estimated by means of a statistical sampling of power system response signals from a transient-stability program. Through the "successive addition" scheme, one of these algorithms easily incorporates mandatory locations such as tie-line busses and large generator step-up transformers. The proposed approaches are first illustrated on the Hydro-Québec transmission grid and then on a 9-area/67-bus/23-machine test network designed with well-defined geographical boundaries and pre-specified weak interties between electrically coherent areas.

Kezunovic, M. *et al* [2004] research aimed at introducing modeling and simulation as a major methodological approach for enhancing power engineering education. The reasons for such an approach are explained first. Different options and uses of the modeling and simulation tools are discussed next. Several implementations of the teaching examples are outlined. The paper ends with the conclusions reached based on the study.

Klump, R. *et al* [2005] explores the ways to highlight threats to power system security by displaying data from phasor measurement units (PMUs) and SCADA data sources simultaneously. SCADA measurements provide a picture of the steady-state health of the system, whereas PMUs capture the faster variations that may indicate small signal stability problems. The software system described in this system gathers SCADA and PMU data and displays them on a geographic map of the system. The system uses contour plots to show the variation of a measurement with location, even when adjacent measurement points are widely spread. The system superimposes trend plots on this

display to show the past variation of a quantity over a user-specified time window. The goal of the system is to help operators gauge the present security of the grid.

Madtharad, C. *et al* [2003] deals with a simple technique for measurement placement method of power system state estimation. The minimum condition number of the measurement matrix is used as the criteria in conjunction with sequential elimination to generalize the measurement placement. The Singular Value Decomposition (SVD) approach will be used to solve the state estimation. The simulation study is performed on the IEEE 14hns test system by linear weighted least square (WLS). It is found that, this algorithm can give a solution of measurement placement of injection current and voltage that make the power system observable.

Madtharad, C. *et al* [2005] focuses on a new technique for optimal measurement placement for power system harmonic state estimation (HSE). The solution provides the optimal number of measurements and the best positions to place them, in order to identify the locations and magnitudes of harmonic sources. The minimum condition number of the measurement matrix is used as the criteria in conjunction with sequential elimination to solve this problem. Two different test systems are provided to validate the measurement placement algorithm. A three-phase asymmetric power system has been tested using the New Zealand test system, while the IEEE 14-bus test system has been used for testing a balanced power system.

Magnago, F. H. and Abur, A. [2000] presents a systematic procedure by which measurement systems can be optimally upgraded. The proposed procedure yields a measurement configuration that can withstand any single branch outage or loss of single measurement, without losing network observability. It is a numerical method based on the measurement Jacobian and sparse triangular factorization, making its implementation easy in existing state estimators. It can be used off-line in planning and meter placement studies or it can be implemented as part of the on-line observability analysis function. Details of the procedure are presented using numerical examples.

Meshram, S. and Sahu, O. P. [2011] presented the artificial neural network technique training against the result obtained by the classical Kirchmayer method and compares the obtained data. After training, the power generation (PGi) for any power demands (PD) can be calculated.

Milosevic, B. and Begovic, M. [2003] will considers a phasor measurement unit (PMU) placement problem requiring simultaneous optimization of two conflicting objectives, such as minimization of the number of PMUs and maximization of the measurement redundancy. The objectives are in conflict since the improvement of one of them leads to the deterioration of another. Instead of a unique optimal solution, it exist a set of best tradeoffs between competing objectives, the so-called Pareto-optimal solutions. A specially tailored non-dominated sorting genetic algorithm (NSGA) for a PMU placement problem is proposed as a methodology to find these Pareto-optimal solutions. The algorithm is combined with the graph-theoretical procedure and a simple GA to reduce the initial number of the PMU's candidate locations. The NSGA parameters are carefully set by performing a number of trial runs and evaluating the NSGA performances based on the number of distinct Pareto-optimal solutions found in the particular run and distance of the obtained Pareto front from the optimal one. Illustrative results on the 39- and 118-bus IEEE systems are presented.

Nuqui, R. F. and Phadke, A. G. [2005] presents techniques for identifying placement sites for phasor measurement units (PMUs) in a power system based on incomplete observability. The novel concept of depth of un-observability is introduced and its impact on the number of PMU placements is explained. Initially, we make use of spanning trees of the power system graph and a tree search technique to find the optimal location of PMUs. We then extend the modeling to recognize limitations in the availability of communication facilities around the network and pose the constrained placement problem within the framework of Simulated Annealing (SA). The SA formulation was further extended to solve the pragmatic phased installation of PMUs. The performance of these methods is tested on two electric utility systems and IEEE test systems. Results show that these techniques provide utilities with systematic approaches for incrementally placing PMUs thereby cushioning their cost impact.

Nwohu, M. N. [2010] proposes an approach for estimating bifurcation point in multi-bus systems. The approach assumes that the generators would violate their Q-limits before the bifurcation point is reached. The result of this assumption clearly raises the voltages along the PV curve which consequently yield an infinitesimal error. Therefore the final estimated point can be obtained after a number of load flow solutions depending on the complexity of the system and the loading pattern among others. Finally, computer

simulations of two system networks are carried out to calculate the bifurcation point at the selected minimum voltage which estimates the bus that violates its Q-limit at a certain load.

Ota, Y. ***et al*** **[2002]** shows the aspect of instability phenomena during midterm is complicated, the stability analysis is significant in order to keep the power system stable. Synchronized phasor angles obtained by the PMU (Phasor Measurement Unit) provide the effective information for evaluating the stability of B bulk power system. This paper proposes a midterm stability evaluation method of the wide-area power system by using the synchronized phasor measurements. Clustering and aggregating the power system to some coherent generator groups, the stability margin of each coherent group is quantitatively evaluated on the basis of the one machine and infinite bus system. The midterm stability of B longitudinal power system model of Japanese 60Hz systems constructed by the PSA (Power system Analyzer), which is a hybrid-type power system simulator is practically evaluated using the proposed method.

Phadke, A.G. [2002] says that Synchronized Phasor Measurements (PMU) was introduced in mid-1980s. Since then, the subject of wide-area measurements in power systems using PMUs and other measuring instruments has been receiving considerable attention from researchers in the field. This paper provides a historical overview of the PMU development. It is pointed out that the PMU is a direct descendant of the Symmetrical Component Distance Relay introduced in late 1970s. From the early prototypes of the PMU built at Virginia Tech, a commercial product evolved which has been installed in the field at various locations around the world. Applications of PMU measurements to power system operation and control remain a very important subject for current research.

Phadke, A.G. ***et al*** **[2009]** are being installed Synchronized Phasor Measurement Units (PMU) in many power systems, around the world. Several of these installations intend to utilize the PMU data to augment features of their state estimators. This paper summarizes results of recent research which have used phasor measurements in novel ways. Beginning with a phasor based state estimation technique the paper considers an innovative approach to incorporating phasor data in conventional state estimators. The paper reviews the concept of complete and incomplete observability with phasor data, and the use of incompletely observed state to achieve pseudo observability. Also included

is a discussion of seams between adjoining state estimates, and a new concept of using phasor measurements to calibrate instrument transformers.

Rahman, K. A. *et al* [2001] presents that Internet can play an important role in Wide Area Information Sharing (WAIS) especially in the non-critical time applications. Moving from Independent System Operators (IS0s) to Regional Transmission Organizations (RTOS) is one example of the need for WAIS. The WAIS system can form the basis for the future RTO communication model or as a national level security coordinator communication model, if such a need should arise in the near future. This paper discusses some of our study results of the effect of wide area measurements on the power system calculations. Most of the calculations for power system operation are primarily based on accurate determination of the state (the voltage and the angle at each bus) of the power system. A comparison study between Integrated State Estimation (lSE), which is based on sharing real time measurements, and Split State Estimation (SSE), that is based on sharing SE outputs will be presented. The factors which affect the accuracy of SSE WIII also be presented.

Rakpenthai C. *et al* [2004] will presents the concept of distributed process to improve the previously proposed measurement placement method for power system state estimation in which the minimum condition number of the measurement matrix is used as a criterion in conjunction with sequential elimination to reach the near optimal measurement placement. Firstly, the entire network of the power system is decomposed into smaller subsystems. Then, in each subsystem, the optimal positions for measurement placement are determined by using the minimum condition number criteria. The numerical experiment results on the IEEE 14 bus system indicate that the proposed technique gives the measurement matrix with smaller condition number and the computation time is much shorter.

Sangrody, H. A. *et al* [2009] used weighted least square state estimator in power industry is nonlinear and formulated by using conventional measurements such as line flow and injection measurements. PMUs (Phasor Measurement Units) are gradually adding them to improve the state estimation process. In this paper the way of corporation the PMU data to the conventional measurements and a linear formulation of the state estimation using only PMU measured data are investigated. Six cases are tested while gradually increasing the number of PMUs which are added to the measurement set and

the effect of PMUs on the accuracy of variables are illustrated and compared by applying them on IEEE 14, 30 test systems.

Tanti, D.K. *et al* [2011] has been considered Voltage sag as one of the most harmful power quality problem as it may significantly affect industrial production. This paper presents an Artificial Neural Network (ANN) based approach for optimal placement of Distribution Static Compensator (DSTATCOM) to mitigate voltage sag under faults. Voltage sag under different type of short circuits has been estimated using MATLAB/SIMULINK software. Optimal location of DSTATCOM has been obtained using a feed forward neural network trained by post-fault voltage magnitude of three phases at different buses. Case studies have been performed on IEEE 14-bus system and effectiveness of proposed approach of DSTATCOM placement has been established.

Weekes M.A. *et al* [2007] investigates the typical challenges encountered while installing phasor measurement instrumentation on power system grid, which aid in power system security, are documented. The project of installing phasor measurement unit (PMU) devices is described from initiation through execution, operational experience, and testing. A brief business case, road map and results are discussed. The documentation is of significant value to prospective new champions for such devices on their system.

Xu, B. and Abur, A. [2004] provides the analysis of network observability and phasor measurement unit (PMU) placement when using a mixed measurement set. The measurements will include conventional power flows and injections as well as phasor measurements for voltages and line currents provided by phasor measurement units. The observability analysis is followed by an optimal meter placement strategy for the PMUs.

Zhao, L. *et al* [2005] investigates the problem of state estimation in very large power systems, which may contain several control areas. An estimation approach which coordinates locally obtained decentralized estimates while improving bad data processing capability at the area boundaries is presented. Each area is held responsible for maintaining a sufficiently redundant measurement set to allow bad data processing among its internal measurements. It is assumed that synchronized phasor measurements from different area buses are available in addition to the conventional measurements provided by the substation remote terminal units. The estimator is implemented and

tested using different measurement configurations for the IEEE 118-bus test system and the 4520-bus ERCOT system.

Zhou, M. *et al* [2006] propose the use of real-time synchronized phasor measurement units, it is necessary to consider applications of these measurements in greater detail. One of the most natural applications of these measurements is in the area of state estimation. A straightforward application of state estimation theory treats phasor measurements of currents and voltages as additional measurements to be appended to traditional measurements now being used in most energy management system (EMS) state estimators. The resulting state estimator is once again nonlinear and requires significant modifications to existing EMS software. This paper proposes an alternative approach, which leaves the traditional state estimation software in place, and discusses a novel method of incorporating the phasor measurements and the results of the traditional state estimator in a post processing linear estimator. This paper presents the underlying theory and provides verification through simulations of the two alternative strategies. It is shown that the new technique provides the same results as the nonlinear state estimator and does not require modification of the existing EMS software.

From the review of above literatures, different researcher worked on the combination of different parameters. But the work has done in this project on the combined effect of change in Voltage, Power Angle, Current, Real Power and Reactive Power on IEEE 6 Bus, IEEE 9 Bus IEEE 14 Bus and IEEE 30 Bus System.

CHAPTER - 3

FULL WEIGHTED LEAST SQUARE STATE ESTIMATION

3.1 Introduction

A state estimator will estimates the voltage magnitudes and phase angles at the buses by using the available measurements in the form

- Power injections,
- Power flows,
- Voltage magnitudes,
- Current through the branches.

The voltage and current phasor measured by the PMUs can be used in a state estimator in two ways [Phadke [2002]] as

- Increase the confidence in the available measurements; and
- Replace the available conventional measurements.

The PMU at a bus can measure the voltage phasor at that bus as well as at the buses at the other end of all the incident lines, using the current phasor and the known line parameters. It is assumed that the PMU has a sufficient number of channels to measure the current phasor through the entire branches incident to the corresponding bus.

WLS state estimation minimizes the weighted sum of squares of the residuals. Consider the set of measurements given by the vector z :

$$z = \begin{bmatrix} z_1 \\ z_2 \\ z_3 \\ . \\ . \\ z_m \end{bmatrix} = \begin{bmatrix} h_1(x_1, x_2, x_3, \ldots\ldots x_n) \\ h_2(x_1, x_2, x_3, \ldots\ldots x_n) \\ h_3(x_1, x_2, x_3, \ldots\ldots x_n) \\ . \\ . \\ h_m(x_1, x_2, x_3, \ldots\ldots x_n) \end{bmatrix} + \begin{bmatrix} e_1 \\ e_2 \\ e_3 \\ . \\ . \\ e_m \end{bmatrix} = h(x) + e \qquad (3.1)$$

Where:

$$h^T = [h_1(x), h_2(x), h_3(x), \ldots . h_m(x)] \tag{3.2}$$

$h_i(x)$ is the nonlinear function relating measurement i to the state vector x

$x^T = [\, x_1, x_2, x_3 \ldots\ldots\ldots\ldots x_n]$ is the system state vector

$e^T = [e_1, e_2, e_3 \ldots\ldots\ldots e_m\,]$ is the vector of measurement errors.

Let $E(e)$ designate the expected value of e, with the following assumptions:

$$E(e_i) = 0 \text{ , } i = 1, \ldots\ldots, m \tag{3.3}$$

$$E\,(e_i, e_j) = 0 \tag{3.4}$$

Measurement errors are assumed to be independent and their covariance matrix is given by a diagonal matrix R :

$$\text{Cov}\,(e) = E\,[e * e^T] = R = \text{diag}\,\{\sigma_1^2, \sigma_2^2, \sigma_3^2 \ldots\ldots \sigma_m^2\} \tag{3.5}$$

The WLS estimator will minimize the following objective function:

$$J(x) = \sum_{i=1}^{m} \frac{(z_i - h_i(x))^2}{R_{ii}} = [z - h(x)]^T R^{-1} [z - h(x)] \tag{3.6}$$

At the minimum value of the objective function, the first-order optimality conditions have to be satisfied. These can be expressed in compact form as follows:

$$g(x) = \frac{\partial J(x)}{\partial x} = -H^T(x) R^{-1} [z - h(x)] = 0, \tag{3.7}$$

Where $H(x) = \dfrac{\partial h(x)}{\partial x}$

The non-linear function $g(x)$ can be expanded into its Taylor series around the state vector x^k neglecting the higher order terms.

$$g(x) = g(x^k) + G(x^k)(x - x^k) + \ldots\ldots = 0 \tag{3.8}$$

An iterative solution scheme known as the Gauss-Newton method is used to solve above equation:

$$x^{k+1} = x^k - [G(x^k)]^{-1}.g(x^k) \tag{3.9}$$

where, k is the iteration index and x^k is the solution vector at iteration k . $G(x)$ is called the gain matrix, and expressed by:

$$G(x) = \frac{\partial g(x^k)}{\partial x} = H^T(x^k)\,R^{-1}\,H(x^k) \tag{3.10}$$

$$g(x^k) = -H^T(x^k)\,R^{-1}[z - h(x^k)] \tag{3.11}$$

Generally, the gain matrix is quite sparse and decomposed into its triangular factors. At each iteration k, the following sparse linear sets of equations are solved using forward/backward substitutions, where $\Delta x^{k+1} = x^{k+1} - x^k$:

$$[G(x^k)]\,\Delta x^{k+1} = H^T(x^k)R^{-1}[z - h(x^k)] = H^T(x^k).R^{-1}\,\Delta z^k \tag{3.12}$$

These iterations are going on until the maximum variable difference satisfies the condition, ' $Max\ \left|\Delta x^k\right| < \varepsilon$ '. A comprehensive flow-chart of this algorithm is shown in next section.

3.2 WLS State Estimation Algorithm

WLS State Estimation involves the iterative solution of the Normal equations [Sangrody *et al* [2009], Xu and Abur [2004]]. An initial guess has to be made for the state vector x^0. As in the case of the power flow solution, this guess typically corresponds to the flat voltage profile, where all bus voltages are assumed to be 1.0 per unit and in phase with each other.

The iterative solution algorithm for WLS state estimation problem [Abur and Exposito [2005]], [Chakrabarti and Kyriakides [2008]], [Gou B [2008]], [Milosevic B. and Begovic M. [2003]] can be outlined as follows:

1. At start, set the iteration index k = 0.

2. For a flat start initialize the state vector x^k .

3. Determine the gain matrix, $G(x^k)$.

4. Calculate the right hand side $t^k = H^T(x^k)R^{-1}[z - h(x^k)]$

5. Decompose $G(x^k)$ and solve for Δx^k

6. Test for convergence, $Max \left|\Delta x^k\right| < \varepsilon$?

7. If no, update k = k + 1, $x^{k+1} = x^k + \Delta x^k$ and go to step 3. Else, stop.

The above algorithm essentially involves the following computations in each iteration, k;

1. Calculation of the right hand side $t^k = H^T(x^k)R^{-1}[z - h(x^k)]$

   (a) Calculating the measurement function, h (x^k).

   (b) Building the measurement Jacobian, H (x^k).

2. Calculation of G (x^k) and solve for Δx^k .

   (a) Building the gain matrix, G (x^k).

   (b) Decomposing G (x^k) into its Cholesky factors.

   (c) Performing the forward/back substitutions to solve for Δx^{k+1}.

Flow-chart of the iterative algorithm for WLS state estimation problem can be outlined in Figure 3.1.

1. Initially set the iteration counter $k = 0$, define the convergence tolerance ε and the iteration limit k_{limit} values.

2. If $k > k_{limit}$, then terminate the iterations.

3. Calculate the measurement function $h(x^k)$, the measurement Jacobian $H(x^k)$, and the gain matrix $G(x^k) = H^T(x^k)\, R^{-1}\, H(x^k)$.

4. Solve Δx^k using above Equation.

5. If $\left|\Delta x^k\right| < \varepsilon$, then go to step 2. Else, stop. Algorithm converged.

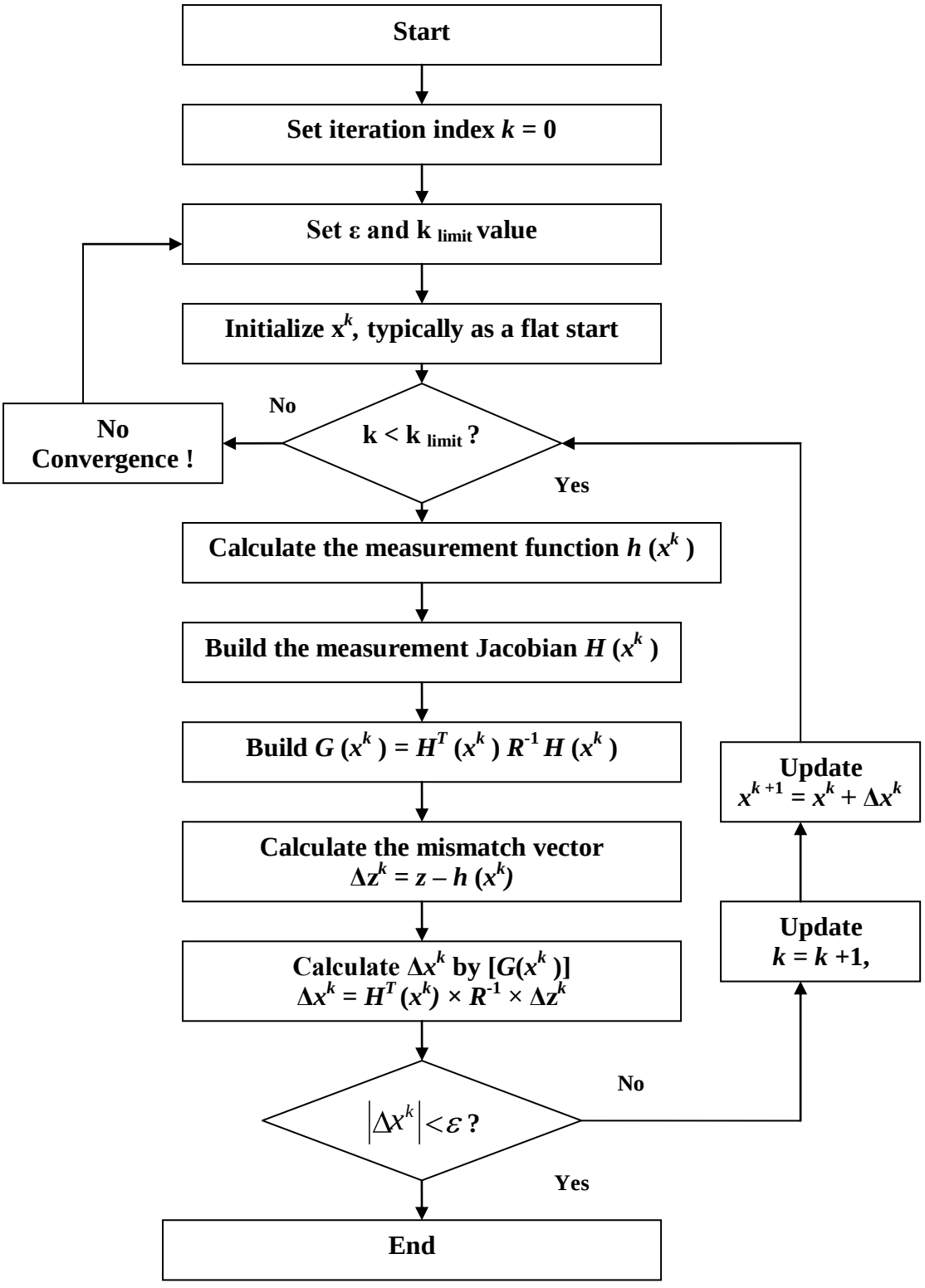

Fig 3.1: Flow-Chart for the WLS State Estimation Algorithm

3.3 Parameter Measurement and their Modeling

In power system analysis most commonly used measurement parameters for state estimation will be

- The bus power injections,
- The line power flows and
- The bus voltage magnitudes.

Such state variables will help in designing the equations for other relevant parameters for power system analysis [Nuqui R.F. and Phadke A. G. [2005]] [Ota Y. et al [2002]].

Consider a system having *N* buses, then their state vector will have (2N - 1) components which are composed of *N* bus voltage magnitudes and (N - 1) phase angles. The state vector is equal to $x^T = [\,|V_1| \angle 0^0, |V_2| \angle \theta_2, |V_3| \angle \theta_3 ..... |V_N| \angle \theta_N\,]$. An arbitrary value, such as 0 is set to be the phase angle of one reference bus. If we define $g_{ij} + jb_{ij}$ as the admittance of the series branch line connecting buses *i* and *j*, and $g_{si} + jb_{si}$ as the admittance of the shunt branch connected at bus *i*, the equivalent π model can be shown in Figure 3.2 below.

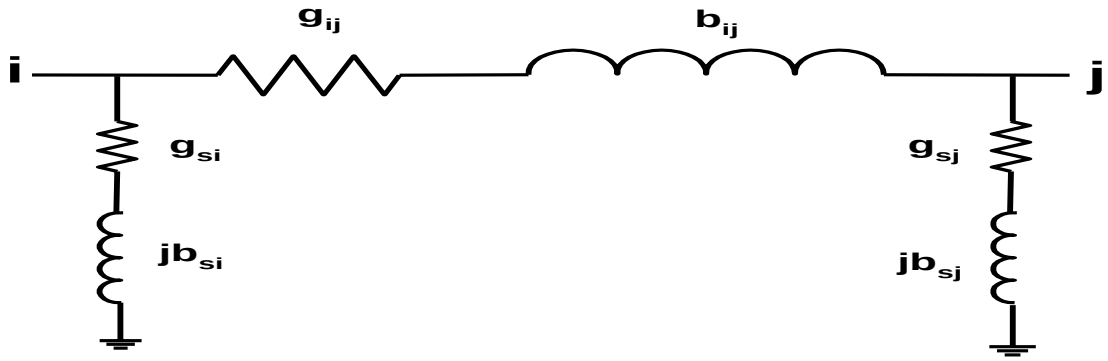

Fig 3.2: Equivalent 'π' Model of Two Bus System

Let the (i, j)th entry of the admittance matrix *Y* be $Y_{ij} = G_{ij} + jB_{ij}$. The expressions for each of the above types of measurements are then given below:

$$I_{ij} = \sqrt{(g_{ij}^{\ 2} + b_{ij}^{\ 2})\,(V_i^{\ 2} + V_j^{\ 2} - 2V_i V_j\, Cos\theta_{ij})}$$
$$= \frac{\sqrt{P_{ij}^{\ 2} + Q_{ij}^{\ 2}}}{V_i} \tag{3.13}$$

Real and reactive power injection at bus *i* can be expressed by,

$$P_i = |V_i| \sum_{j=1}^{N} |V_j| (G_{ij} \cos\theta_{ij} + B_{ij} \sin\theta_{ij}) \tag{3.14}$$

$$Q_i = |V_i| \sum_{j=1}^{N} |V_j| (G_{ij} \sin\theta_{ij} - B_{ij} \cos\theta_{ij}) \tag{3.15}$$

Real and reactive power flow from bus *i* to bus *j* are,

$$P_{ij} = |V_i|^{\,2}(g_{si} + g_{ij}) - |V_i||V_j|(g_{ij} \cos\theta_{ij} + b_{ij} \sin\theta_{ij}) \tag{3.16}$$

$$Q_{ij} = -|V_i|^{\,2}(b_{si} + b_{ij}) - |V_i||V_j|(g_{ij} \sin\theta_{ij} - b_{ij} \cos\theta_{ij}) \tag{3.17}$$

The structure of the measurement of Jacobian H will be as

$$\boldsymbol{H} = \begin{bmatrix} \frac{\partial \boldsymbol{P}_{inj}}{\partial \boldsymbol{\theta}} & \frac{\partial \boldsymbol{P}_{inj}}{\partial \boldsymbol{V}} \\ \frac{\partial \boldsymbol{P}_{flow}}{\partial \boldsymbol{\theta}} & \frac{\partial \boldsymbol{P}_{flow}}{\partial \boldsymbol{V}} \\ \frac{\partial \boldsymbol{Q}_{inj}}{\partial \boldsymbol{\theta}} & \frac{\partial \boldsymbol{Q}_{inj}}{\partial \boldsymbol{V}} \\ \frac{\partial \boldsymbol{Q}_{flow}}{\partial \boldsymbol{\theta}} & \frac{\partial \boldsymbol{Q}_{flow}}{\partial \boldsymbol{V}} \\ \frac{\partial \boldsymbol{I}_{mag}}{\partial \boldsymbol{\theta}} & \frac{\partial \boldsymbol{I}_{mag}}{\partial \boldsymbol{V}} \\ \mathbf{0} & \frac{\partial \boldsymbol{V}_{mag}}{\partial \boldsymbol{V}} \end{bmatrix} \tag{3.18}$$

Jacobian matrix *H* components for real power injection measurement are,

$$\frac{\partial P_i}{\partial \theta_i} = \sum_{j=1}^{N} |V_i||V_j|(-G_{ij} \sin\theta_{ij} + B_{ij} \cos\theta_{ij}) - |V_i|^2 B_{ii} \tag{3.19}$$

$$\frac{\partial P_i}{\partial \theta_j} = |V_i||V_j|(G_{ij}\sin\theta_{ij} - B_{ij}\cos\theta_{ij}) \tag{3.20}$$

$$\frac{\partial P_i}{\partial |V_i|} = \sum_{j=1}^{N} |V_j|(G_{ij}\cos\theta_{ij} + B_{ij}\sin\theta_{ij}) - |V_i|^2 G_{ii} \tag{3.21}$$

$$\frac{\partial P_i}{\partial |V_j|} = |V_i|(G_{ij}\cos\theta_{ij} + B_{ij}\sin\theta_{ij}) \tag{3.22}$$

Jacobian matrix *H* components for reactive power injection measurement are,

$$\frac{\partial Q_i}{\partial \theta_i} = \sum_{j=1}^{N} |V_i||V_j|(G_{ij}\cos\theta_{ij} + B_{ij}\sin\theta_{ij}) - |V_i|^2 G_{ii} \tag{3.23}$$

$$\frac{\partial Q_i}{\partial \theta_j} = |V_i||V_j|(-G_{ij}\sin\theta_{ij} - B_{ij}\cos\theta_{ij}) \tag{3.24}$$

$$\frac{\partial Q_i}{\partial |V_i|} = \sum_{j=1}^{N} |V_j|(G_{ij}\sin\theta_{ij} - B_{ij}\cos\theta_{ij}) - |V_i|^2 B_{ii} \tag{3.25}$$

$$\frac{\partial Q_i}{\partial |V_j|} = |V_i|(G_{ij}\sin\theta_{ij} - B_{ij}\cos\theta_{ij}) \tag{3.26}$$

Jacobian matrix *H* components for real power flow measurement are,

$$\frac{\partial P_{ij}}{\partial \theta_i} = |V_i||V_j|(g_{ij}\sin\theta_{ij} - b_{ij}\cos\theta_{ij}) \tag{3.27}$$

$$\frac{\partial P_{ij}}{\partial \theta_j} = -|V_i||V_j|(g_{ij}\sin\theta_{ij} - b_{ij}\cos\theta_{ij}) \tag{3.28}$$

$$\frac{\partial P_{ij}}{\partial |V_i|} = -|V_i||V_j|(g_{ij}\cos\theta_{ij} - b_{ij}\sin\theta_{ij}) + 2(g_{ij} + g_{si})|V_i| \tag{3.29}$$

$$\frac{\partial P_{ij}}{\partial |V_j|} = -|V_i|(g_{ij}\cos\theta_{ij} + b_{ij}\sin\theta_{ij}) \tag{3.30}$$

Jacobian matrix *H* components for reactive power flow measurement are,

$$\frac{\partial Q_{ij}}{\partial \theta_i} = -|V_i||V_j|(g_{ij}\cos\theta_{ij} + b_{ij}\sin\theta_{ij}) \tag{3.31}$$

$$\frac{\partial Q_{ij}}{\partial \theta_j} = |V_i||V_j|(g_{ij}\cos\theta_{ij} + b_{ij}\sin\theta_{ij}) \tag{3.32}$$

$$\frac{\partial Q_{ij}}{\partial |V_i|} = -|V_j|(g_{ij}\sin\theta_{ij} - b_{ij}\cos\theta_{ij}) - 2(b_{ij} + b_{si})|V_i| \tag{3.33}$$

$$\frac{\partial Q_{ij}}{\partial |V_j|} = -|V_i|(g_{ij}\sin\theta_{ij} - b_{ij}\cos\theta_{ij}) \tag{3.34}$$

The *H* matrix has rows at each measurement and columns at each variable. If the system is large, the *H* matrix has more zero components. Therefore, usually the sparse matrix technique is used to build this matrix.

3.4 PMUs Algorithm with State Estimation Technique

One PMU can measure not only the voltage phasor, but also the current phasor. Figure 3.3 shows a 4-bus system example which has single PMU at bus 1. It has one voltage phasor measurement and three current phasor measurements, namely $V_1 \angle \theta_1$, $I_1 \angle \delta_1$, $I_2 \angle \delta_2$ and $I_3 \angle \delta_3$

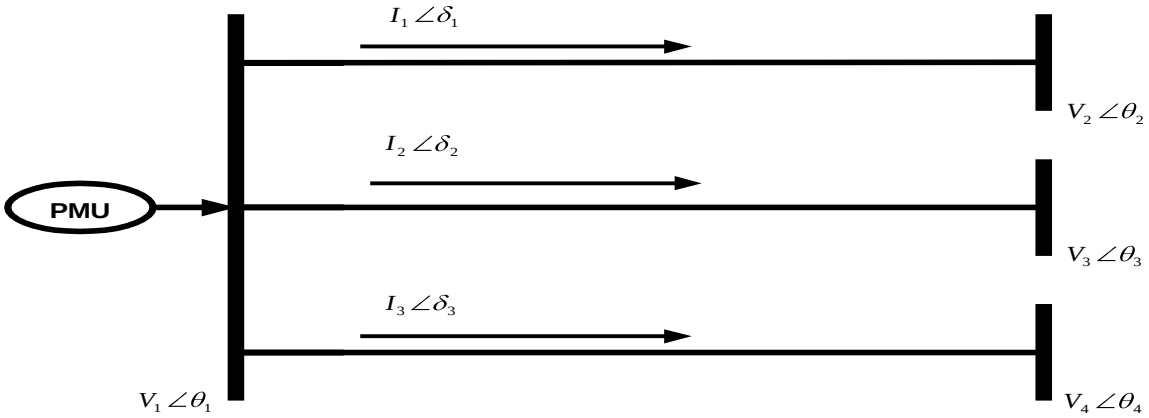

Fig 3.3: Single PMU Measurement Model

If we define *y* as the series admittance and y_{shunt} as the shunt admittance, current phasor measurements can be written in rectangular coordinates as shown in Figure 3.4.

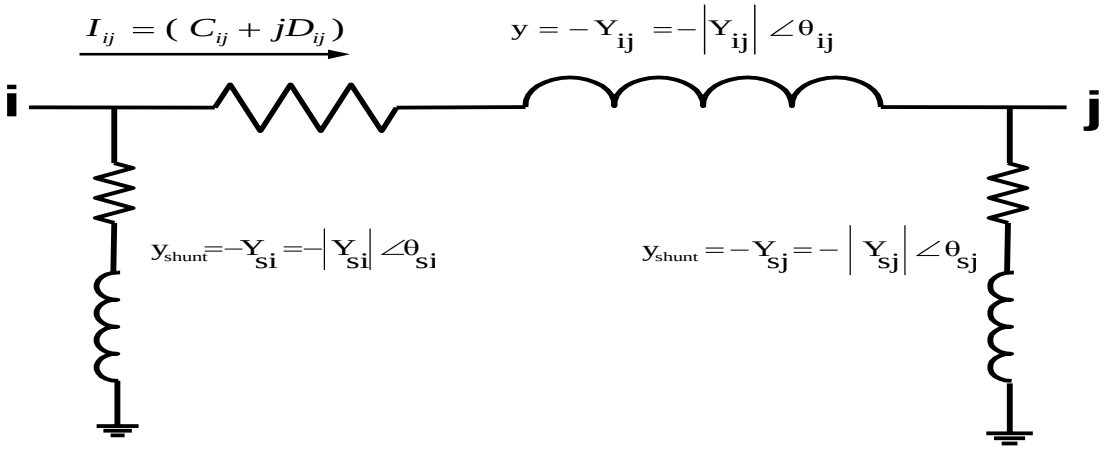

Fig 3.4: Transmission Line Model

The expressions for C_{ij} and D_{ij} are:

$$C_{ij} = |V_i Y_{si}| \cos(\delta_i + \theta_{si}) + |V_j Y_{ij}| \cos(\delta_j + \theta_{ij}) - |V_i Y_{ij}| \cos(\delta_i + \theta_{ij}) \quad (3.35)$$

$$D_{ij} = |V_i Y_{si}| \sin(\delta_i + \theta_{si}) + |V_j Y_{ij}| \sin(\delta_j + \theta_{ij}) - |V_i Y_{ij}| \sin(\delta_i + \theta_{ij}) \quad (3.36)$$

where, the state vector is given as:

$$x = [|V_1| \angle 0^0, |V_2| \angle \delta_2, |V_3| \angle \delta_3 \ldots\ldots |.V_N| \angle \delta_N]^T \quad (3.37)$$

The entries of the measurement Jacobian H corresponding to the real and reactive parts of the current phasor is:

$$\frac{\partial C_{ij}}{\partial V_i} = |Y_{si}| \cos(\delta_i + \theta_{si}) - |Y_{ij}| \cos(\delta_i + \theta_{ij}) \quad (3.38)$$

$$\frac{\partial C_{ij}}{\partial V_j} = |Y_{ij}| \cos(\delta_j + \theta_{ij}) \quad (3.39)$$

$$\frac{\partial C_{ij}}{\partial \delta_i} = -|V_i Y_{si}| \sin(\delta_i + \theta_{si}) + |V_i Y_{ij}| \sin(\delta_i + \theta_{ij}) \quad (3.40)$$

$$\frac{\partial C_{ij}}{\partial \delta_j} = -|V_j Y_{ij}| \sin(\delta_j + \theta_{ij}) \quad (3.41)$$

$$\frac{\partial D_{ij}}{\partial V_i} = |Y_{si}|\sin(\delta_i + \theta_{si}) - |Y_{ij}|\sin(\delta_i + \theta_{ij}) \tag{3.42}$$

$$\frac{\partial D_{ij}}{\partial V_j} = |Y_{ij}|\sin(\delta_j + \theta_{ij}) \tag{3.43}$$

$$\frac{\partial D_{ij}}{\partial \delta_i} = |V_i Y_{si}|\cos(\delta_i + \theta_{si}) - |V_i Y_{ij}|\cos(\delta_i + \theta_{ij}) \tag{3.44}$$

$$\frac{\partial D_{ij}}{\partial \delta_j} = |V_j Y_{ij}|\cos(\delta_j + \theta_{ij}) \tag{3.45}$$

The measurement vector *z* contains δ, C_{ij}, D_{ij} as well as the power injections, power flows and voltage magnitude measurements.

$$z = [P_{inj}{}^T,\ Q_{inj}{}^T,\ P_{flow}{}^T,\ Q_{flow}{}^T,\ |V|^T,\ \delta^T,\ C_{ij}{}^T,\ D_{ij}{}^T]^T \tag{3.46}$$

Generally, measurements obtained from PMUs are more precise with small variances as compared to the variances obtained from conventional measurements. Therefore, measurements done with the help of PMU are expected to generate more accurate result as estimated by conventional methods.

CHAPTER - 4

LINEAR FORMULATION OF STATE ESTIMATION USING PMUs

4.1 Introduction

One phasor measurement unit can measure a synchronized voltage phasor and several synchronized current phasor. If the measurement set is composed of only voltages and currents which measured by PMUs, then the state estimation can be formulated as a linear problem [Abur and Exposito [2005], Bretas *et al* [2001], Chakrabarti and Albu [2007], Ebrahimian and Baldick [2000], Filho *et al* [2001]]. The state vector and measurement data can be expressed in rectangular coordinate system. The voltage measurement ($V = |V| \angle \theta$) can be expressed as ($V = E + jF$), and the current measurement can be expressed as ($I = C + jD$).

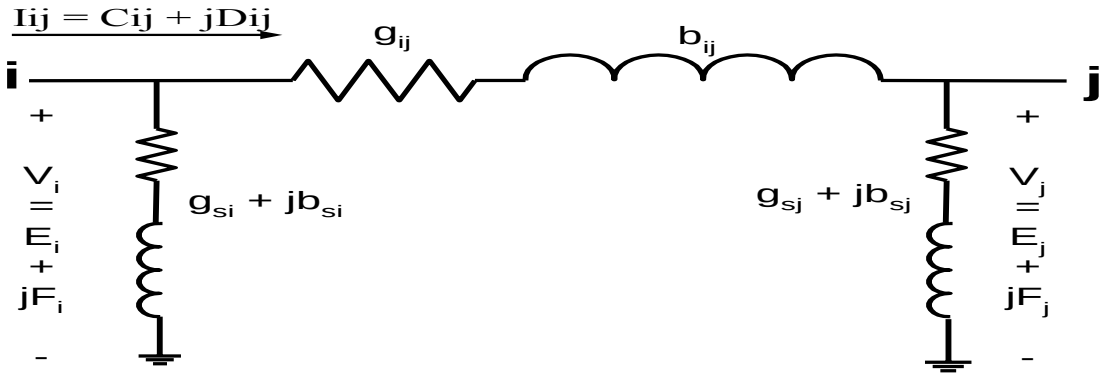

Fig 4.1: Transmission Line Model with Rectangular Form

In the Figure 4.1, ($g_{ij} + jb_{ij}$) is the series admittance of the line and ($g_{si} + jb_{si}$) is the shunt admittance of the transmission line. Line current flow I_{ij} can be expressed as a linear function of voltages.

$$\begin{aligned} I_{ij} &= [(V_i - V_j) \times (g_{ij} + jb_{ij})] + [V_i \times (g_{si} + jb_{si})] \\ &= V_i \times [(g_{ij} + jb_{ij}) + (g_{si} + jb_{si})] - V_j \times (g_{ij} + jb_{ij}) \end{aligned} \quad (4.1)$$

The measurement vector z is expressed as $z = h(x) + e$, (where x is a state vector, $h(x)$ is a matrix of the linear equations and e is an error vector). In rectangular coordinates:

$$z = (H_r + jH_m)(E + jF) + e \quad (4.2)$$

where, $H = H_r + jH_m$, $x = E + jF$ and $z = A + jB$.

A and B are expressed by:

$$A = H_r \times E - H_m \times F \tag{4.3}$$

$$B = H_m \times E + H_r \times F \tag{4.4}$$

In matrix form,

$$\begin{bmatrix} A \\ B \end{bmatrix} = \begin{bmatrix} H_r & -H_m \\ -H_m & H_r \end{bmatrix} \begin{bmatrix} E \\ F \end{bmatrix} + e \tag{4.5}$$

Then, the estimated value $\hat{x} = \hat{E} + j\hat{F}$ can be obtained by solving the linear equation below:

$$\Delta\hat{x} = (H^T R^{-1} H)^{-1} H^T R^{-1} \Delta z = G^{-1} H^T R^{-1} \Delta z \tag{4.6}$$

If we define the linear matrix H_{new} as $H_{new} = \begin{bmatrix} H_r & -H_m \\ -H_m & H_r \end{bmatrix}$, then the above equation can be rewritten as: $\hat{x} = \begin{bmatrix} \hat{E} \\ \hat{F} \end{bmatrix} = (H_{new}{}^T R^{-1} H_{new})^{-1} H_{new}{}^T R^{-1} \begin{bmatrix} A \\ B \end{bmatrix}$ (4.7)

Therefore, the equation for rectangular formed variable $\hat{x}$ can be given by the rectangular forms of H matrix and z vector. They are all real numbers.

4.2 Algorithm for Linear State Estimation

Consider the two bus system shown in Figure 4.2. Note that PMU located at bus 1 measures voltage V_1 and line current I_{12} [Huang and Lei [2002], Jiang *et al* [2007], Jiang *and* Vittal [2006] Madtharad *et a*l [2005], Phadke [2009], Xu and Abur [2004]]. According to (3.1), the line current flow I_{12} can be expressed as:

$$I_{12} = k_1 \times V + k_2 \times V \text{ (k_1, k_2 are constant complex value)} \tag{4.8}$$

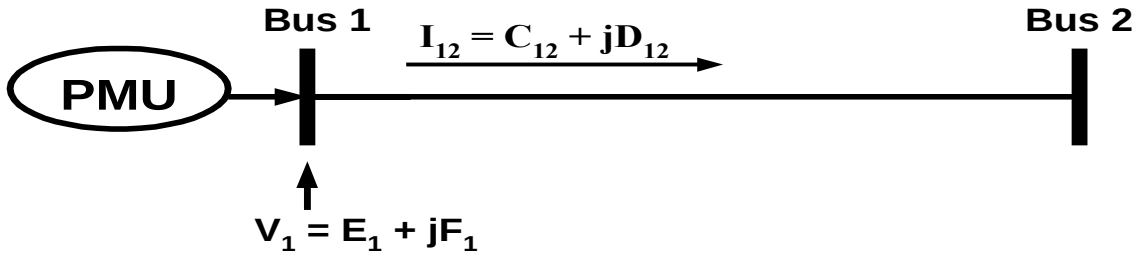

Fig 4.2: Two Bus Systems with Measurements

Measurement vector *z* has two entries, V_1 and I_{12}.

$$z = \begin{bmatrix} V_1 \\ I_{12} \end{bmatrix} = \begin{bmatrix} 1 & 0 \\ k_1 & k_2 \end{bmatrix} \begin{bmatrix} E \\ F \end{bmatrix} + e \tag{4.9}$$

Expressing (3.8) in rectangular coordinates:

$$\begin{bmatrix} 1 & 0 \\ k_1 & k_2 \end{bmatrix} = \begin{bmatrix} 1 & 0 \\ k_{r1} + jk_{m1} & k_{r2} + jk_{m2} \end{bmatrix}$$
$$= \begin{bmatrix} 1 & 0 \\ k_{r1} & k_{r2} \end{bmatrix} + j \begin{bmatrix} 0 & 0 \\ k_{m1} & k_{m2} \end{bmatrix} = H_r + jH_m \tag{4.10}$$

where,

$$V_1 = E_1 + jF_1, \quad I_{12} = C_{12} + jD_{12}$$
$$k_1 = k_{r1} + jk_{m1}, \quad k_2 = k_{r2} + jk_{m2} \tag{4.11}$$

The measurement vector *z* becomes,

$$z = \begin{bmatrix} E_1 \\ C_{12} \\ F_1 \\ D_{12} \end{bmatrix} = \begin{bmatrix} 1 & 0 & 0 & 0 \\ k_{r1} & k_{r2} & -k_{m1} & -k_{m2} \\ 0 & 0 & 1 & 0 \\ k_{m1} & k_{m2} & k_{r1} & k_{r2} \end{bmatrix} \begin{bmatrix} E_1 \\ E_2 \\ F_1 \\ F_2 \end{bmatrix} + e \tag{4.12}$$

Finally, $\hat{x}$ is calculated using (3.6):

$$\hat{x} = \begin{bmatrix} \hat{E} \\ \hat{F} \end{bmatrix} = \begin{bmatrix} E_1 \\ E_2 \\ F_1 \\ F_2 \end{bmatrix}, \quad z = \begin{bmatrix} A \\ B \end{bmatrix} = \begin{bmatrix} E_1 \\ C_{12} \\ F_1 \\ D_{12} \end{bmatrix} \tag{4.13}$$

This is very simple and fast, because it doesn't need any iteration.

In respect of system accuracy and reliability, PMU can deliver more precise measurement data. Several cases to be tested with different number of PMUs added to the conventional set of measurement. The simulations and analysis of different cases are as shown in Table 4.1 are done with several IEEE bus systems in the next section.

Table 4.1: Measurements with their PMU Cases

Cases	Measurements
1	**Conventional with No PMUs**
2	**Conventional with 1 PMUs**
3	**Conventional with 2 PMUs**
4	**Conventional with 3 PMUs**
5	**Conventional with 4 PMUs**
6	**Conventional with 5 PMUs**
7	**Conventional with 6 PMUs**
8	**Conventional with 7 PMUs**
9	**Conventional with 8 PMUs**
P	**Only PMUs**

4.3 Simulation Results

Four different IEEE test systems (IEEE 6, IEEE 9, IEEE 14 & IEEE 30 bus system) are used for the simulations [Kezunovic *et al* [2004], Madtharad *et al* [2005], Magnago and Abur [2000], Nwohu [2010], Phadke *et al* [2009], Sangrody *et al* [2009]. The Gaussian random errors are imposed on each measurement. The error variance of measurements is set to be 0.00001. Table 4.2 shows the locations of PMUs at each system. These PMUs are placed as a minimum required number.

Each PMU has one voltage measurement and several current flow measurements connected to the neighboring buses.

Table 4.2: PMU Locations for Each Bus System

Type of System	PMU locations at Bus							
IEEE 6 Bus	Bus 2	-	-	-	-	-	-	-
IEEE 9 Bus	Bus 2	Bus 3	-	-	-	-	-	-
IEEE 14 Bus	Bus 2	Bus 3	Bus 6	Bus 8	Bus 14	-	-	-
IEEE 30 Bus	Bus 2	Bus 5	Bus 8	Bus 11	Bus 13	Bus 19	Bus 23	Bus 30

Network diagrams showing the PMU locations for the test systems are given as

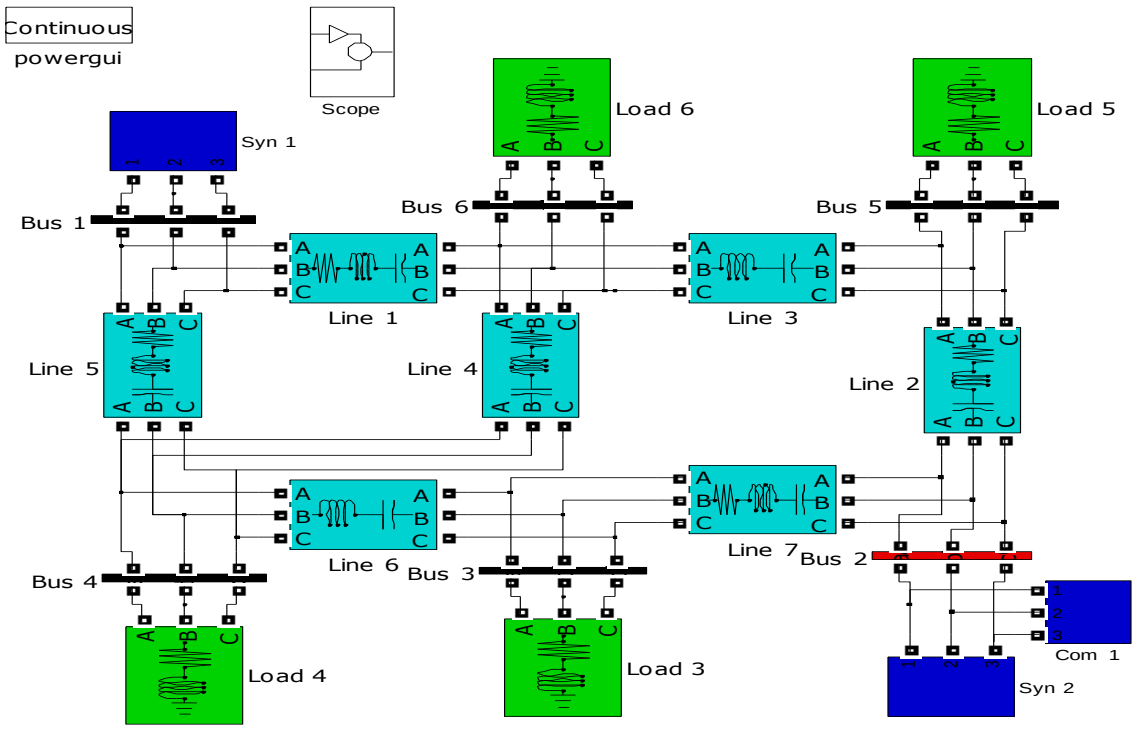

Fig 4.3: IEEE 6 bus system

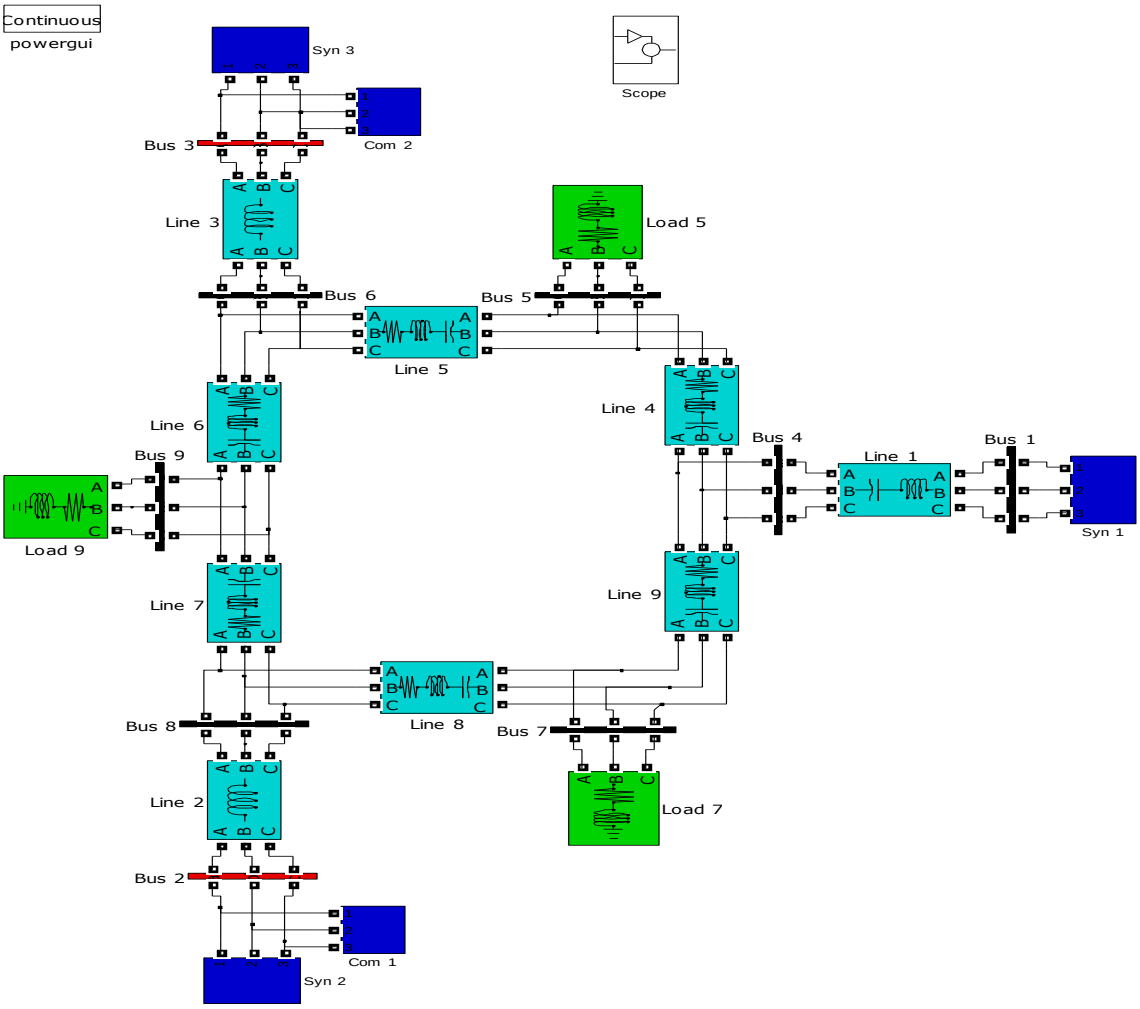

Fig 4.4: IEEE 9 bus system

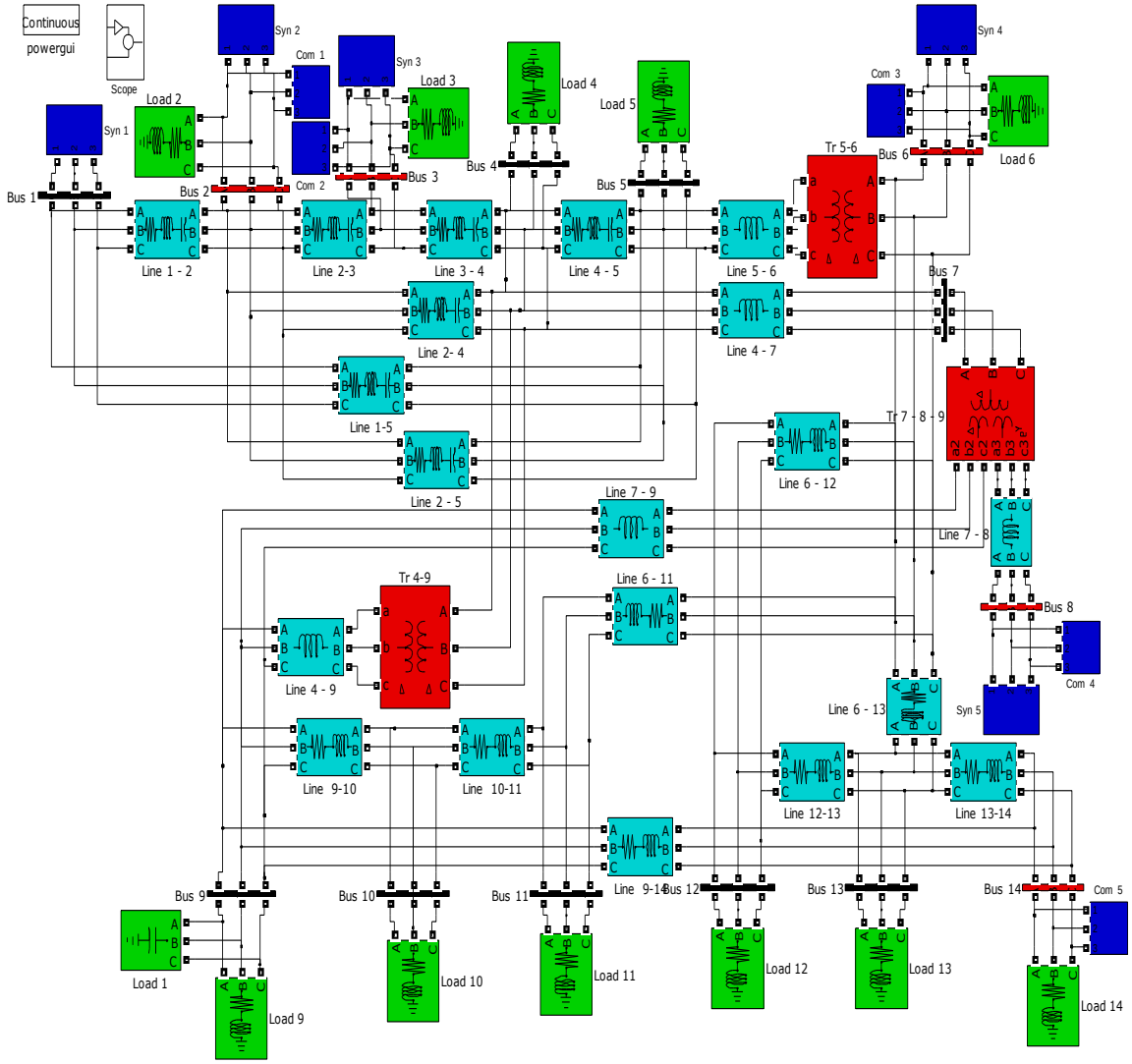

Fig 4.5: IEEE 14 bus system

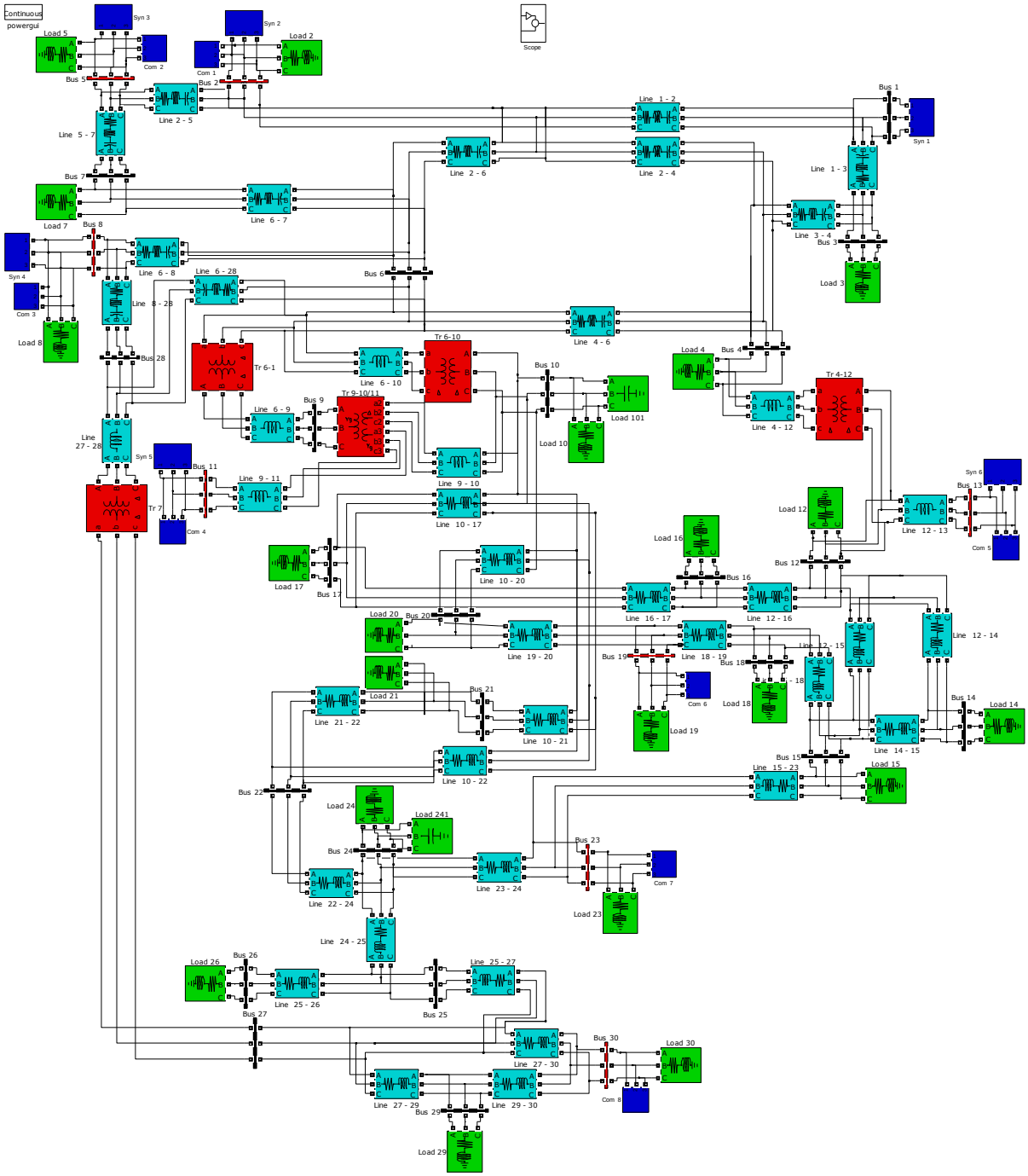

Fig 4.6: IEEE 30 bus system

CHAPTER - 5

BENEFITS OF USING PMUs

5.1 PMU improved Variables Accuracy

In this, the effects of increasing the number of PMUs on the accuracy of the estimated variables are investigated. If some PMU measurements are added to the state estimation, the state estimation accuracy will be affected, as the PMU measurements have less significant error variances compared to other measurements. The PMU has measure

- One voltage phasor
- Several current phasor measurements at any branch connected to the PMU installed bus.
- The real and reactive part of the phasor for each voltage or current.

Firstly, judge estimated variables and then their accuracy as compare to the conventional measured data. One of the ways of representing the level of state estimation accuracy is in refer to the covariance of the estimated variables. From (4.6), the covariance of the estimated variable vector $\hat{x}$ can be expressed as:

$$Cov(\hat{x}) = Cov((H^T R^{-1} H)^{-1} H^T R^{-1} z) = Cov(G^{-1} H^T R^{-1} z) \quad (5.1)$$

The covariance of the measurement vector z is R from:

$$Cov(z) = Cov(h(x) + e) = Cov(e) = R \quad (5.2)$$

Then eq (5.1), can be rewritten as:

$$Cov(\hat{x}) = (G^{-1} H^T R^{-1}) \, Cov(z) \, (G^{-1} H^T R^{-1})^T \quad (5.3)$$

$$= (G^{-1} H^T R^{-1}) \, R \, ((H^T R^{-1} H)^{-1} H^T R^{-1})^T$$

$$= (G^{-1} H^T R^{-1}) \, R \, (H^T R^{-1})^T \, ((H^T R^{-1} H)^{-1})^T$$

$$= (G^{-1} H^T R^{-1}) \, R^{-1} H^{-1} R \, (H^T)^{-1}$$

$$= G^{-1} H^T R^{-1} R (H^T)^{-1}$$

$$= G^{-1}$$

Therefore, the inverse of the gain matrix is equal to the covariance of $\hat{x}$.

In regard of the accuracy of the system, PMU be able to deliver more precise in data measurement. Some cases are tested with different number of additional PMUs to the conventional measurement set Simulations and analysis of different cases which are shown in Table 5.1 are done with several IEEE bus systems in the next section.

5.2 Simulations Results

In this segment, IEEE bus systems as IEEE 6 bus system [Meshram and Sahu [2011], IEEE 9 bus system [Ebrahimpour et al [2011]], IEEE 14 bus system [Fitiwi D.Z. and Rao K.S.R[2009]], [Iyambo, P.K. and Tzoneva, R. [2007]], [Tanti, D.K. *et al* [2011]] and IEEE 30 bus system[Sangrody, H. A. *et al* [2009]] are tested with their respected cases to find out the significance of the PMUs on the precision of the estimated variables. The measured parameters are transformed from abc to dq0 by using Clark Transformation into relevant measured parameter for high accuracy and low harmonic component [APPENDIX A].

Assume *n* as the number of variables, *m* as the number of measurements and ε as the ratio of the number of measurements per the number of variables. During the tests, maintained ε as 1.6. Table 5.1 has more detailed information about the measurement numbers for the tests.

Table 5.1: Type of Variables and Measurement

Types of System	Variables (n)	Measurements				Ratio $\varepsilon = (m/n)$
		Power Injection	Power Flow	Voltage Magnitude	Total (m)	
IEEE 6 Bus	11	6	10	1	17	1.6
IEEE 9 Bus	17	10	16	1	27	1.6
IEEE 14 Bus	27	16	26	1	43	1.6
IEEE 30 Bus	59	38	56	1	95	1.6

For IEEE 6 bus system example, variable number is $n = 6 \times 2 - 1 = 11$ (excluding slack bus angle), and to maintain $\varepsilon = 1.6$ there m must be 17. To place measurement evenly at each system, 40% of injection measurements and 60% of flow measurements are distributed to each system. Therefore, the '6' injection measurement and '10' flow measurement in IEEE 6 bus systems. Lastly one voltage magnitude measurement is placed at each system. The settings for error standard deviations for measurements are shown in Table 5.2. A PMU has much smaller error deviations than other conventional measurements as 0.00000001.

Table 5.2: Standard Deviations of the Measurements for the Test

Voltage Magnitude (Max)	Voltage Magnitude (Min)	Power (Max)	Power (Min)
0.0001	0.00001	0.000001	0.00000001

Figures 5.1 – 5.4 show the network diagrams for each system. The parameters measured are as

- The real and reactive power injection measurements,
- The voltage magnitude measurement.
- The real and reactive power flow measurements.
- The power flow direction.

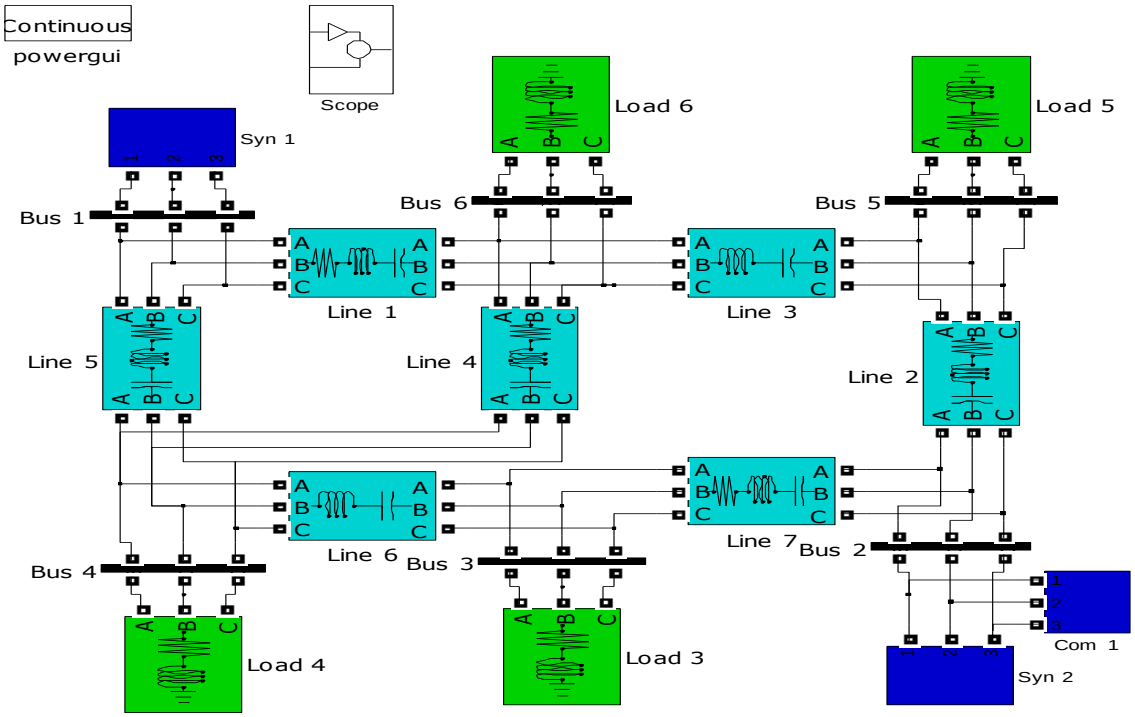

Fig. 5.1: IEEE 6 bus system

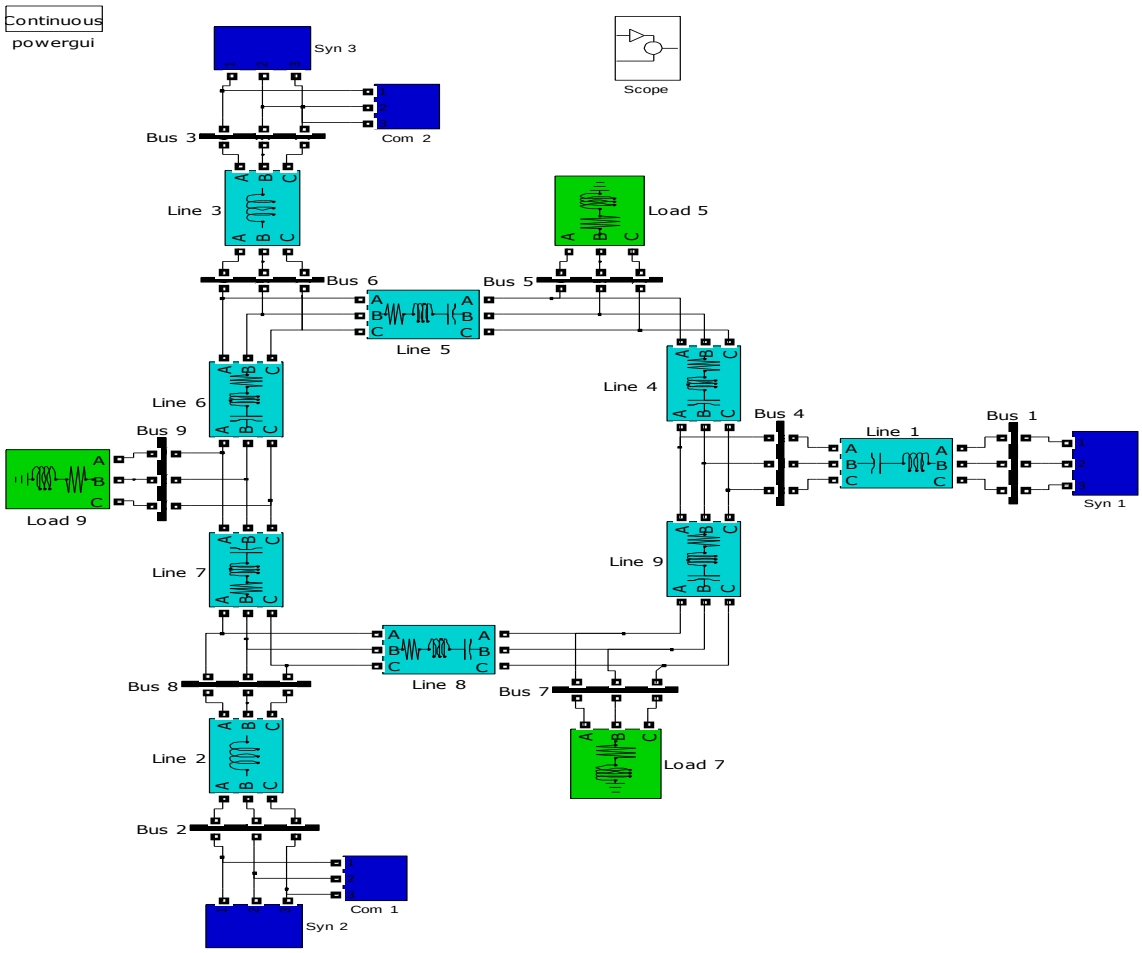

Fig. 5.2: IEEE 9 bus system

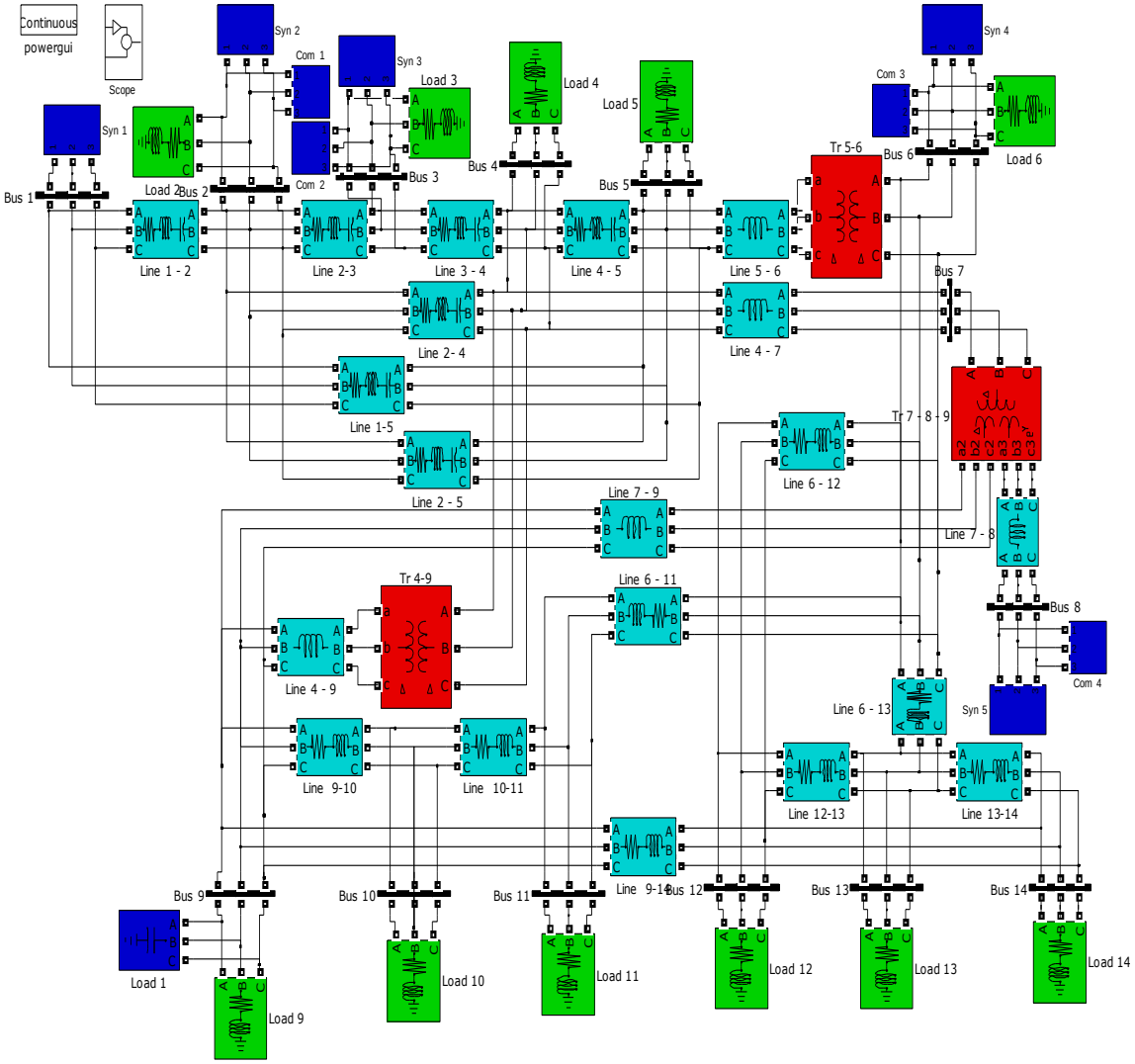

Fig 5.3: IEEE 14 bus system

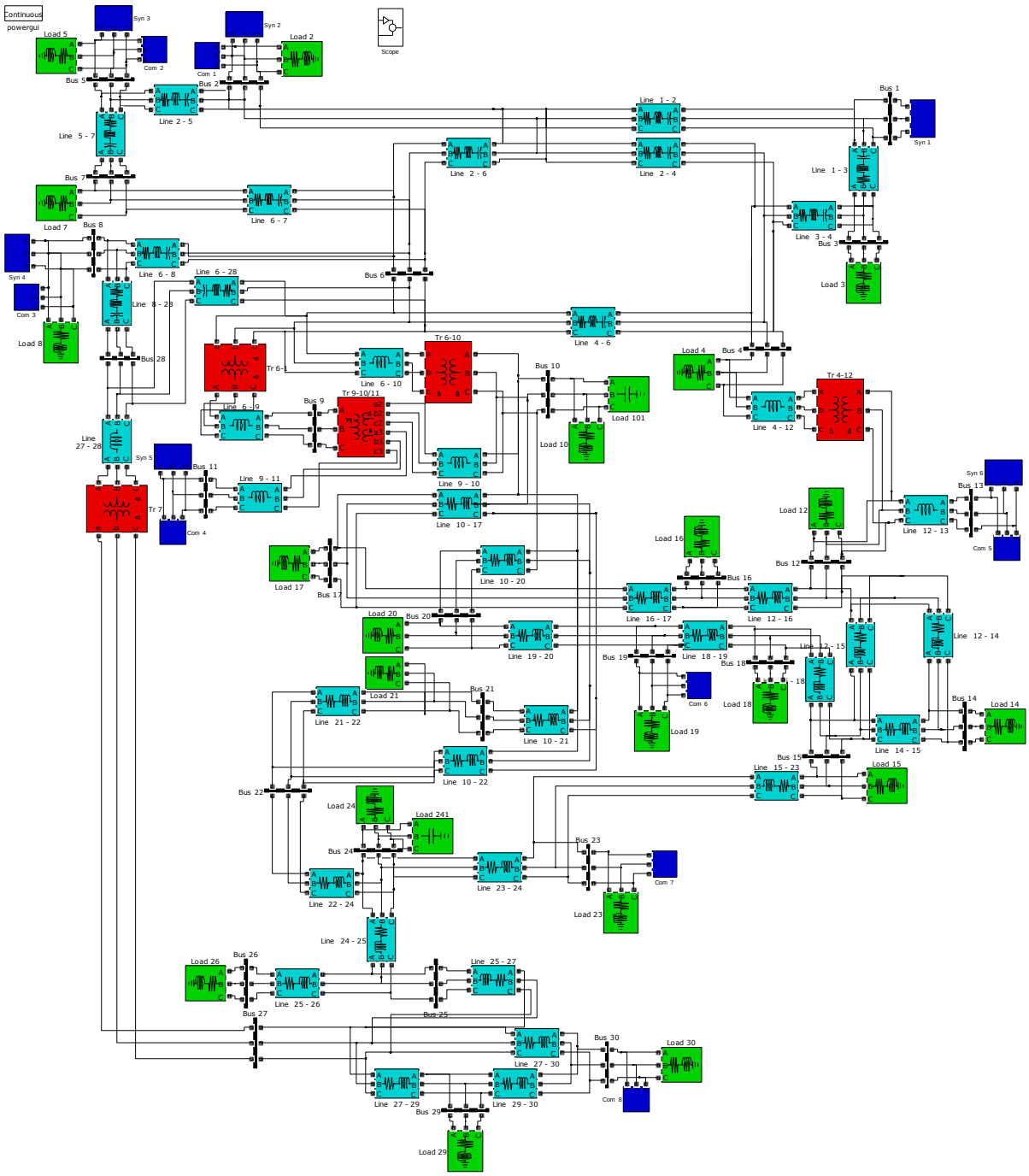

Fig 5.4: IEEE 30 bus system

The accuracy of two variables (voltage magnitude and power (injection or flow)) is investigated separately. The standard deviations of variables are obtained from the inverse diagonal elements of 'G' matrix. The variance is a square of the standard deviation. Figures 5.5 – 5.12 show the accuracy of the estimated voltage (V) magnitudes of each system, Figures 5.13 – 5.20 show the accuracy of the estimated voltage angle (θ) magnitudes of each system, Figures 5.21 – 5.28 show the accuracy of the estimated current (I) magnitudes of each system, Figures 5.29 – 5.36 show the accuracy of the

estimated real power (P) of each system and Figures 5.37 – 5.44 show the accuracy of the estimated reactive power (Q) of each system

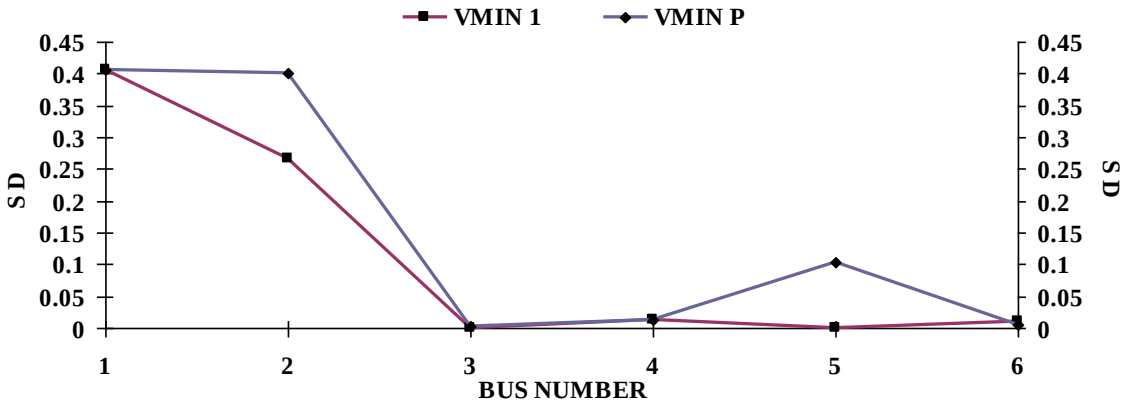

Fig. 5.5 : GRAPH BETWEEN MAG OF V (S D) vs BUS NUMBER

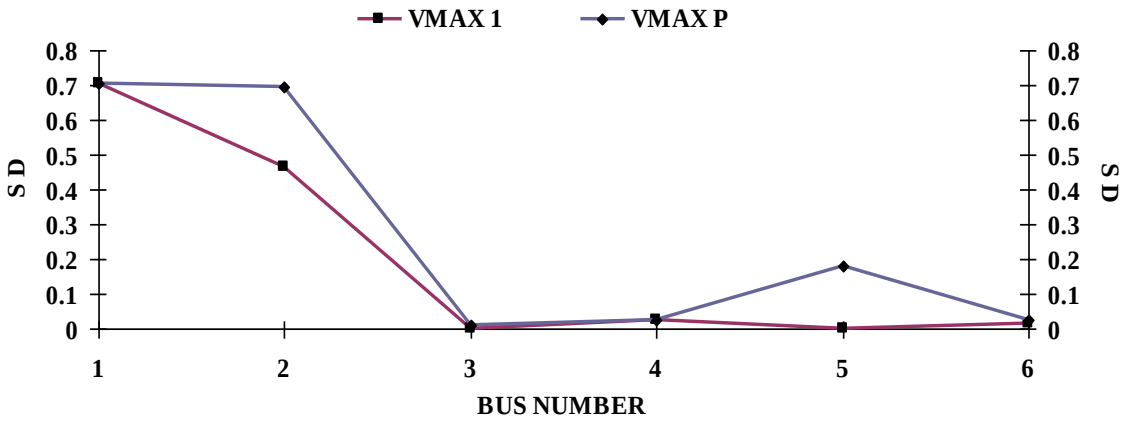

Fig. 5.6 : GRAPH BETWEEN MAG OF V (S D) vs BUS NUMBER

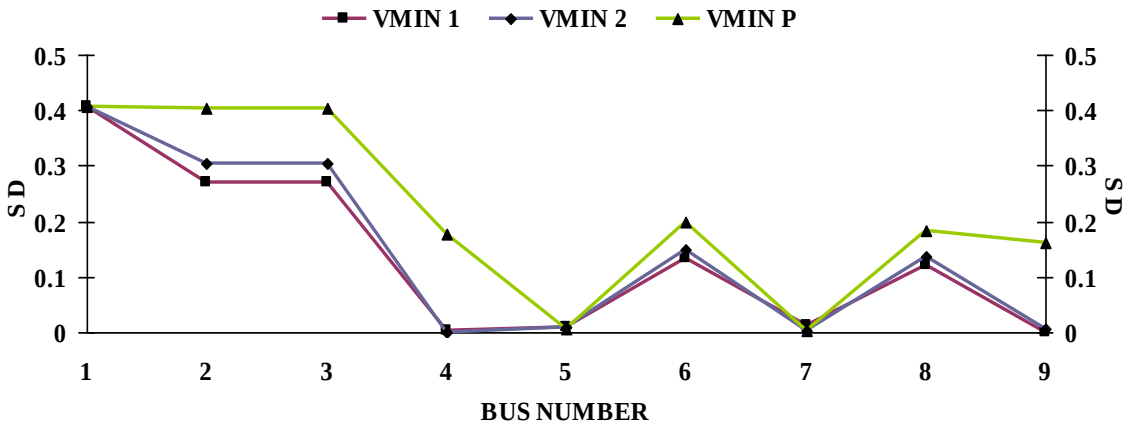

Fig. 5.7 : GRAPH BETWEEN MAG OF V (S D) vs BUS NUMBER

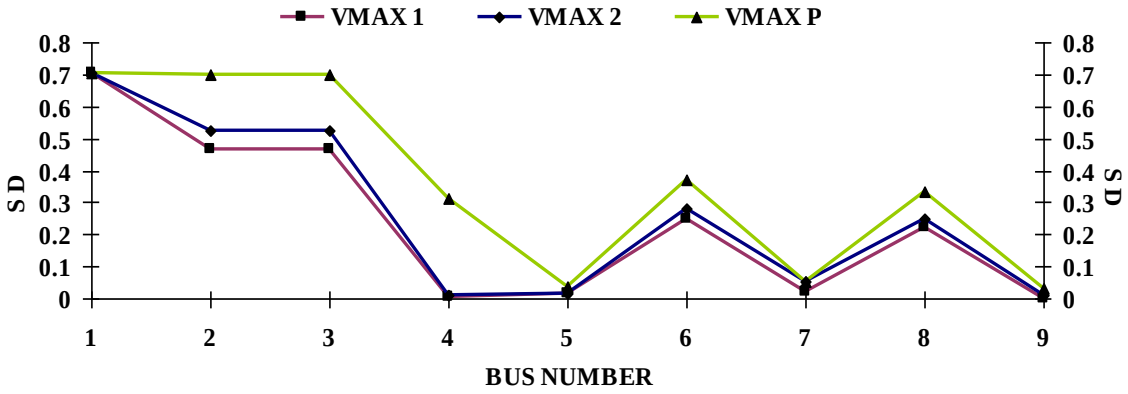

Fig. 5. 8 : GRAPH BETWEEN MAG OF V (S D) vs BUS NUMBER

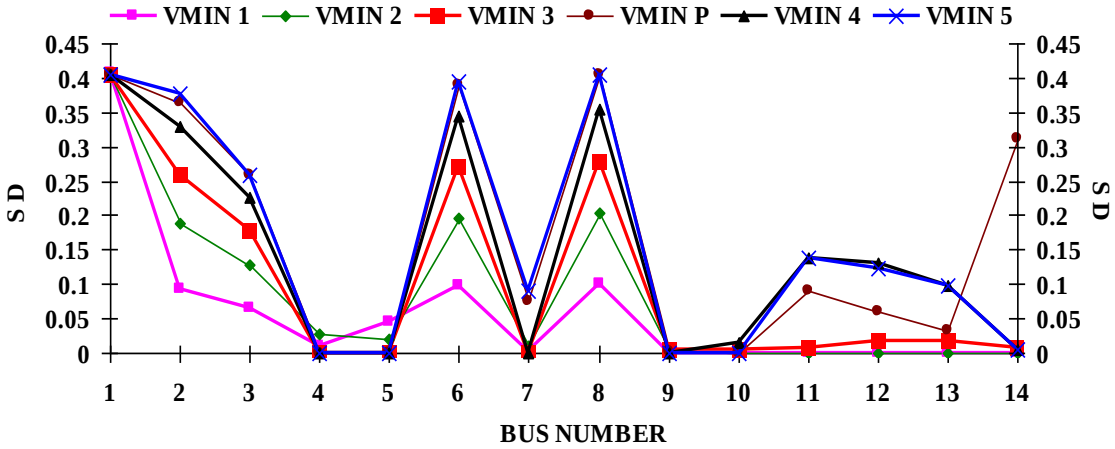

Fig. 5.9 GRAPH BETWEEN MAG OF V (S D) vs BUS NUMBER

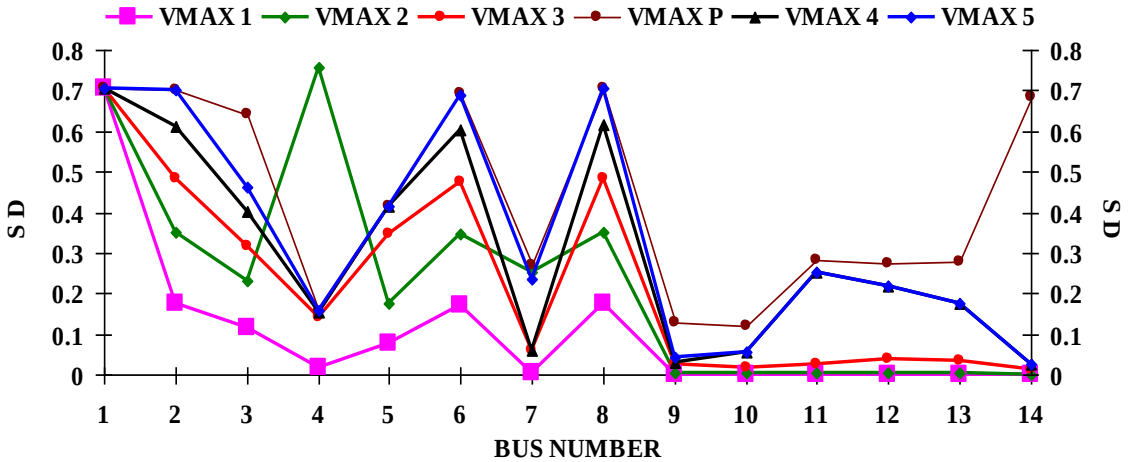

Fig. 5.10 GRAPH BETWEEN MAG OF V (S D) vs BUS NUMBER

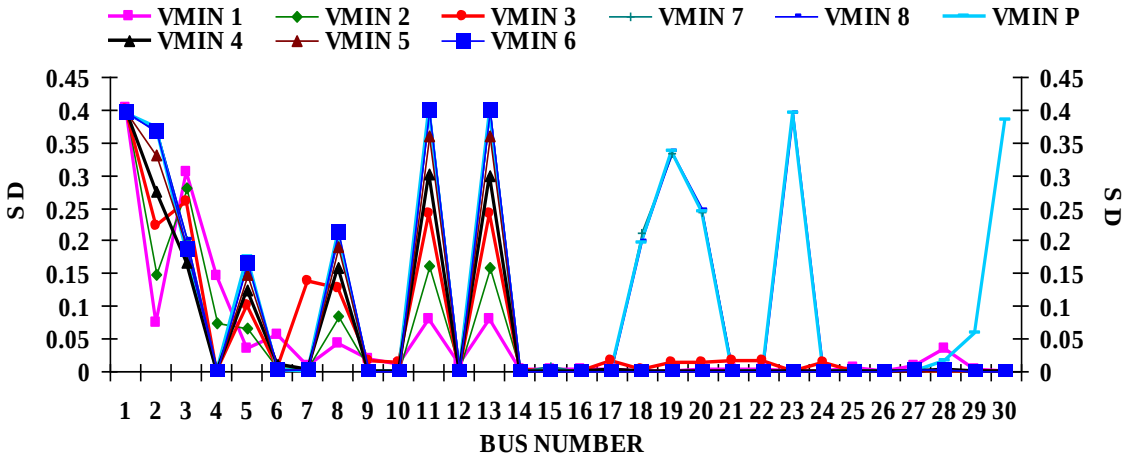

Fig. 5.11 GRAPH BETWEEN MAG OF V (S D) vs BUS NUMBER

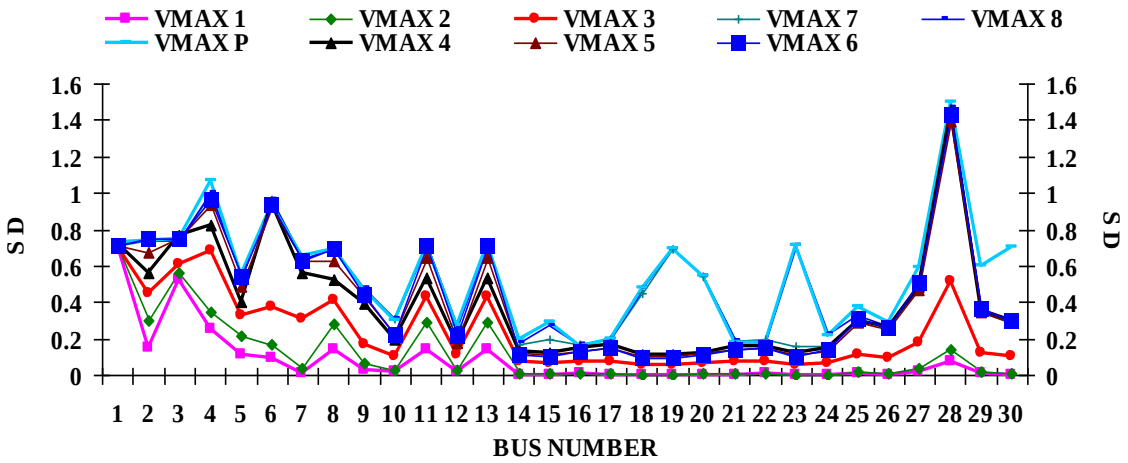

Fig. 5.12 GRAPH BETWEEN MAG OF V (S D) vs BUS NUMBER

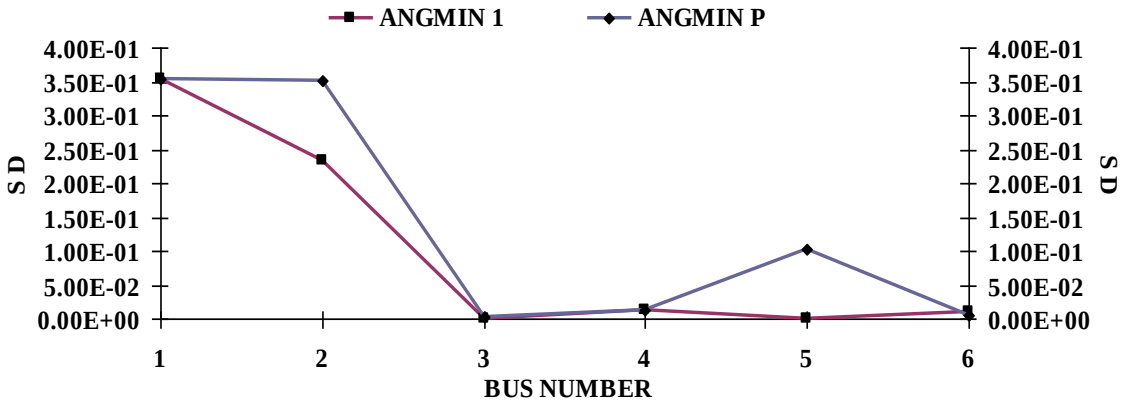

Fig. 5.13 : GRAPH BETWEEN ANGLE (S D) vs BUS NUMBER

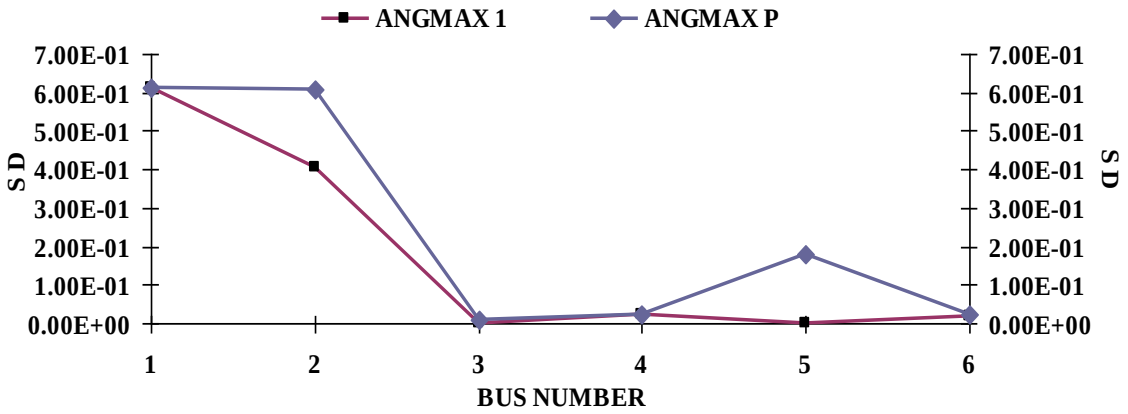

Fig. 5.14 : GRAPH BETWEEN ANGLE (S D) vs BUS NUMBER

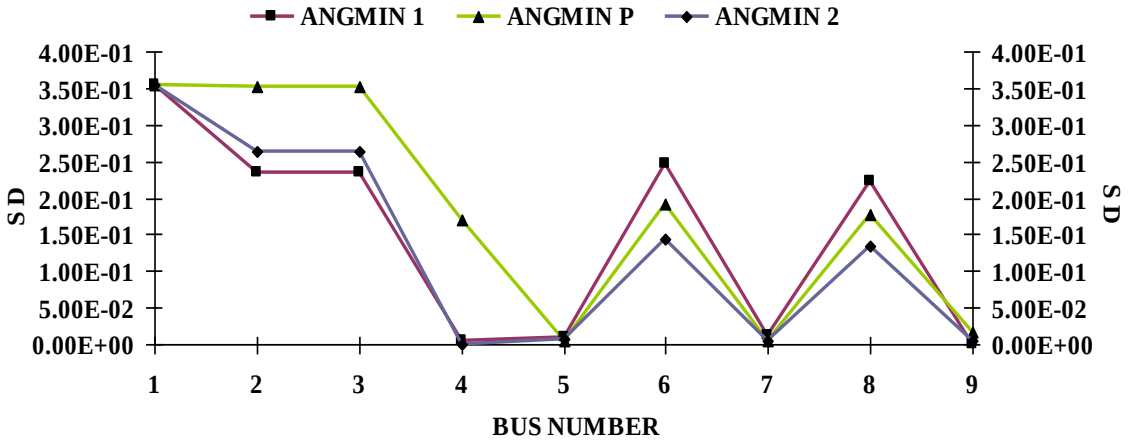

Fig.5.15 : GRAPH BETWEEN ANGLE (S D) vs BUS NUMBER

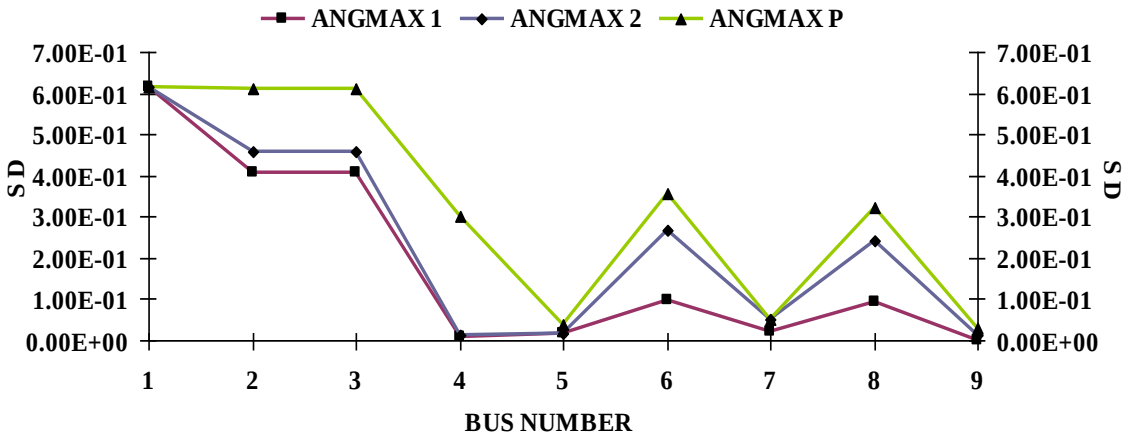

Fig. 5.16 : GRAPH BETWEEN ANGLE (S D) vs BUS NUMBER

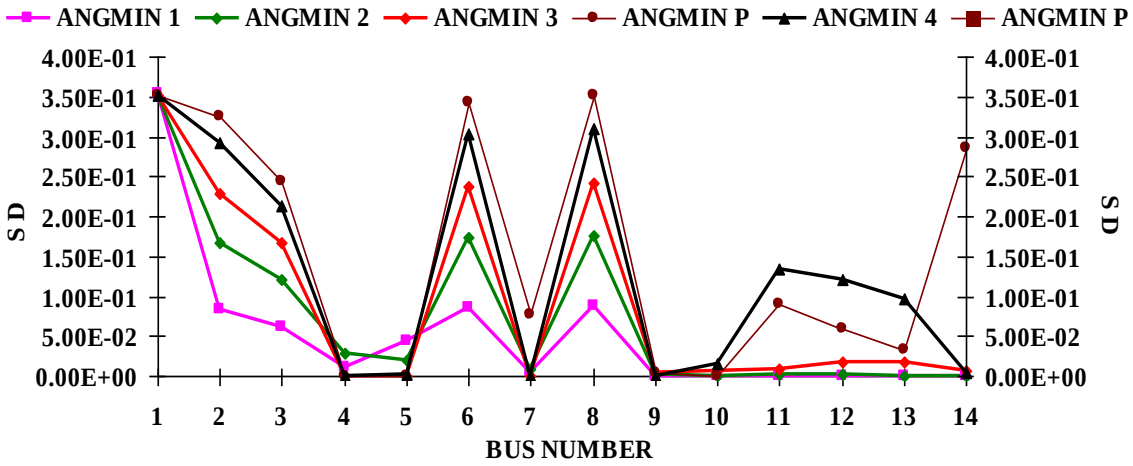

Fig. 5.17 GRAPH BETWEEN ANGLE (S D) vs BUS NUMBER

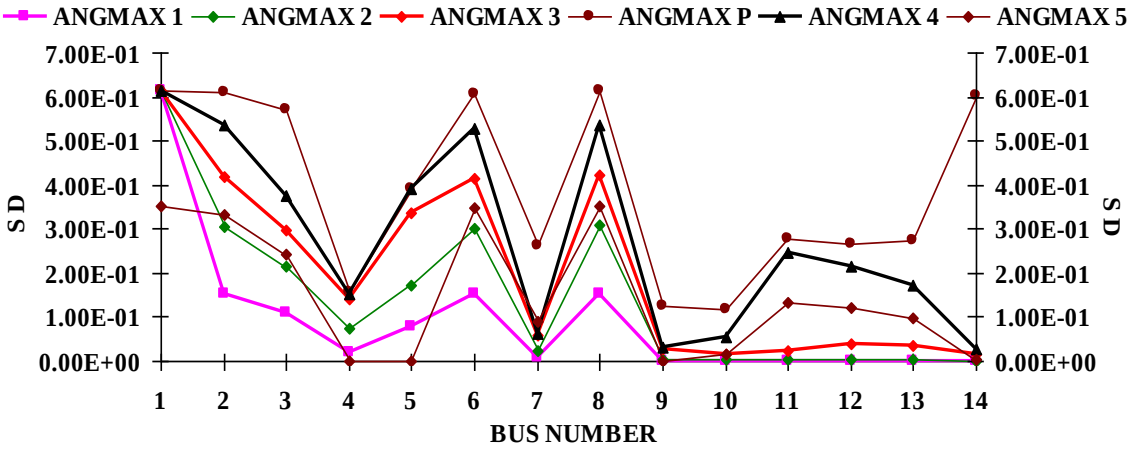

Fig. 5.18 GRAPH BETWEEN ANGLE (S D) vs BUS NUMBER

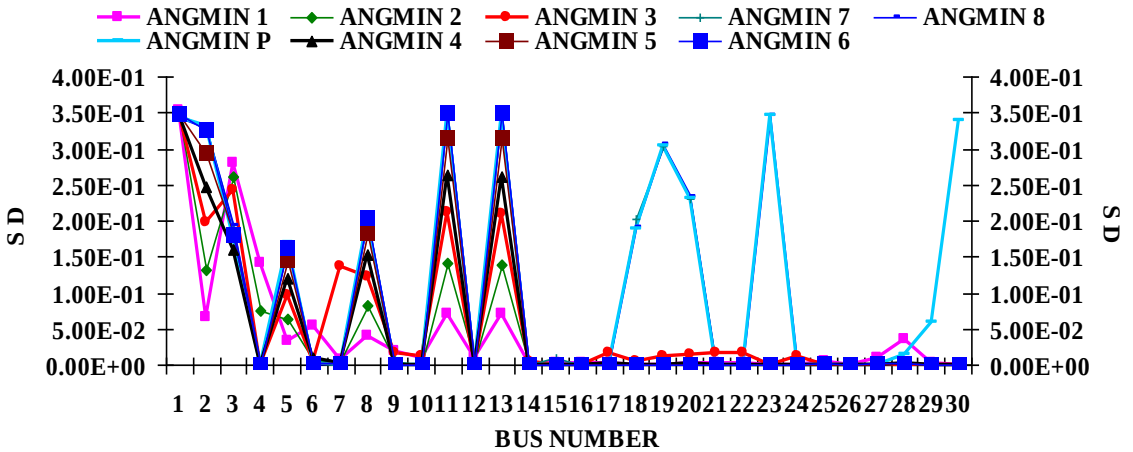

Fig. 5.19 GRAPH BETWEEN ANGLE (S D) vs BUS NUMBER

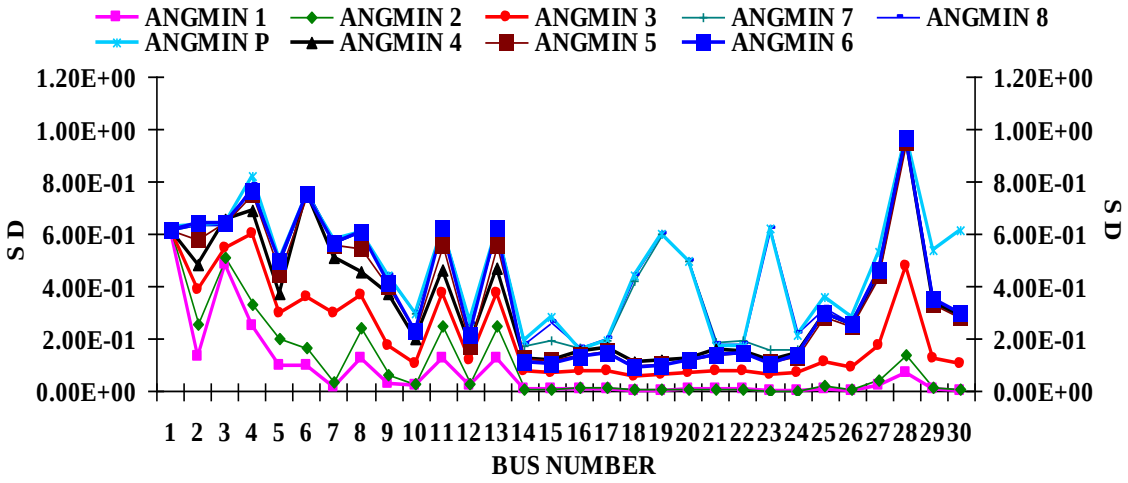

Fig. 5.20 GRAPH BETWEEN ANGLE (S D) vs BUS NUMBER

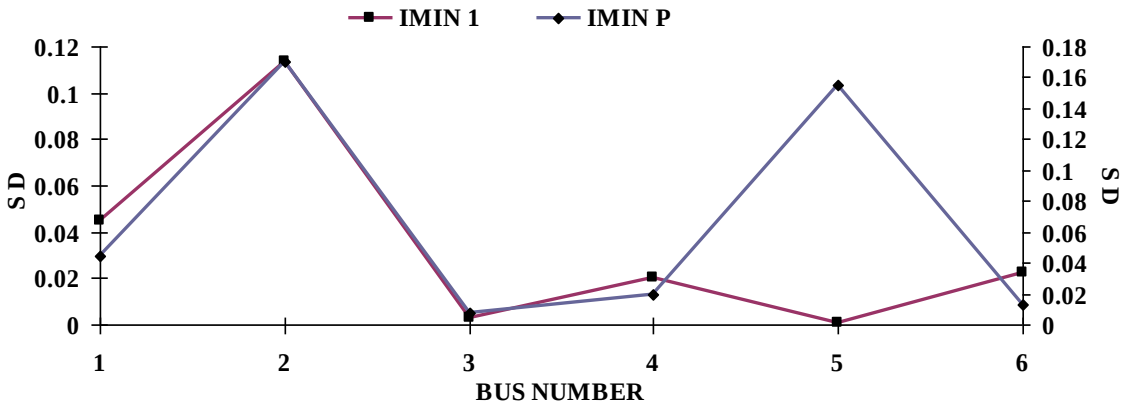

Fig. 5.21 : GRAPH BETWEEN I (S D) vs BUS NUMBER

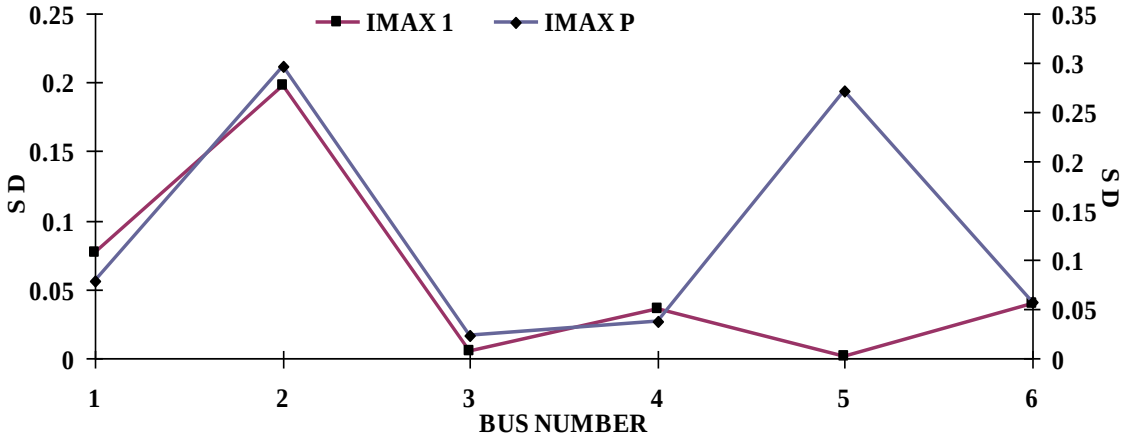

Fig. 5.22 : GRAPH BETWEEN I (S D) vs BUS NUMBER

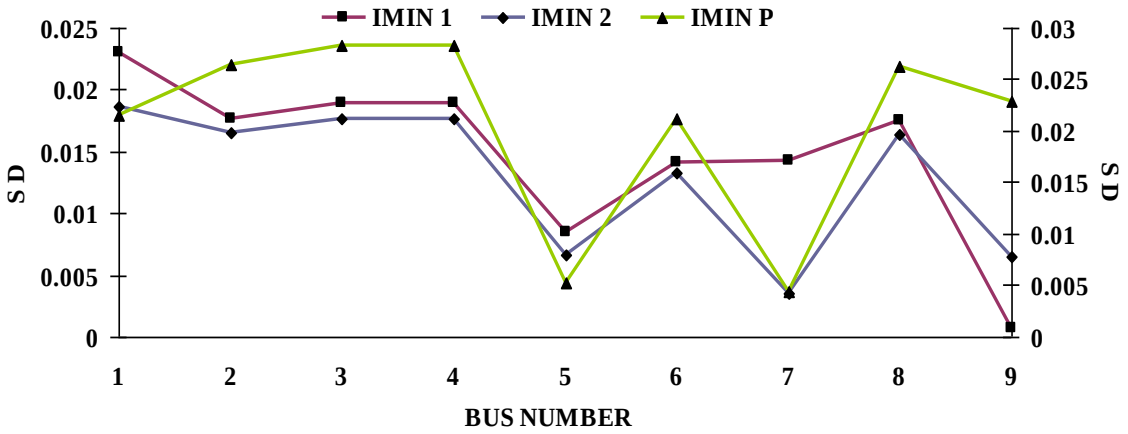

Fig. 5.23 : GRAPH BETWEEN MAG OF I (S D) vs BUS NUMBER

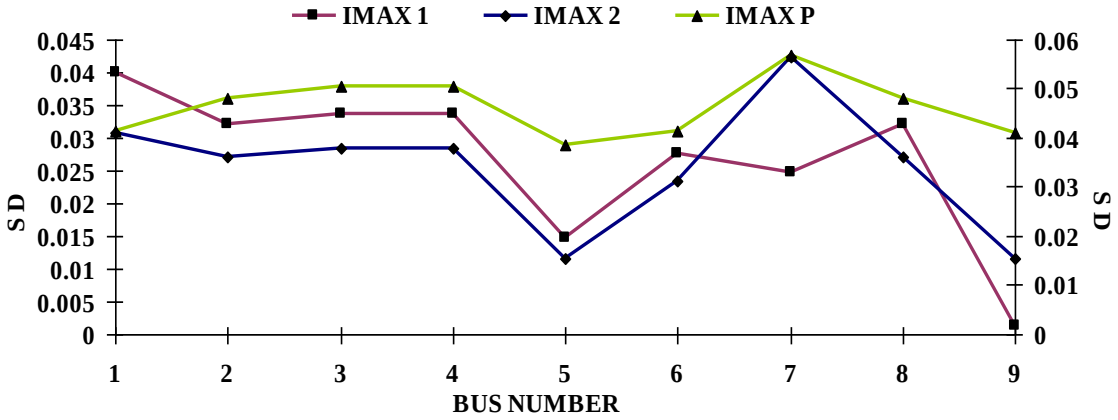

Fig. 5. 24 : GRAPH BETWEEN MAG OF I (S D) vs BUS NUMBER

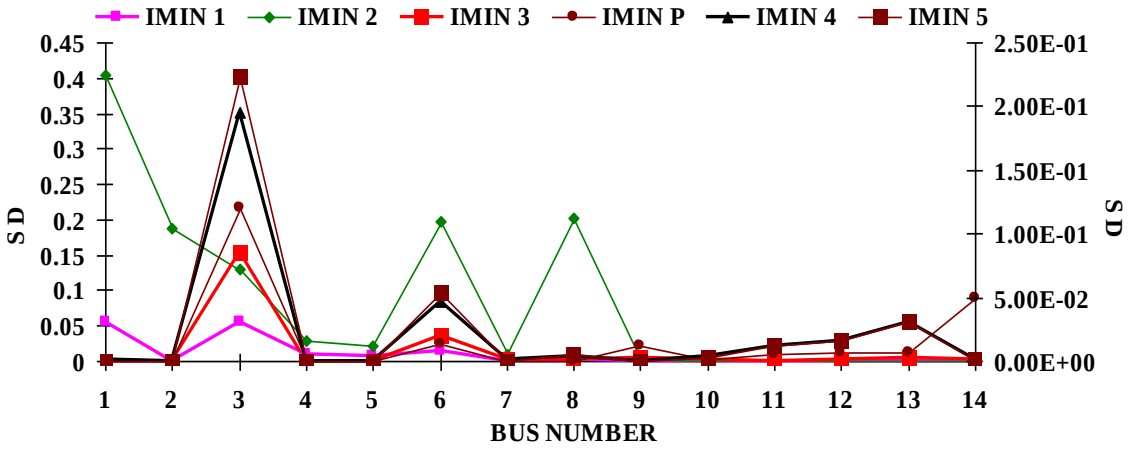

Fig. 5.25 GRAPH BETWEEN MAG OF I (S D) vs BUS NUMBER

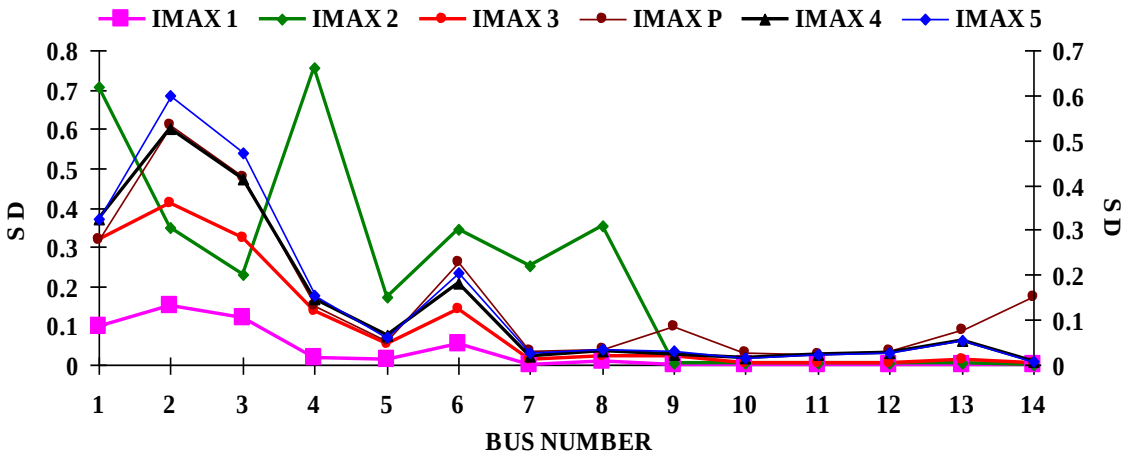

Fig. 5.26 GRAPH BETWEEN MAG OF I (S D) vs BUS NUMBER

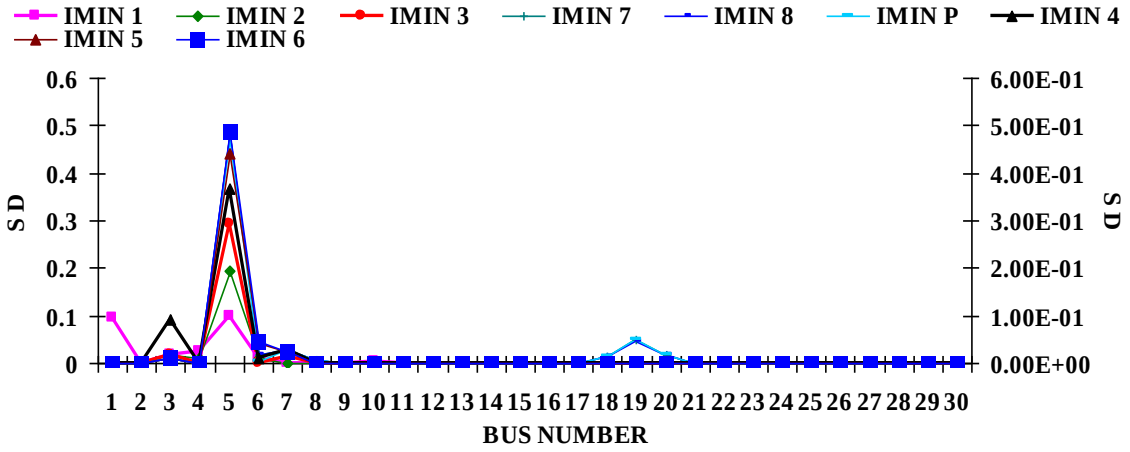

Fig. 5.27 GRAPH BETWEEN MAG OF I (S D) vs BUS NUMBER

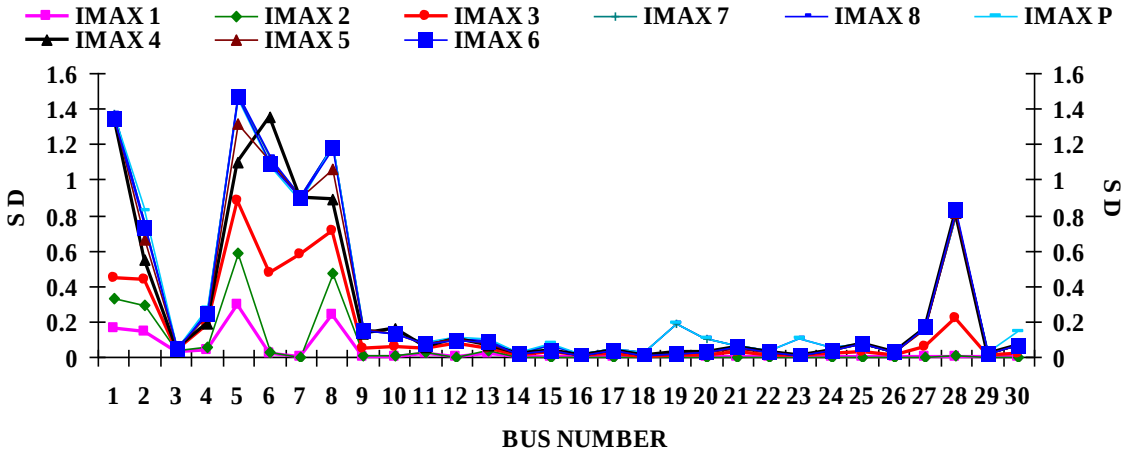

Fig. 5.28 GRAPH BETWEEN MAG OF I (S D) vs BUS NUMBER

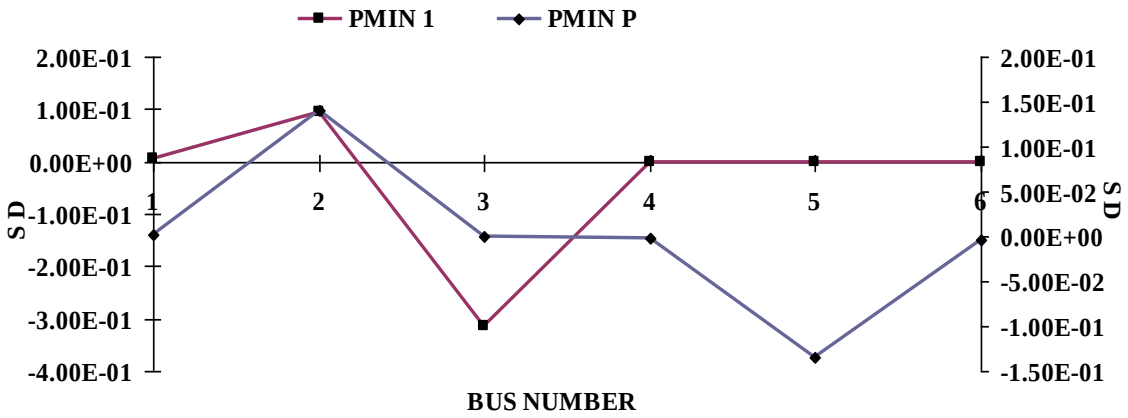

Fig. 5.29 : GRAPH BETWEEN P (S D) vs BUS NUMBER

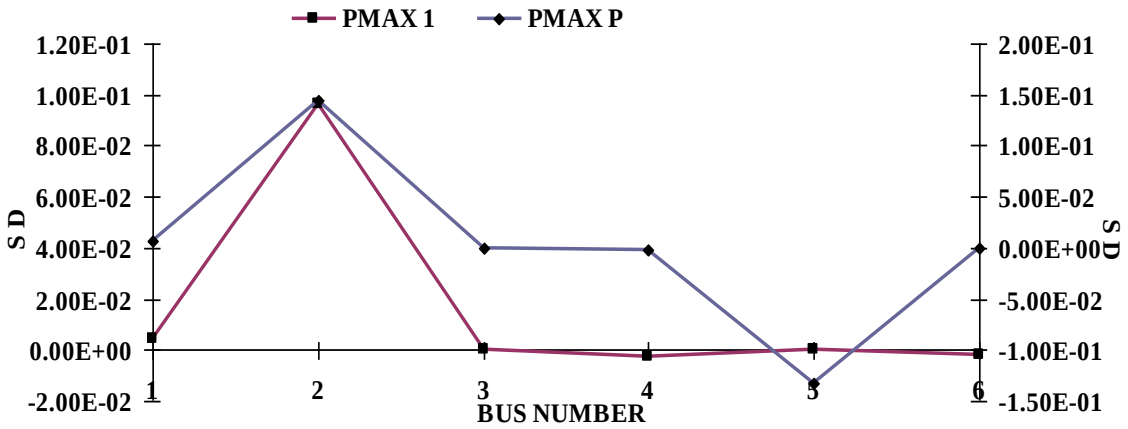

Fig. 5.30 : GRAPH BETWEEN P (S D) vs BUS NUMBER

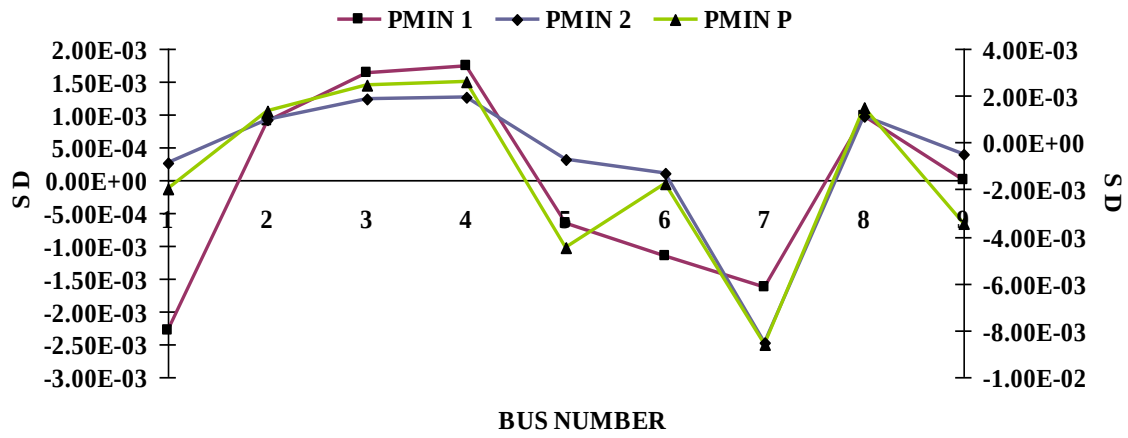

Fig. 5.31 : GRAPH BETWEEN P (S D) vs BUS NUMBER

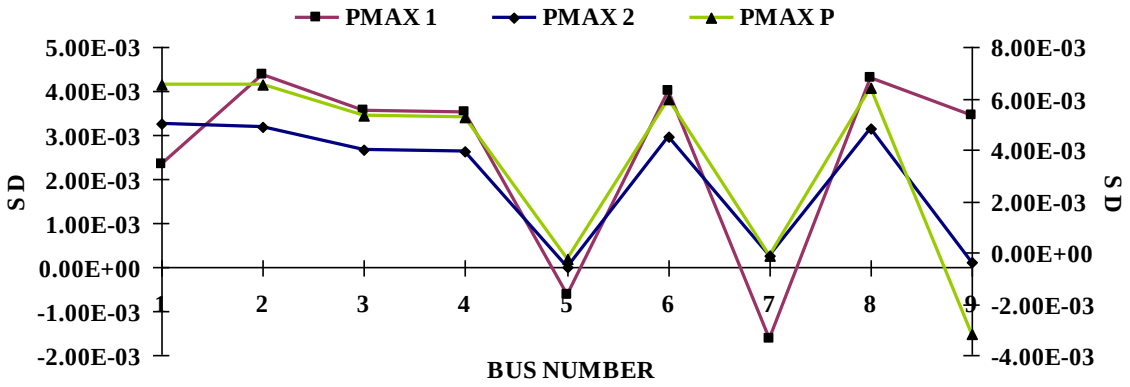

Fig. 5.32 : GRAPH BETWEEN P (S D) vs BUS NUMBER

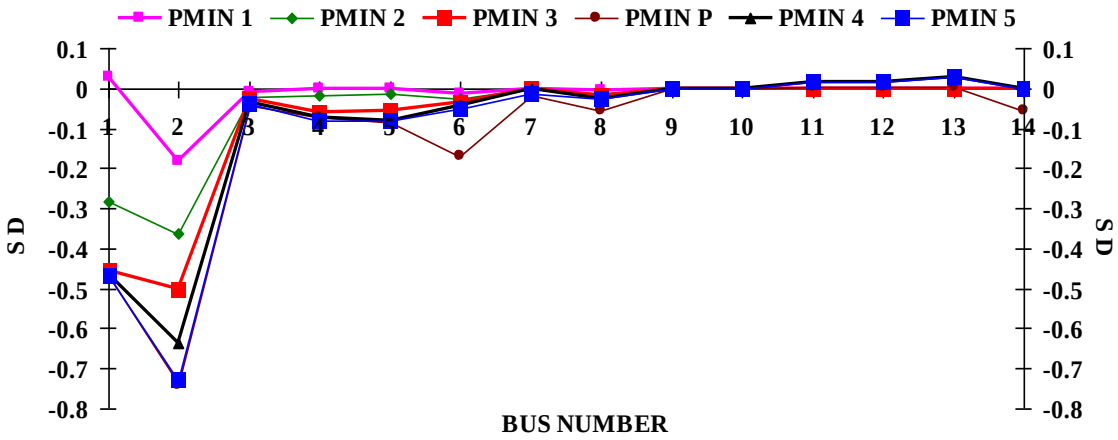

Fig. 5.33 GRAPH BETWEEN P (S D) vs BUS NUMBER

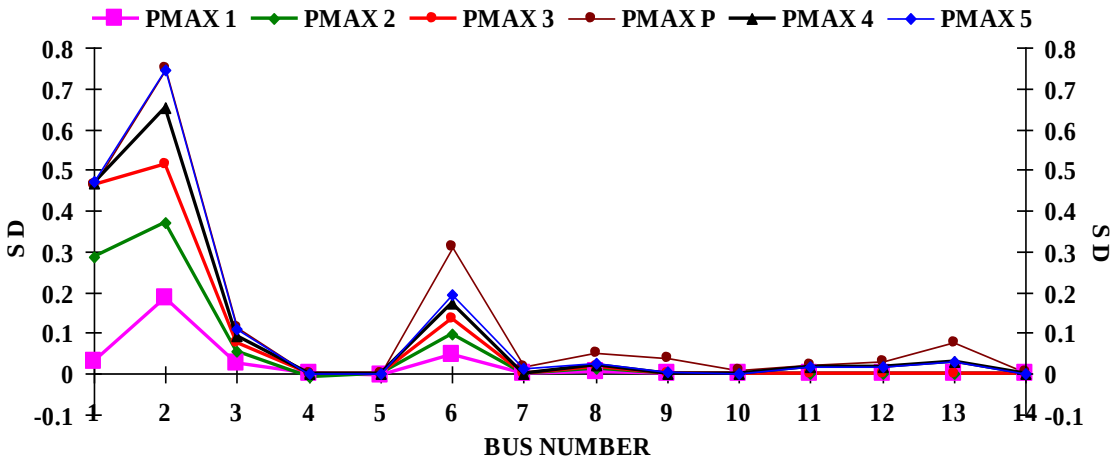

Fig. 5.34 GRAPH BETWEEN P (S D) vs BUS NUMBER

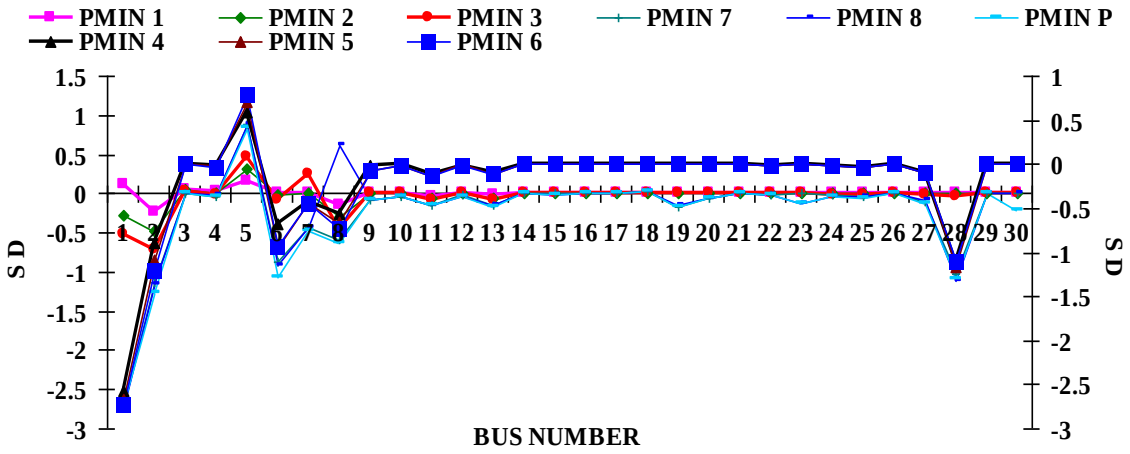

Fig. 5.35 GRAPH BETWEEN P (S D) vs BUS NUMBER

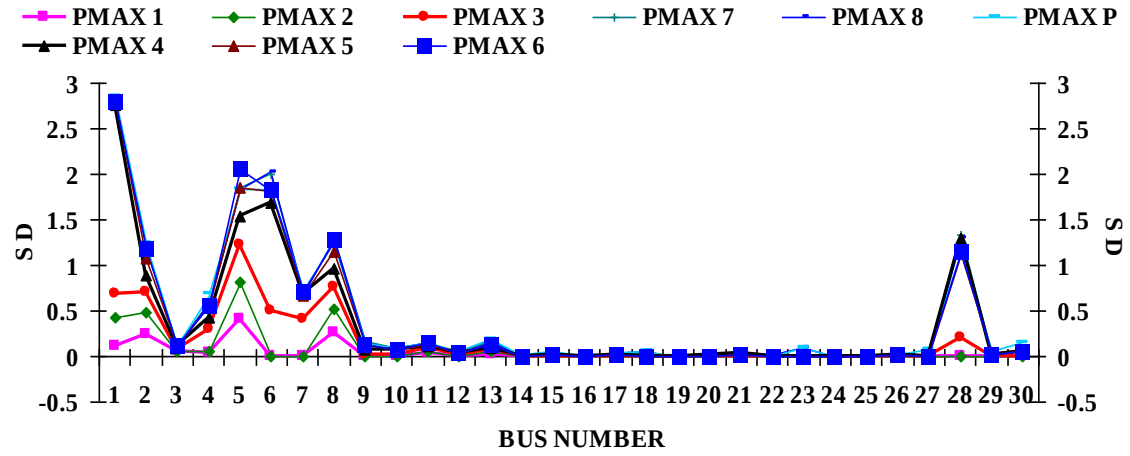

Fig. 5.36 GRAPH BETWEEN P (S D) vs BUS NUMBER

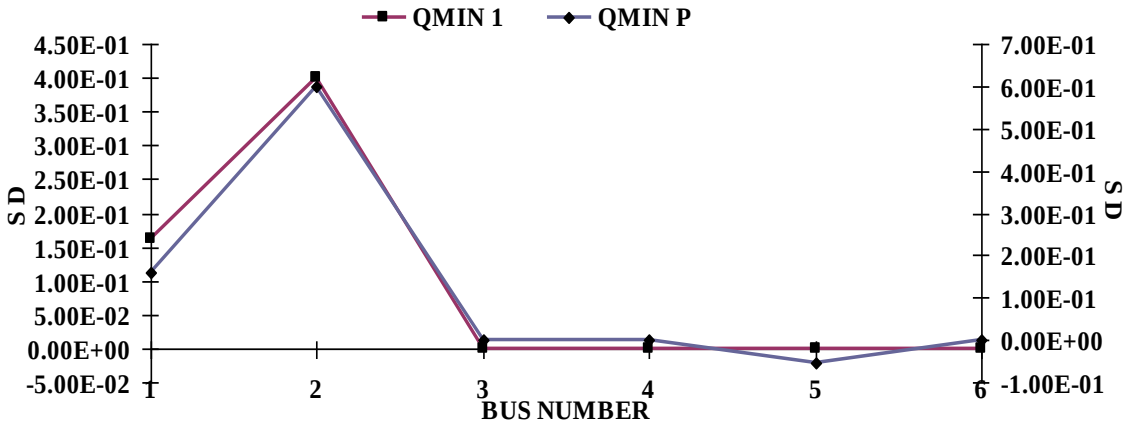

Fig. 5.37 : GRAPH BETWEEN Q (S D) vs BUS NUMBER

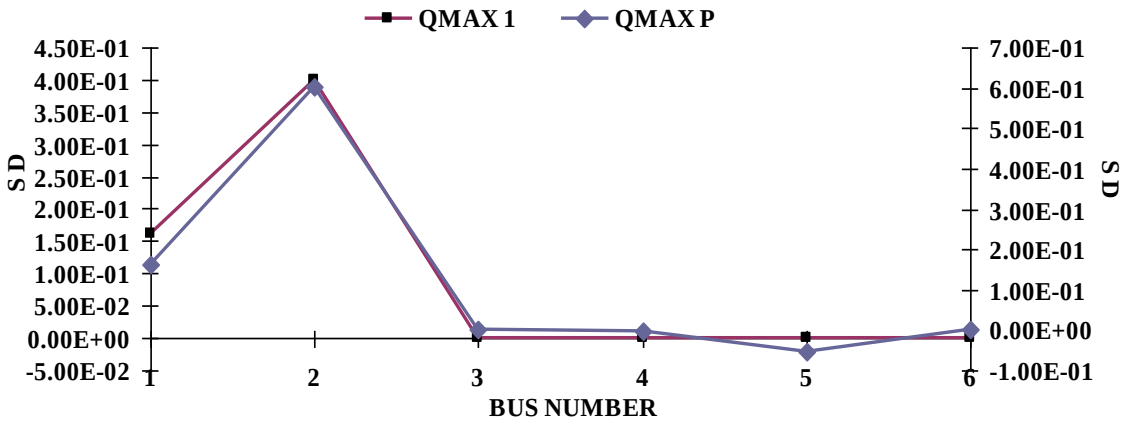

Fig. 5.38 : GRAPH BETWEEN Q (S D) vs BUS NUMBER

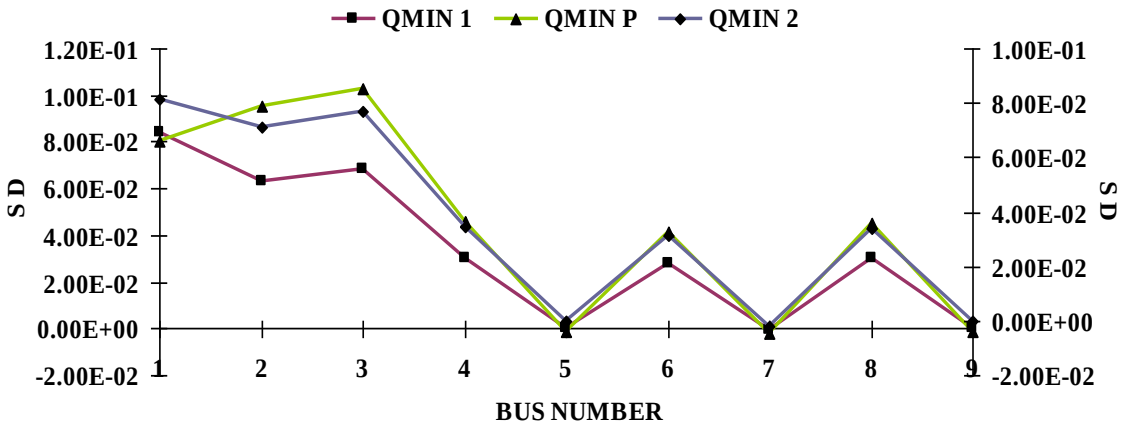

Fig.5.39 : GRAPH BETWEEN Q (S D) vs BUS NUMBER

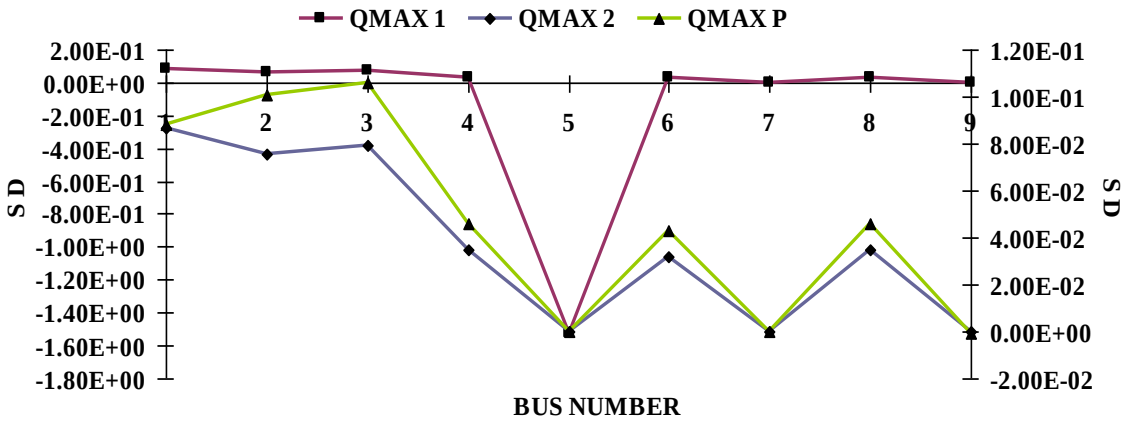

Fig. 5.40 : GRAPH BETWEEN Q (S D) vs BUS NUMBER

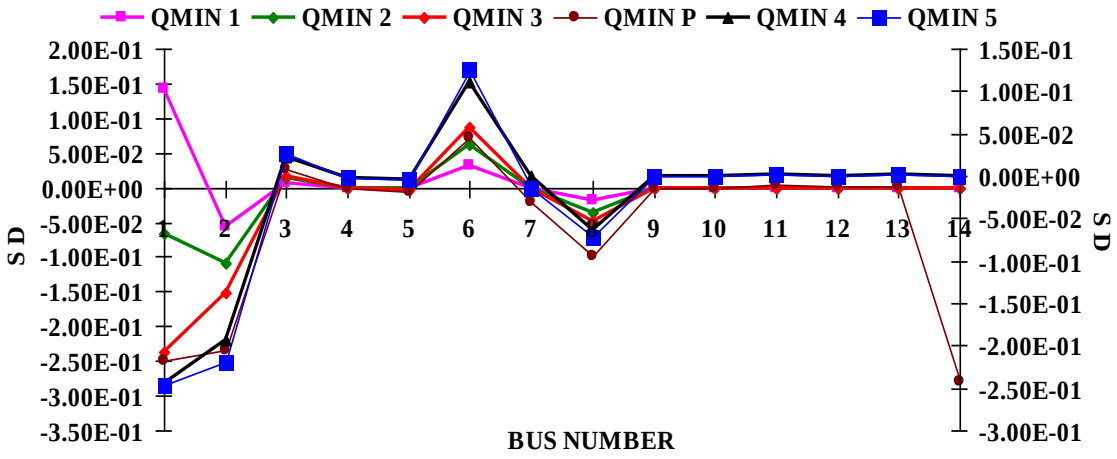

Fig. 5.41 GRAPH BETWEEN Q (S D) vs BUS NUMBER

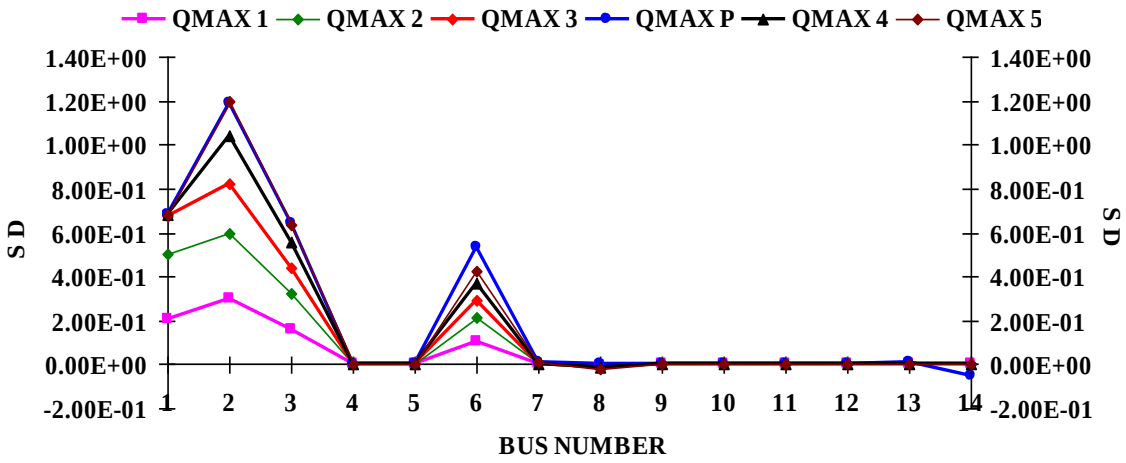

Fig. 5.42 GRAPH BETWEEN Q (S D) vs BUS NUMBER

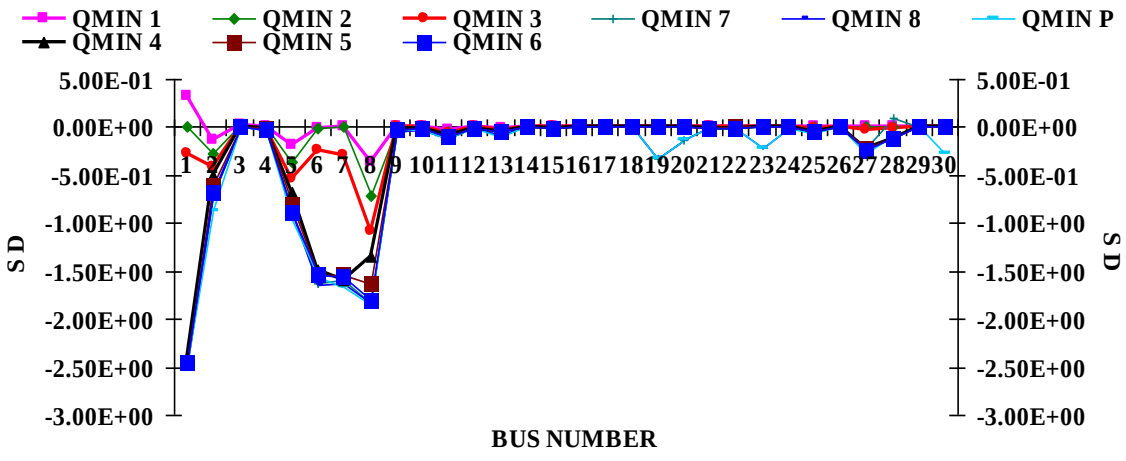

Fig. 5.43 GRAPH BETWEEN Q (S D) vs BUS NUMBER

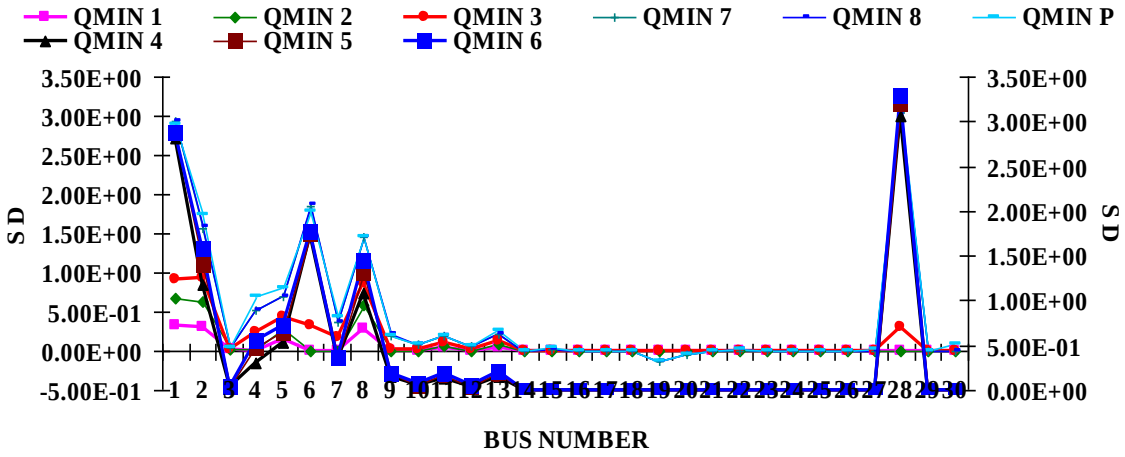

Fig. 5.44 GRAPH BETWEEN Q (S D) vs BUS NUMBER

Average valued Standard Deviation (S D) of each variable is shown in Figures 5.45 – 5.52 for voltage (V) magnitudes, in Figures 5.53 – 5.60 for voltage angle (θ) magnitudes, in Figures 5.61 – 5.68 for current (I) magnitudes, in Figures 5.69 – 5.76 for real power (P) and in Figures 5.77 – 5.84 for reactive power (Q).

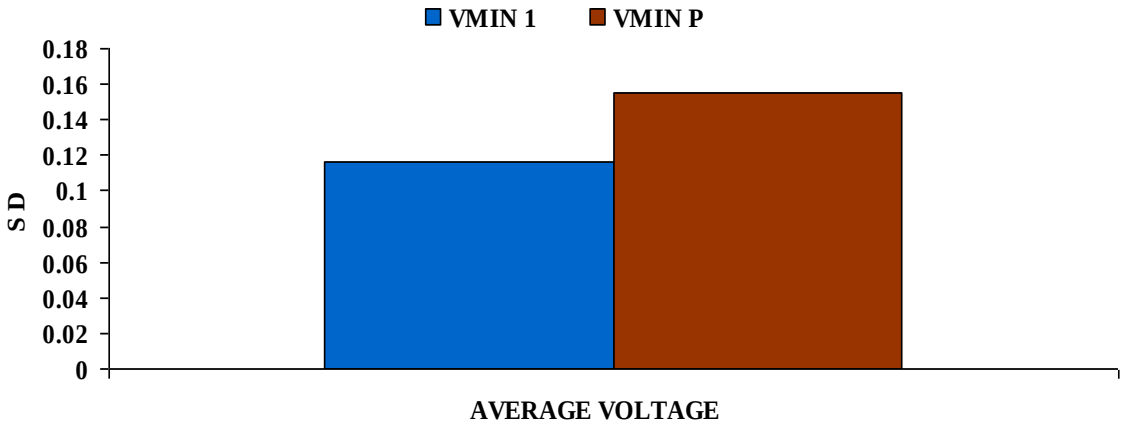

Fig. 5.45 : AVERAGE VOLTAGE vs STANDARD DEVIATION

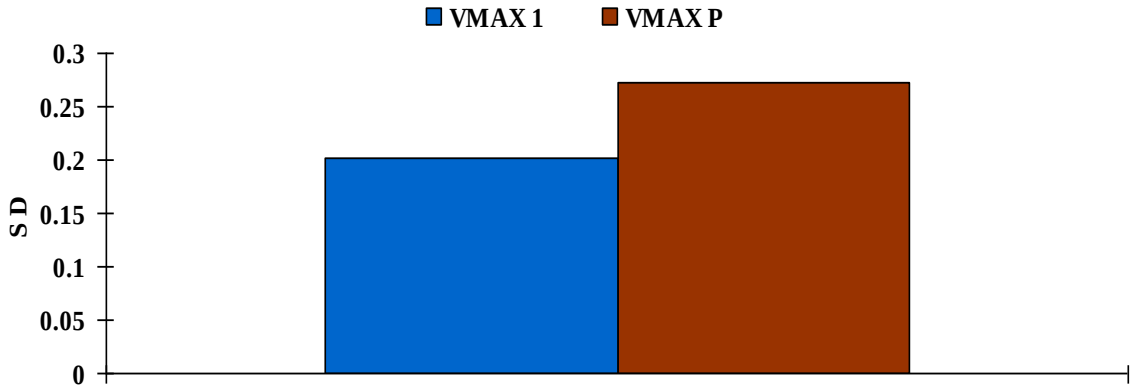

Fig. 5.46 : AVERAGE VOLTAGE vs STANDARD DEVIATION

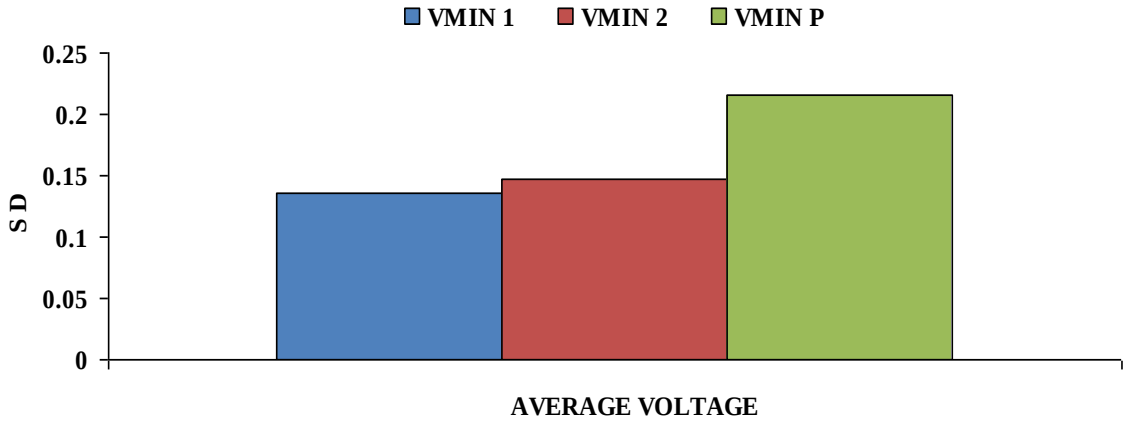

Fig. 5.47 : AVERAGE VOLTAGE vs STANDARD DEVIATION

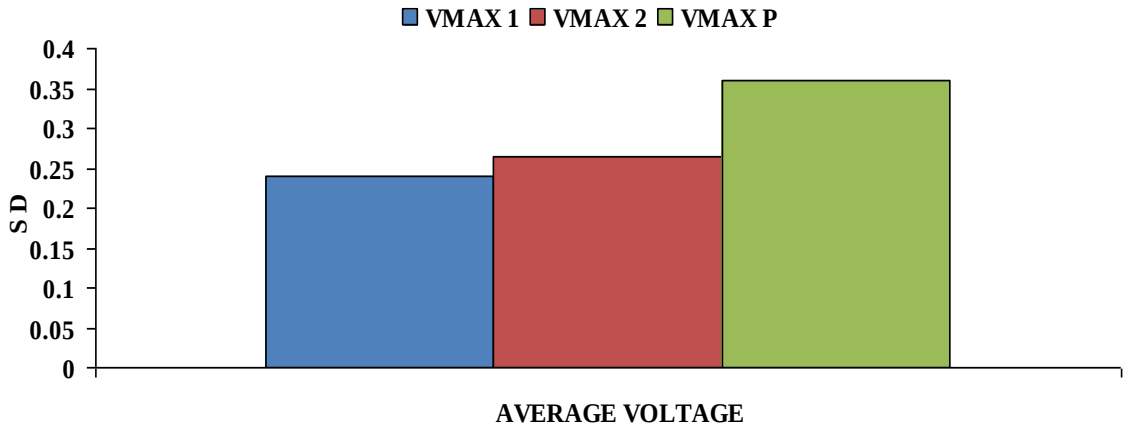

Fig. 5.48 : AVERAGE VOLTAGE vs STANDARD DEVIATION

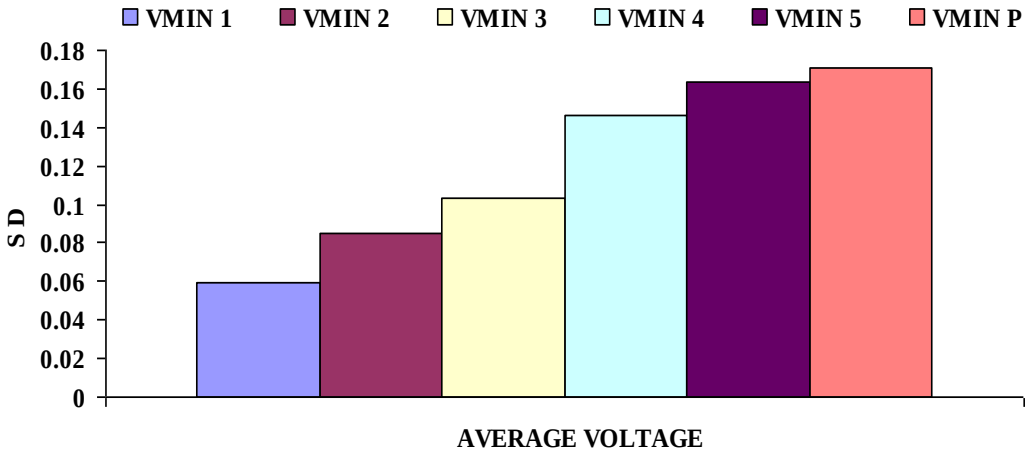

Fig. 5.49 AVERAGE VOLTAGE STANDARD DEVIATION

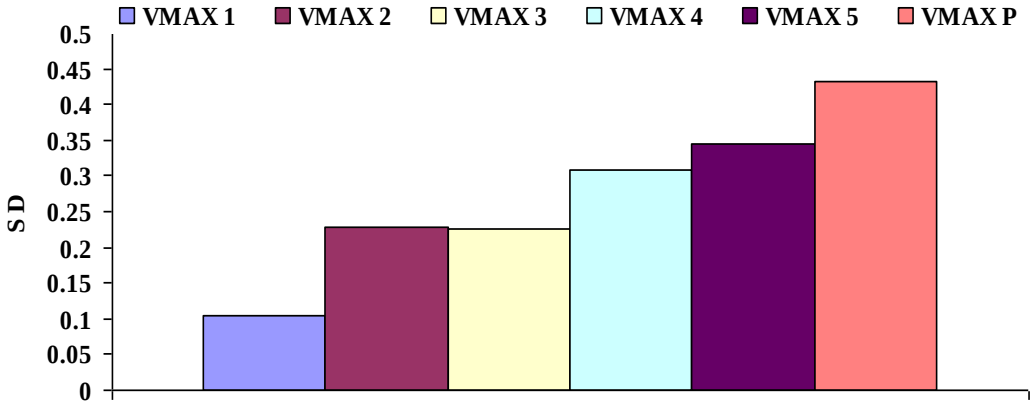

Fig. 5.50 AVERAGE VOLTAGE vs STANDARD DEVIATION

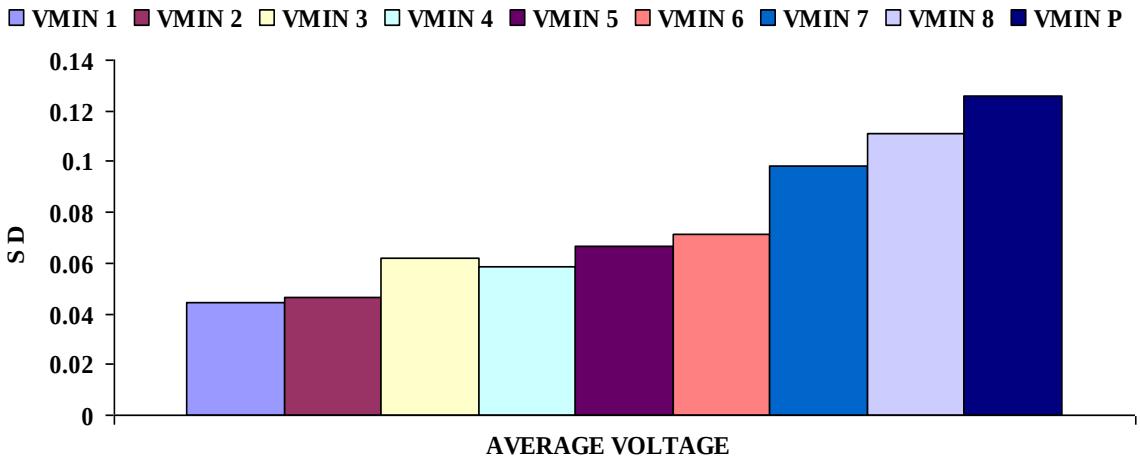

Fig. 5.51 AVERAGE VOLTAGE vs STANDARD DEVIATION

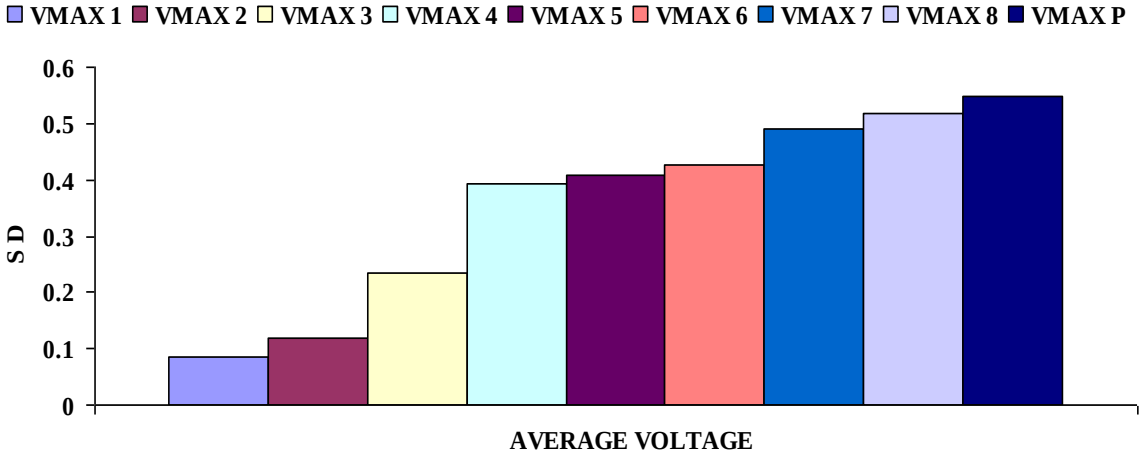

Fig. 5.52 AVERAGE VOLTAGE vs STANDARD DEVIATION

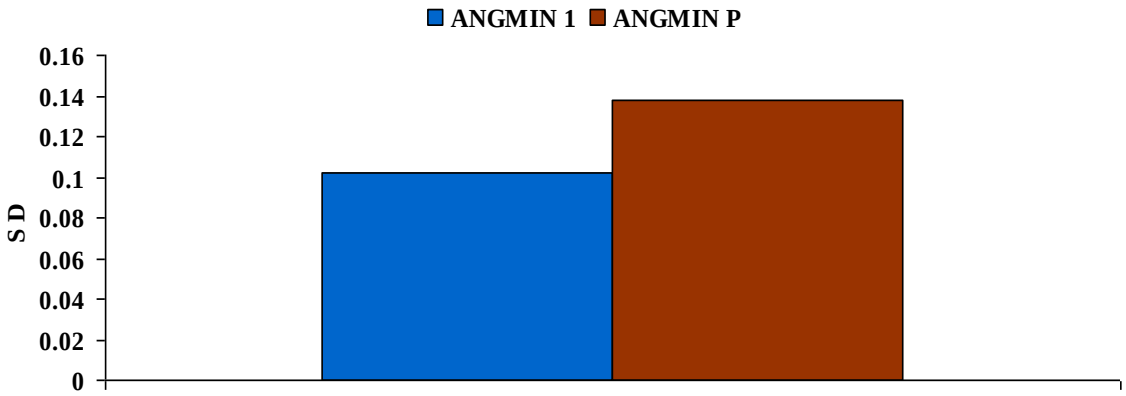

Fig. 5.53 :AVERAGE VOLTAGE ANGLE vs STANDARD DEVIATION

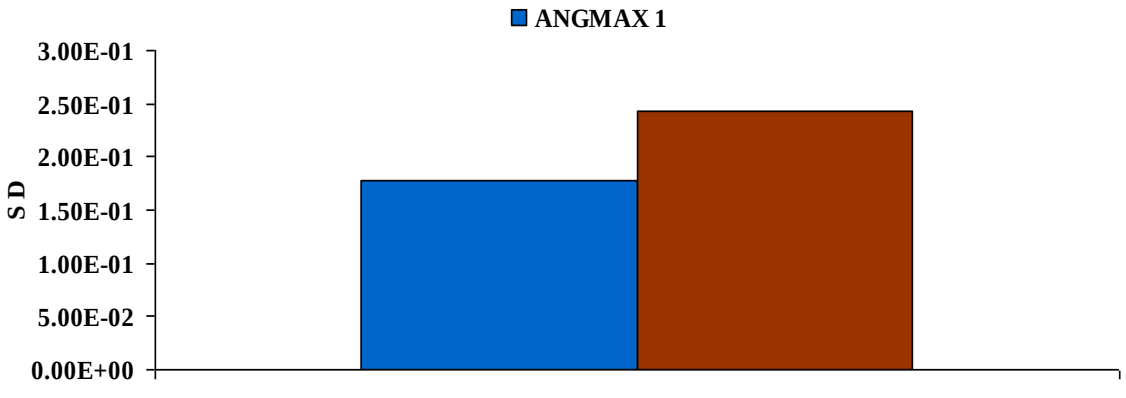

Fig.5.54 : AVERAGE VOLTAGE ANGLE vs STANDARD DEVIATION

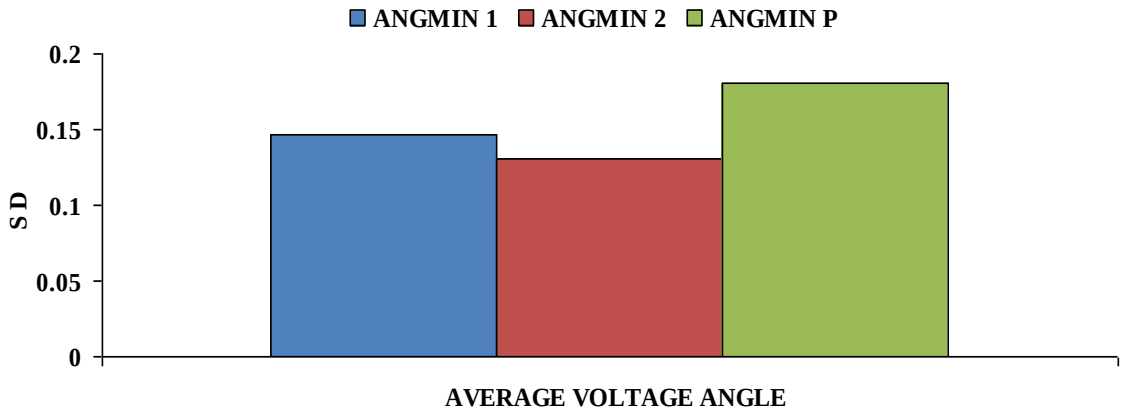

Fig. 5.55 : AVERAGE VOLTAGE ANGLE vs STANDARD DEVIATION

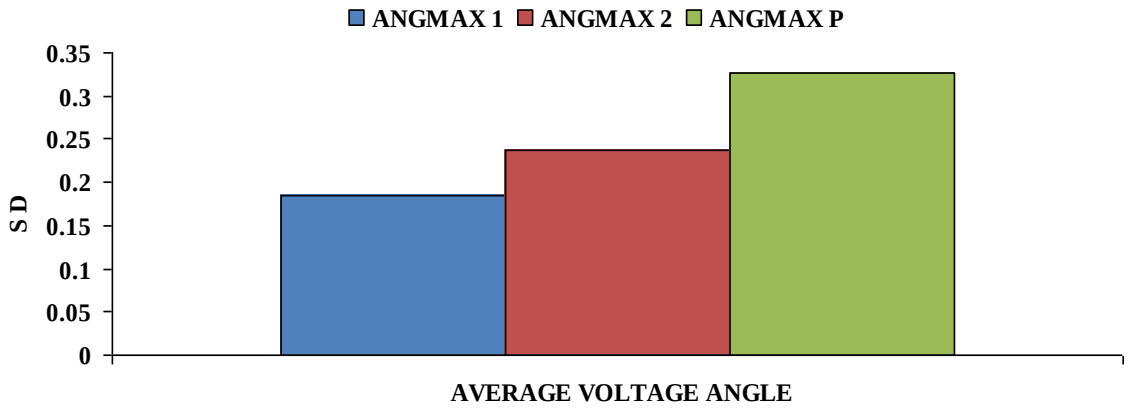

Fig. 5.56 : AVERAGE VOLTAGE ANGLE vs STANDARD DEVIATION

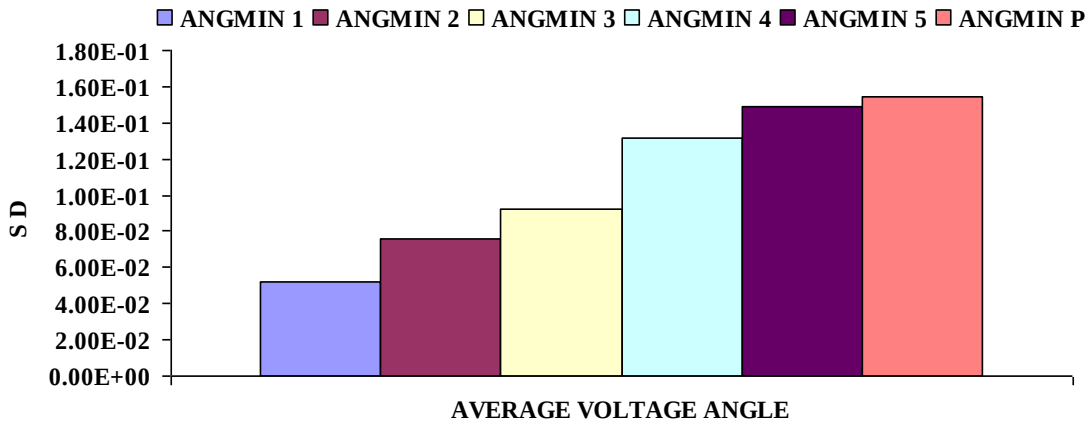

Fig. 5.57 AVERAGE VOLTAGE ANGLE vs STANDARD DEVIATION

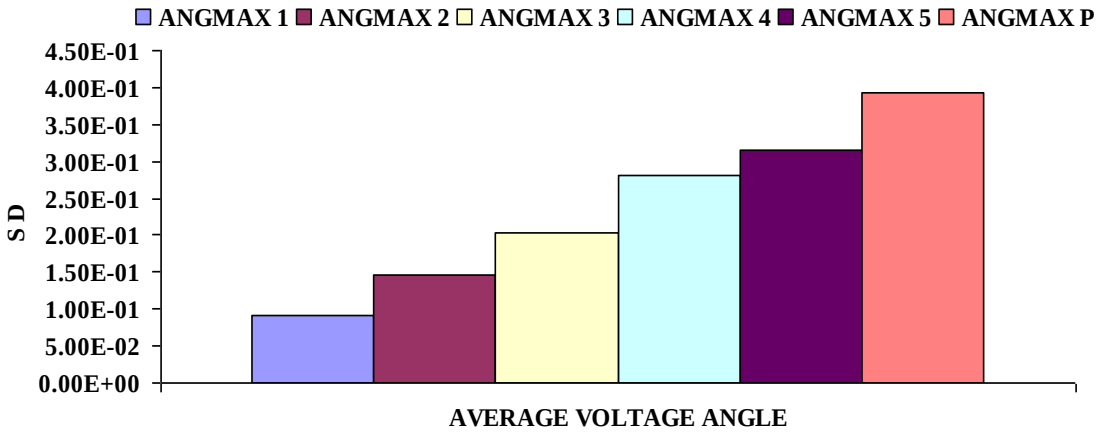

Fig. 5.58 AVERAGE VOLTAGE ANGLE vs STANDARD DEVIATION

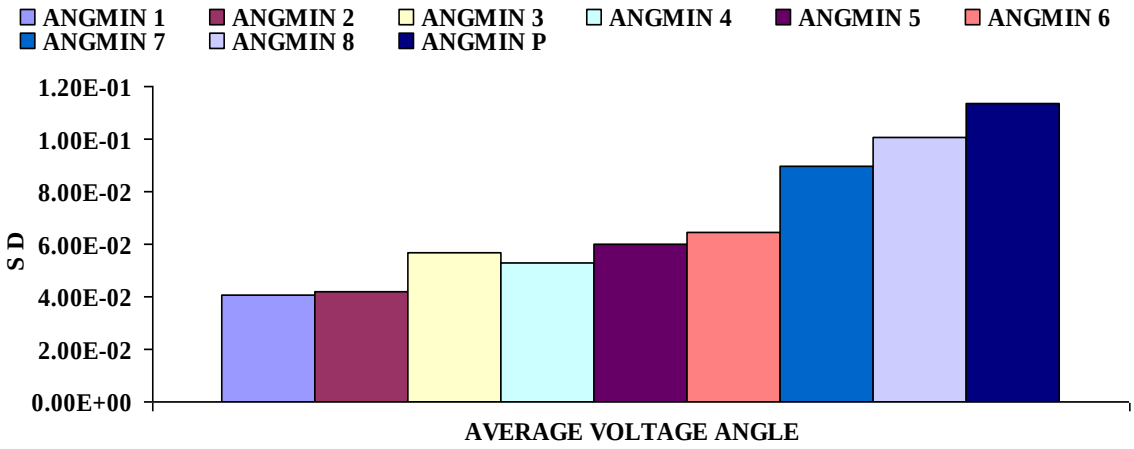

Fig. 5.59 AVERAGE VOLTAGE ANGLE vs STANDARD DEVIATION

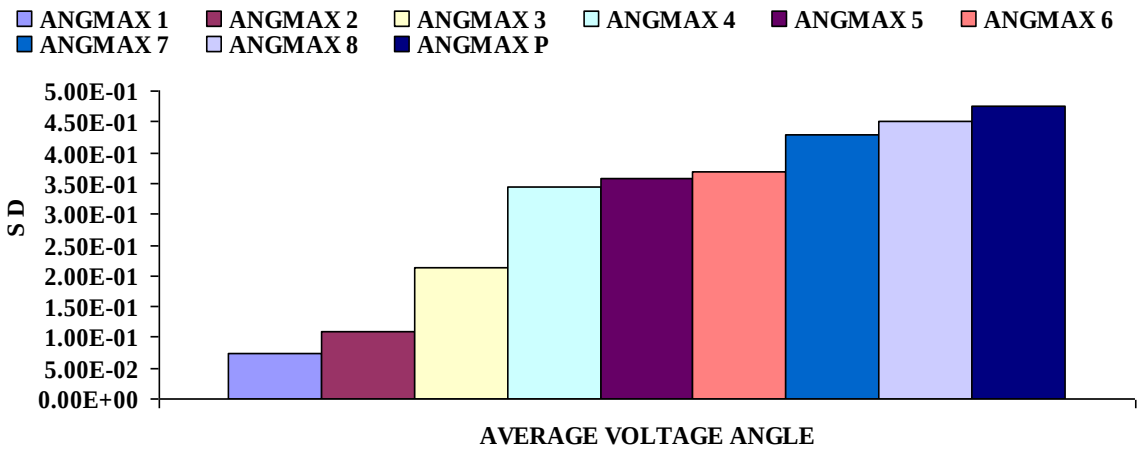

Fig. 5.60 AVERAGE VOLTAGE ANGLE vs STANDARD DEVIATION

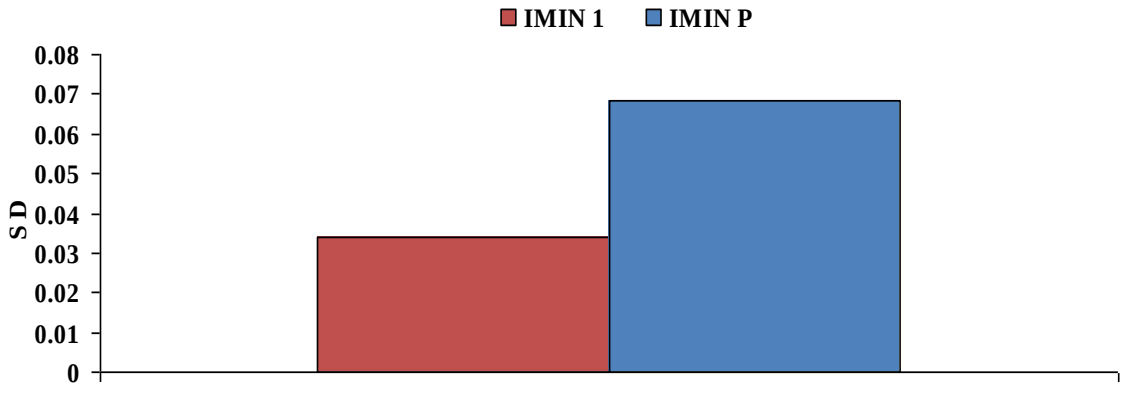

Fig. 5.61 : AVERAGE CURRENT vs STANDARD DEVIATION

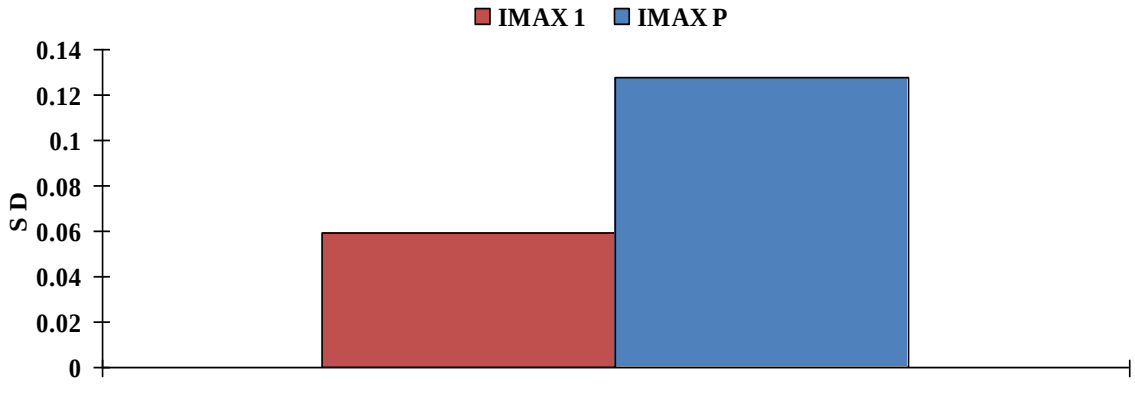

Fig. 5.62 : AVERAGE CURRENT vs STANDARD DEVIATION

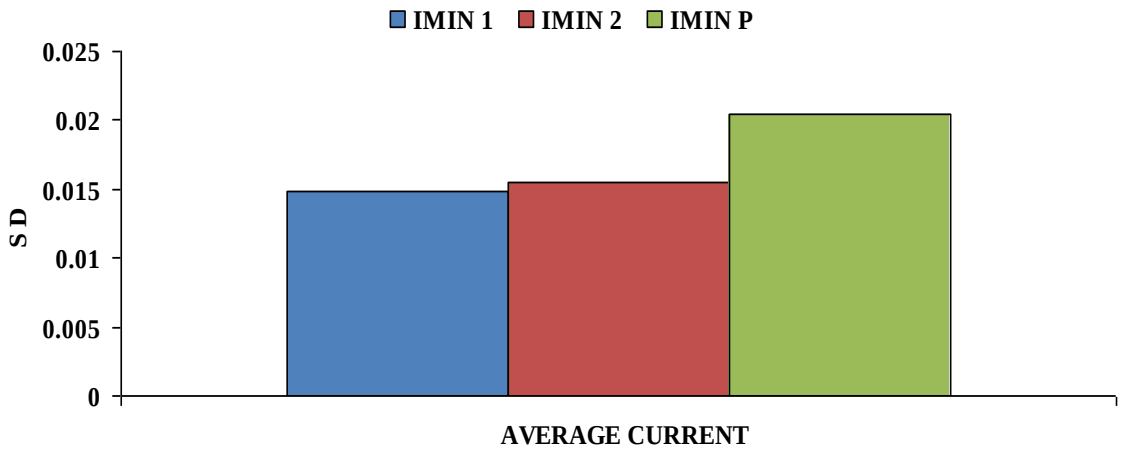

Fig. 5.63 : AVERAGE CURRENT vs STANDARD DEVIATION

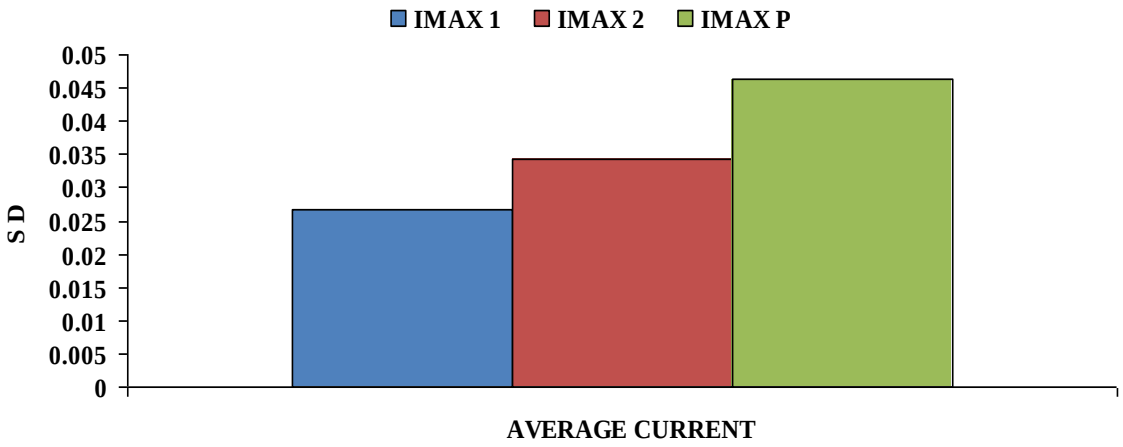

Fig. 5.64 : AVERAGE CURRENT vs STANDARD DEVIATION

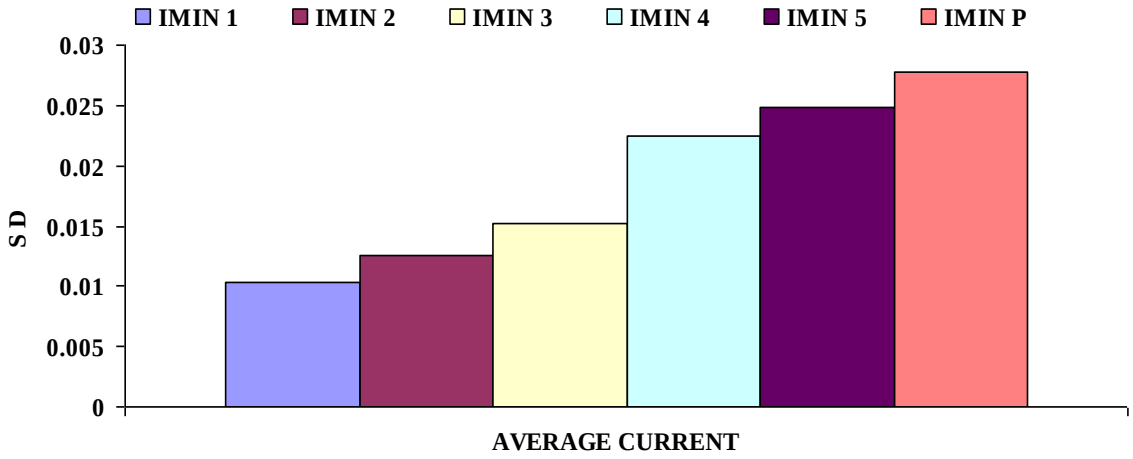

Fig. 5.65 AVERAGE CURRENT vs STANDARD DEVIATION

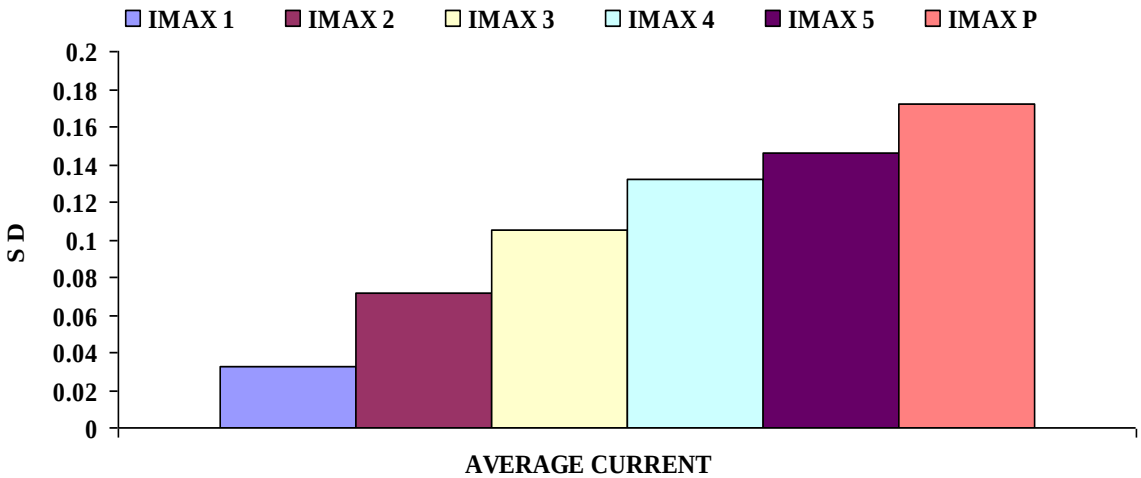

Fig. 5.66 AVERAGE CURRENT vs STANDARD DEVIATION

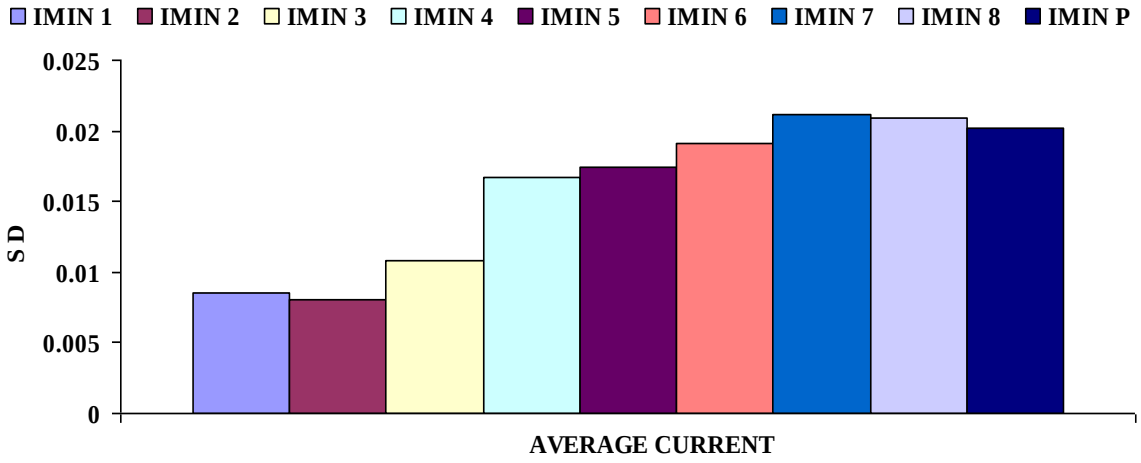

Fig. 5.67 AVERAGE CURRENT vs STANDARD DEVIATION

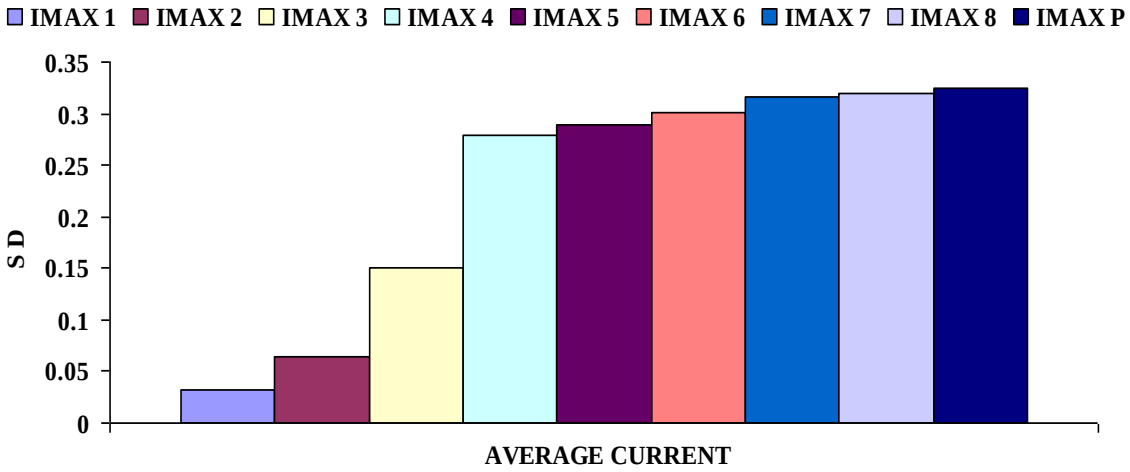

Fig. 5.68 AVERAGE CURRENT vs STANDARD DEVIATION

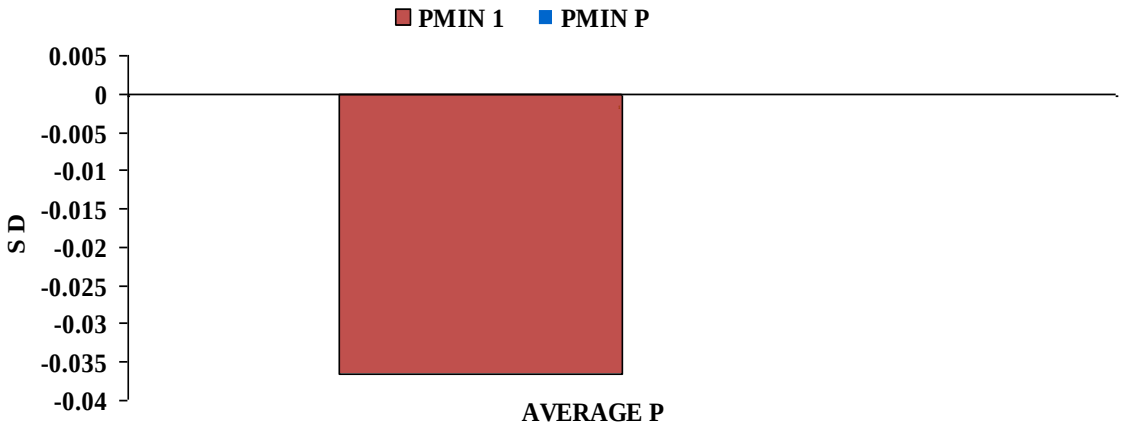

Fig. 5.69 : AVERAGE P vs STANDARD DEVIATION

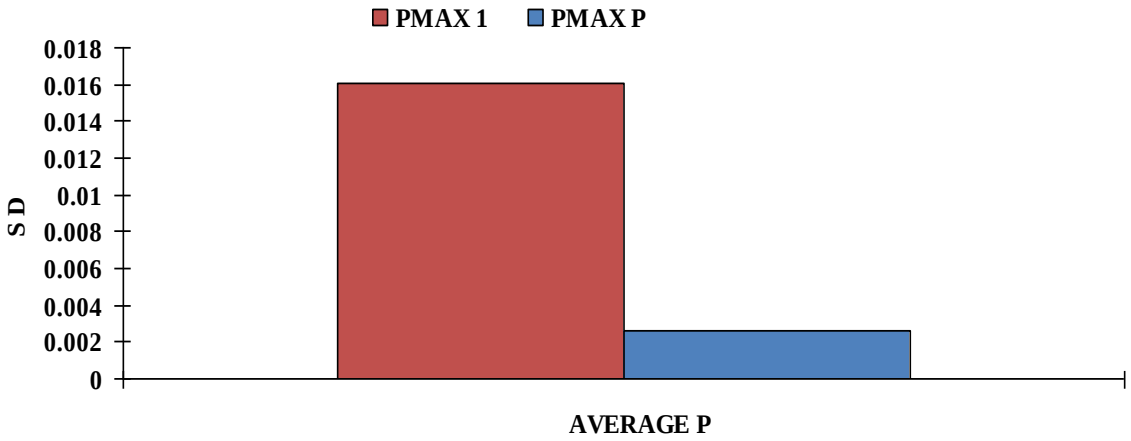

Fig. 5.70 : AVERAGE P vs STANDARD DEVIATION

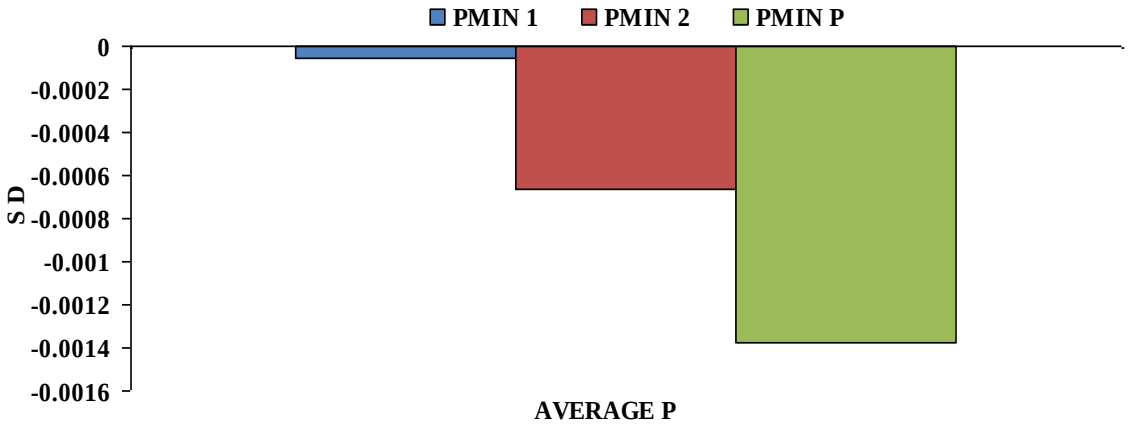

Fig. 5.71 : AVERAGE P vs STANDARD DEVIATION

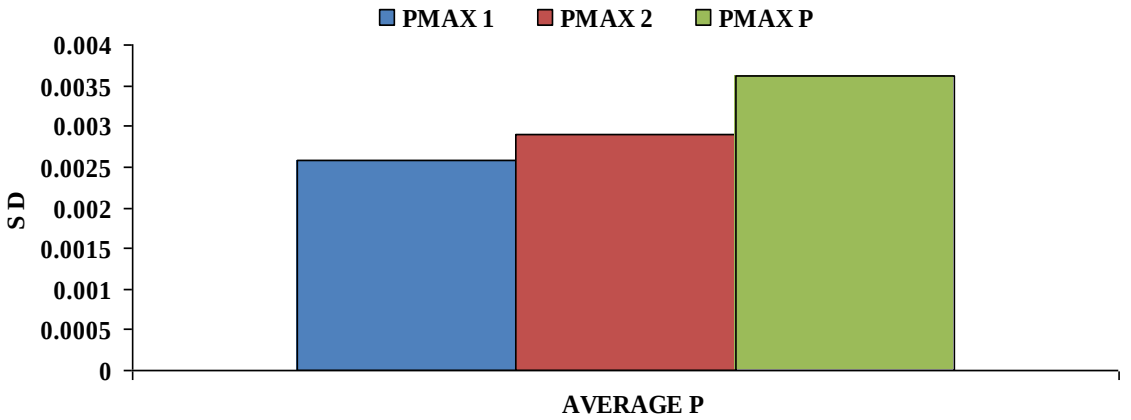

Fig. 5.72 : AVERAGE P vs STANDARD DEVIATION

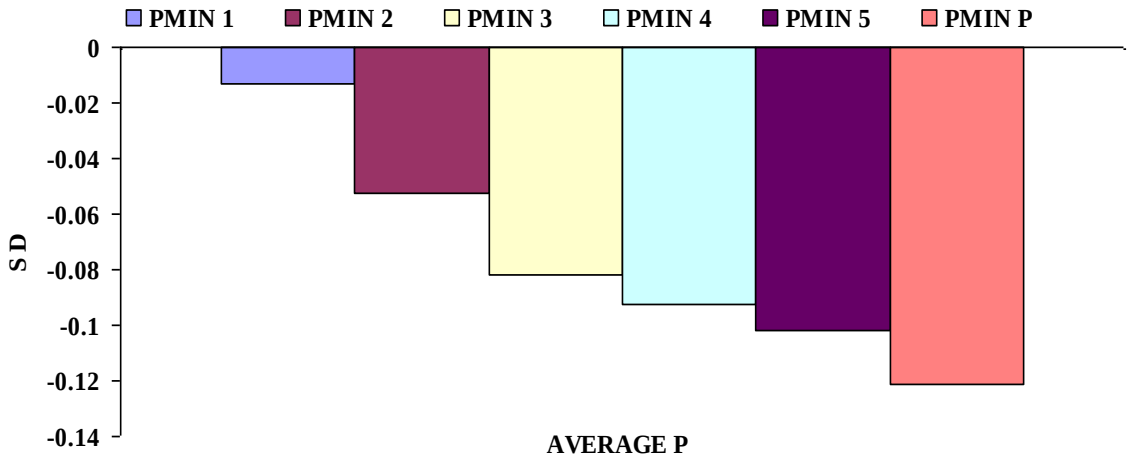

Fig. 5.73 AVERAGE P vs STANDARD DEVIATION

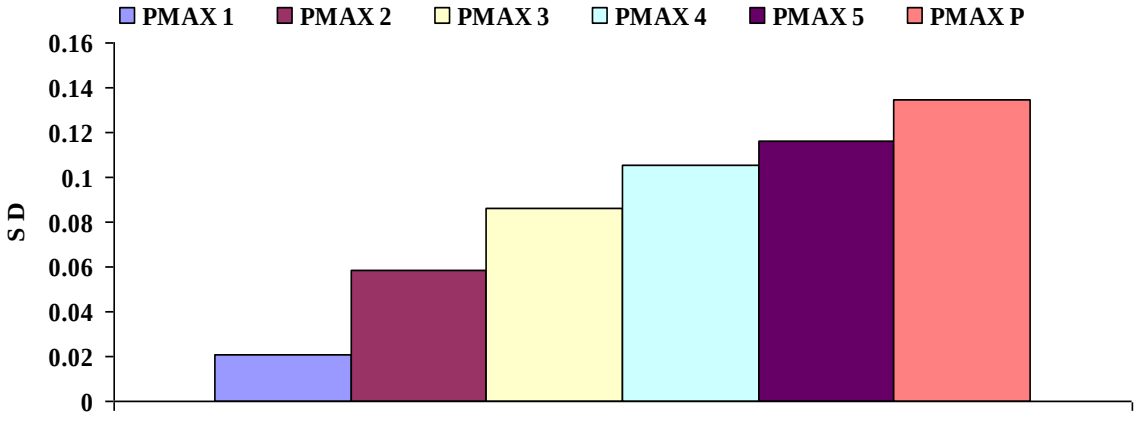

Fig. 5.74 AVERAGE P vs STANDARD DEVIATION

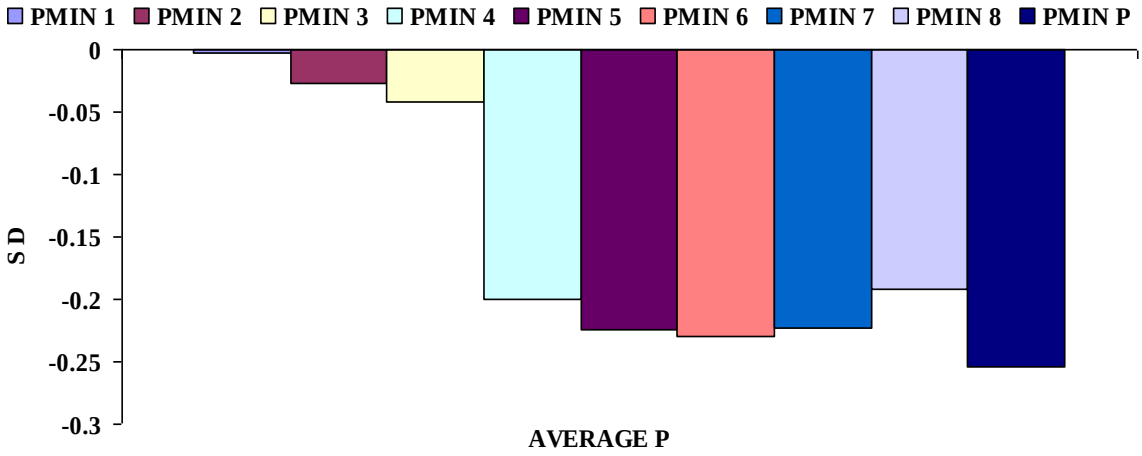

Fig. 5.75 AVERAGE P vs STANDARD DEVIATION

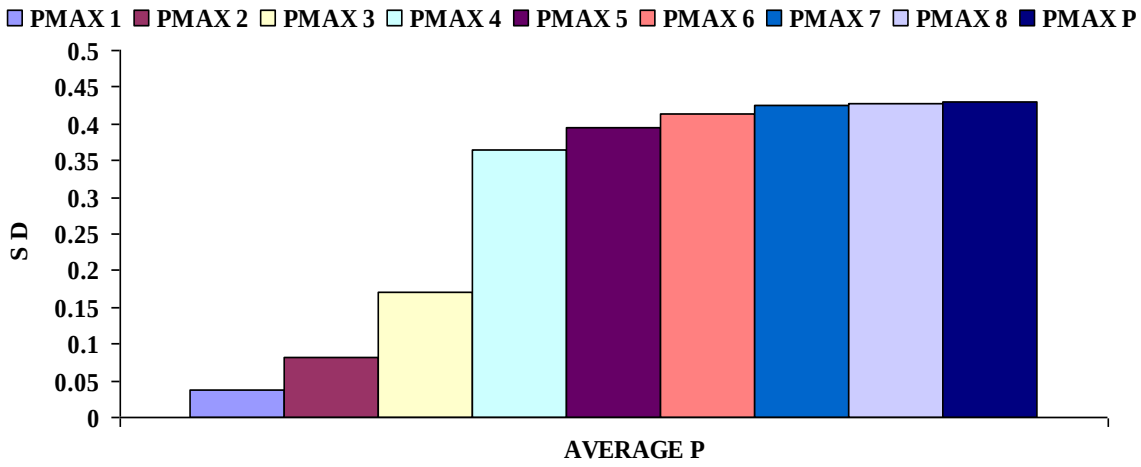

Fig. 5.76 AVERAGE P vs STANDARD DEVIATION

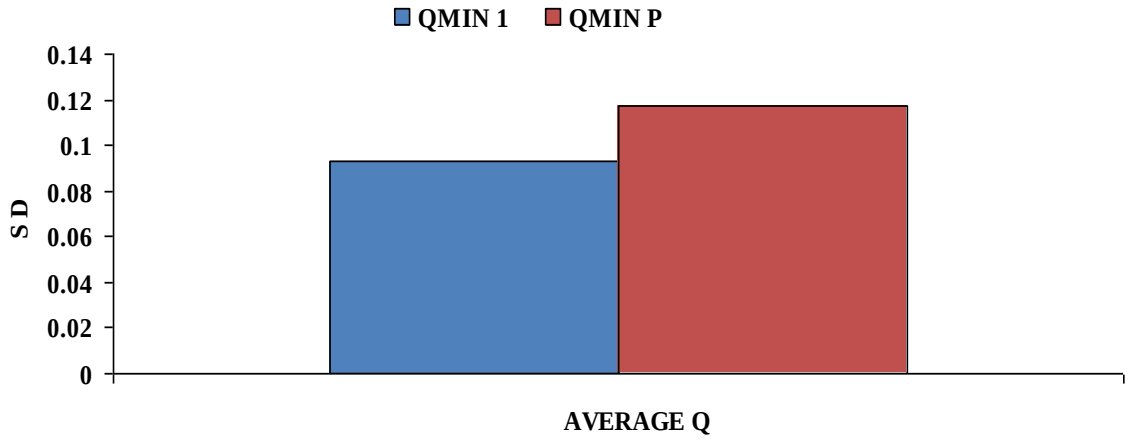

Fig. 5.77 : AVERAGE Q vs STANDARD DEVIATION

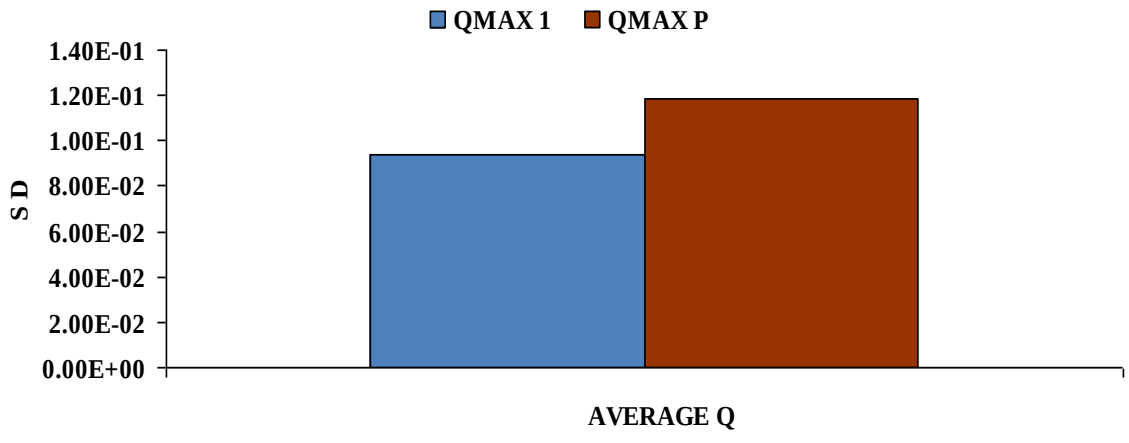

Fig.5.78 : AVERAGE Q vs STANDARD DEVIATION

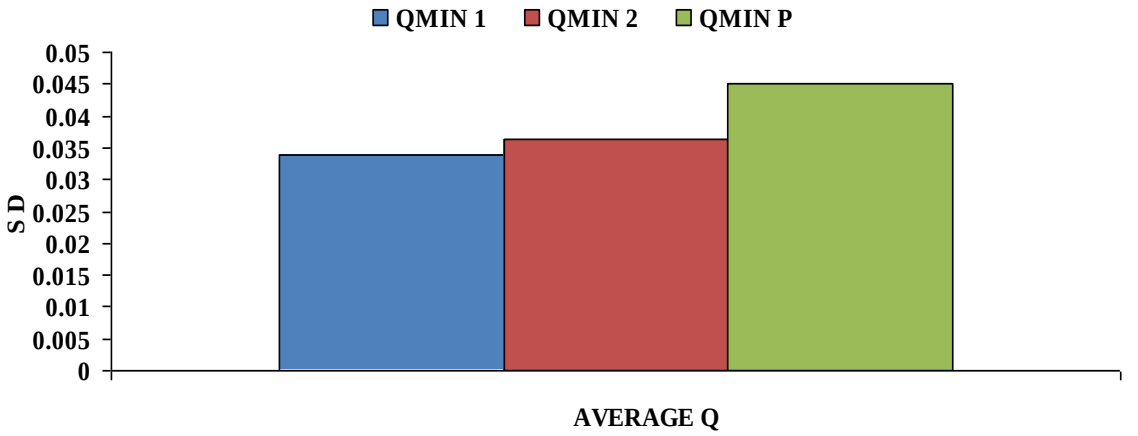

Fig. 5.79 : AVERAGE Q vs STANDARD DEVIATION

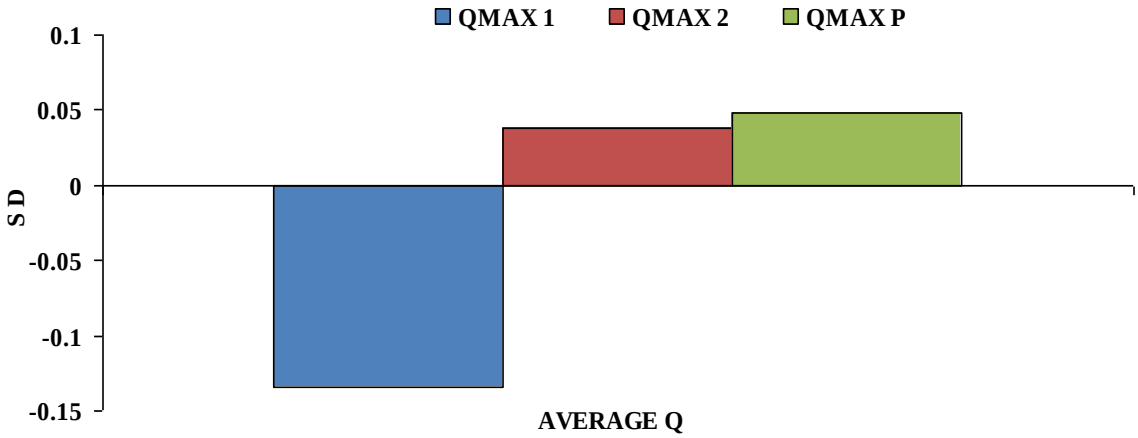

Fig. 5.80 : AVERAGE Q vs STANDARD DEVIATION

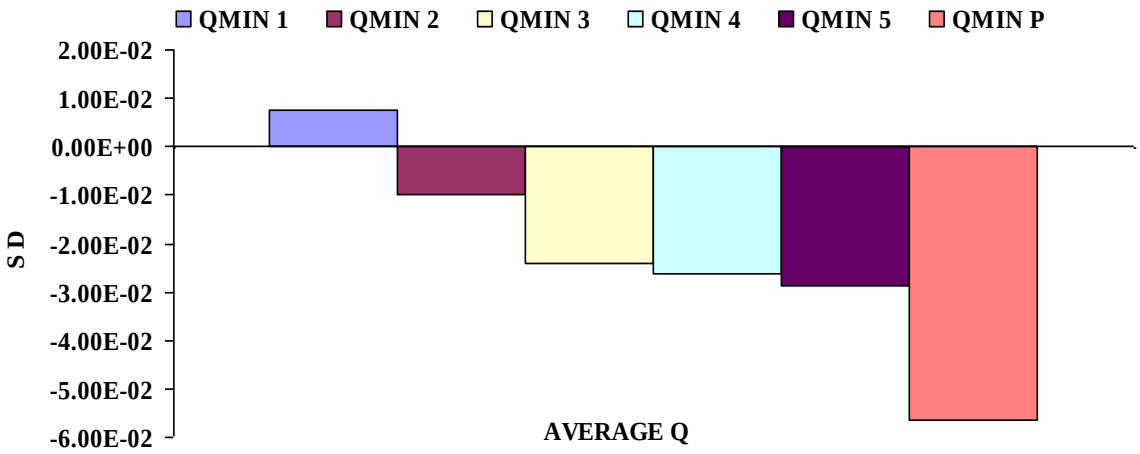

Fig. 5.81 AVERAGE Q vs STANDARD DEVIATION

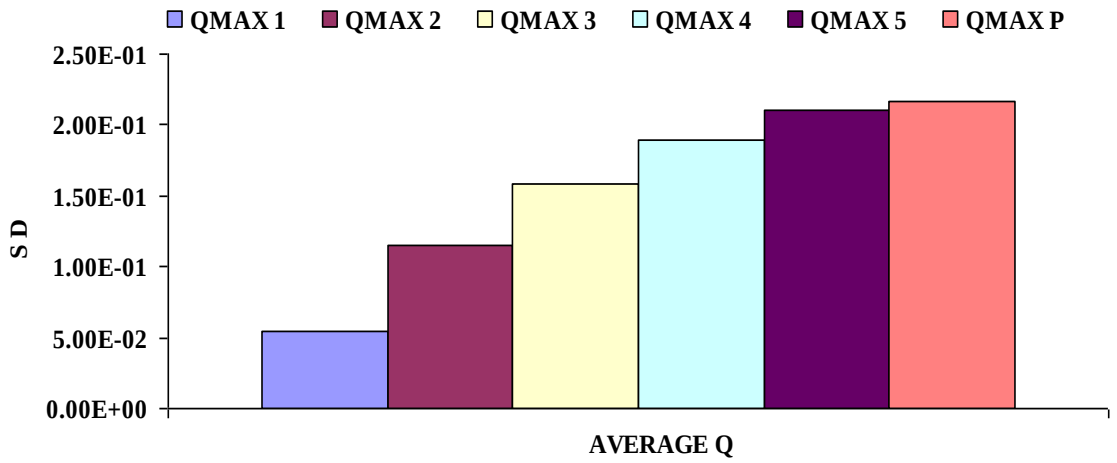

Fig. 5.82 AVERAGE Q vs STANDARD DEVIATION

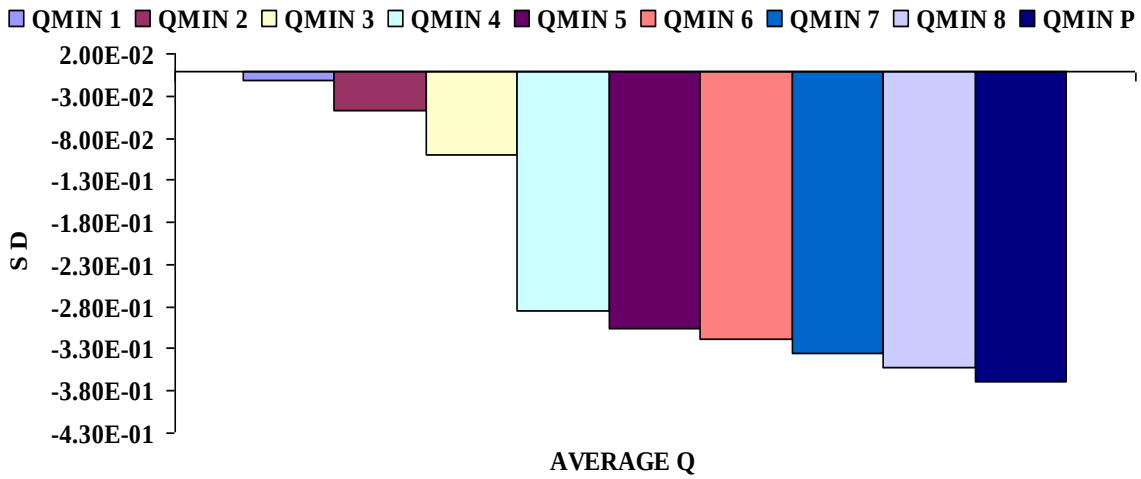

Fig. 5.83 AVERAGE Q vs STANDARD DEVIATION

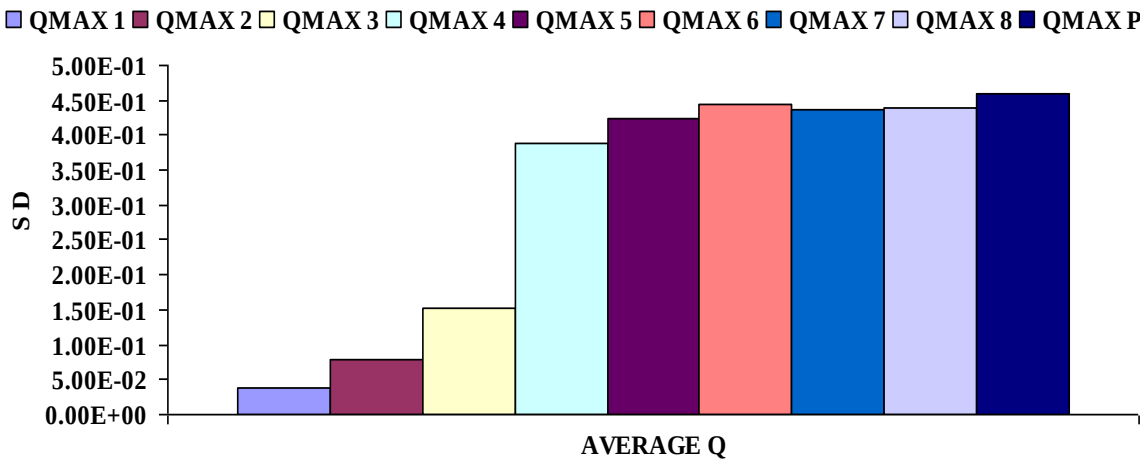

Fig. 5.84 AVERAGE Q vs STANDARD DEVIATION

Table 5.3 : Average Standard Deviations of the Estimated Variables

Type of Variables	Type of Systems	No PMUs		1 PMUs		2 PMUs	
		Min	Max	Min	Max	Min	Max
Voltage Magnitude (V)	6 Bus	0.116451	0.201764	-	-	-	-
	9 Bus	0.136364	0.239584	0.146453	0.264089	-	-
	14 Bus	0.059018	0.103501	0.084794	0.227837	0.103686	0.226238
	30 Bus	0.044502	0.085112	0.046551	0.120107	0.061803	0.233047
Voltage Angle (θ)	6 Bus	0.102129	1.77E-01	-	-	-	-
	9 Bus	0.146942	0.18511	0.130961	0.236817	-	-
	14 Bus	5.24E-02	9.17E-02	7.55E-02	1.46E-01	9.22E-02	2.04E-01
	30 Bus	4.09E-02	7.51E-02	4.22E-02	1.09E-01	5.65E-02	2.14E-01
Current Magnitude (I)	6 Bus	0.034145	0.059283	-	-	-	-
	9 Bus	0.01483	0.026632	0.015556	0.034175	-	-
	14 Bus	0.010323	0.032592	0.012579	0.071714	1.52E-02	0.105263
	30 Bus	0.008583	0.032904	0.008	0.063981	0.010793246	0.150697
Real Power (P)	6 Bus	-0.03661	0.016088	-	-	-	-
	9 Bus	-5.44E-05	0.0025782	-0.00066	0.0028995	-	-
	14 Bus	-0.01324	0.02107	-0.05253	0.058474	-0.08218	0.086179
	30 Bus	-0.003203	0.03823817	-0.02640	0.08202461	-0.041412	0.170698
Reactive Power (Q)	6 Bus	0.093373	9.37E-02	-	-	-	-
	9 Bus	0.0337751	-0.134730	0.036288	0.03812	-	-
	14 Bus	7.54E-03	5.44E-02	-9.85E-03	1.16E-01	-2.42E-02	1.58E-01
	30 Bus	-1.19E-02	3.92E-02	-4.68E-02	7.94E-02	-9.90E-02	1.51E-01

Type of Variables	Type of Systems	3 PMUs		4 PMUs		5 PMUs	
		Min	Max	Min	Max	Min	Max
Voltage Magnitude (V)	6 Bus	-	-	-	-	-	-
	9 Bus	-	-	-	-	-	-
	14 Bus	0.146055	0.309194	0.16371	0.345643	-	-
	30 Bus	0.058245	0.393268	0.066334	0.409227	0.071556	0.42564
Voltage Angle (θ)	6 Bus	-	-	-	-	-	-
	9 Bus	-	-	-	-	-	-
	14 Bus	1.32E-01	2.82E-01	1.49E-01	3.15E-01	-	-
	30 Bus	5.27E-02	3.43E-01	5.99E-02	3.57E-01	6.45E-02	3.70E-01
Current Magnitude (I)	6 Bus	-	-	-	-	-	-
	9 Bus	-	-	-	-	-	-
	14 Bus	0.02244	0.132364	0.024797	0.145976	-	-
	30 Bus	0.016752	0.279389	0.017378	0.289197	0.019126	0.300657
Real Power (P)	6 Bus	-	-	-	-	-	-
	9 Bus	-	-	-	-	-	-
	14 Bus	-0.09272	0.105609	-0.10191	0.116409	-	-
	30 Bus	-0.200673	0.365447	-0.22395	0.394325	-0.229368	0.412551

Type of Variables	Type of Systems	3 PMUs		4 PMUs		5 PMUs	
		Min	Max	Min	Max	Min	Max
Reactive Power (Q)	6 Bus	-	-	-	-	-	-
	9 Bus	-	-	-	-	-	-
	14 Bus	-2.63E-02	1.89E-01	-2.88E-02	2.10E-01	-	-
	30 Bus	-2.85E-01	3.88E-01	-3.05E-01	4.24E-01	-3.19E-01	4.45E-01

Type of Variables	Type of Systems	6 PMUs		7 PMUs		P PMUs	
		Min	Max	Min	Max	Min	Max
Voltage Magnitude (V)	6 Bus	-	-	-	-	0.155211	0.273
	9 Bus	-	-	-	-	0.21618603	0.3607
	14 Bus	-	-	-	-	0.171281	0.432693
	30 Bus	0.098532	0.491333	0.111073	0.5174	0.12556645	0.5494
Voltage Angle (θ)	6 Bus	-	-	-	-	0.137928	0.243
	9 Bus	-	-	-	-	0.18056381	0.3266
	14 Bus	-	-	-	-	0.154652	0.392193
	30 Bus	8.96E-02	4.28E-01	1.01E-01	4.50E-01	0.11367311	0.47576
Current Magnitude (I)	6 Bus	-	-	-	-	0.068248	0.127333
	9 Bus	-	-	-	-	0.02050078	0.04625556
	14 Bus	-	-	-	-	0.02479694	0.14597602
	30 Bus	0.021099	0.31592	0.020952	0.3202	2.02E-02	0.324087
Real Power (P)	6 Bus	-	-	-	-	0.000126	0.002653
	9 Bus	-	-	-	-	0.00361395	-0.0010843
	14 Bus	-	-	-	-	-0.12102	0.1349
	30 Bus	-0.222593	0.4258915	-0.19249	0.4277428	-0.2544753	0.43010183
Reactive Power (Q)	6 Bus	-	-	-	-	0.117138	0.118
	9 Bus	-	-	-	-	0.0451682	0.04766911
	14 Bus	-	-	-	-	-0.05637	0.216507
	30 Bus	-3.36E-01	4.38E-01	-3.52E-01	4.40E-01	-0.3699197	0.45857718

The table 5.3 shows that how the average standard deviation varies on increasing the number of PMUs on the same bus system. The system parameters with conventional method to the only PMUs will reflect that how the controllability of the system improves as follows:-

- The voltage magnitude varies from conventional method to only PMU in IEEE 6 Bus system is 24.97 % (Min) & 26.09 % (Max), in IEEE 9 Bus system is 36.92 % (Min) & 33.58 % (Max), in IEEE 14 Bus system is 65.54 % (Min) & 76.08 % (Max) and in IEEE 30 Bus system is 64.56 % (Min) & 84.51 % (Max).
- The voltage angle varies from conventional method to only PMU in IEEE 6 Bus system is 25.95 % (Min) & 27.18 % (Max), in IEEE 9 Bus system is 18.62 %

(Min) & 43.32 % (Max), in IEEE 14 Bus system is 66.09 % (Min) & 76.61 % (Max) and in IEEE 30 Bus system is 64.06 % (Min) & 84.22 % (Max).

- The current magnitude varies from conventional method to only PMU in IEEE 6 Bus system is 49.97 % (Min) & 53.44 % (Max), in IEEE 9 Bus system is 27.66 % (Min) & 42.42 % (Max), in IEEE 14 Bus system is 62.89 % (Min) & 81.06 % (Max) and in IEEE 30 Bus system is 57.50 % (Min) & 89.85 % (Max).

Also in case of IEEE 30 bus system, the average standard deviation of the estimated P is approximately -0.003203 (Min) & 0.03823817 (Max) when there is conventional method, but after adding '4 PMUs' to the system, it becomes nearly -0.22395 (Min) & 0.394325 (Max) and at 'P PMUs' it become -0.2544753 (Min) & 0.43010183 (Max). The system will not produce any effective variation on system performance on further increasing from '4 PMUs' & onwards. Similarly, reactive power is showing the same impact on the system performance as in the case of real power. It means that the system controllability of 'No PMUs' to only PMUs is enhanced. The interesting thing is that the standard deviation increasing as increasing PMU and become nearly steady after '4 PMUs'. Therefore, this result shows that the most cost effective way of installing PMUs is to add '13 %' of the total bus numbers to the system, for decreasing the chances of errors on the estimated variables.

CHAPTER - 6

CONCLUSIONS AND FUTURE WORK

6.1 Conclusions

The conventional measurement method discussed with the PMU and is able to measure the voltage and current with their magnitude and phasors. The current measurement is implemented to the measurement set as in rectangular form. Equations for the measurements are illustrated in detail including the elements of the Jacobian matrix. It is expected that PMU measured data provide smaller error standard deviations of PMU which may improve the measurement redundancy and accuracy.

The state estimation in the linear formulation is investigated with PMU. All the variables and measurements are improved as in rectangular form, and then treated separately during the estimation process. Such linear formulation of the PMU data can produce the estimation result by a single calculation not requiring any iteration. If only PMU data measurement set is exist in the real world, the improvement of the computation time and accuracy is estimated, with the linear formulation of the state estimation.

The advantages of using PMU will advances the accuracy of the estimated variables. Some cases are tested while gradually increasing the number of PMUs which are added to the measurement set. With the help of advanced accuracy of PMU, it was seen that the estimated accuracy is also gradually increases. One of the motivating thing is that the accuracy improves most effectively when the number of implemented PMUs are around '13 %' of the system buses. It is proved that the quality of the estimation is bettered by adopting PMU data to the measurement set. The PMU will provide us various parameters with improved accuracy and redundancy.

6.2 Future Work

The following method may be used for estimation of the system parameters for further study:

- Singular Value Decomposition (SVD),
- Distributed state estimation
- Harmonic state estimation (HSE),
- Simulated Annealing(SA)
- Integer linear programming,
- hybrid state estimation,
- Artificial Neural Networks (ANN),
- Time domain simulation method,
- Improvement level of the accuracy with their cost.
- More number of buses may be used.

REFERENCES

Abur and Exposito A. G., Power System State Estimation, Theory and Implementation, MAECEL DEKKER, 2005, pp. 9-27.

Angelo Baggini, Handbook of Power Quality, JOHN WILEY & SONS LTD, 2008, pp.309 - 313

Bretas N.G., London J.B.A. Jr., Carlos E. de E. de S., Carlos S., "Measurement placement design and reinforcement for state estimation Purposes", 2001 IEEE Porto Power Tech Conference, Porto, Portugal, pp.1-6

Chakrabarti S. and Albu M., "Measurement Uncertainty Considerations in Optimal Sensor Deployment for State Estimation", 1 -4244-0830-X/07 ©2007 IEEE, pp.1–6

Chakrabarti S. and Kyriakides E., "Optimal Placement of Phasor Measurement Units for Power System Observability", IEEE TRANSACTIONS ON POWER SYSTEMS, VOL. 23, NO. 3, AUGUST 2008, 0885-8950 © 2008 IEEE, pp.1433–1440

Cheng Y., Hu X., and Gou B., "A New State Estimation Using Synchronized Phasor Measurements", 978-1-4244-1684-4/08 ©2008 IEEE, pp.2817–2820

Ebrahimian R. and Baldick R., "State Estimation Distributed Processing", IEEE TRANSACTIONS ON POWER SYSTEMS, VOL. 15, NO. 4, NOVEMBER 2000, 0885–8950/00 © 2000 IEEE, pp.1240–1246

Ebrahimpour R., Abharian E. K., Moussavi S. Z. and Birjandi A. A. M., "Transient Stability Assessment of a Power System by Mixture of Experts", INTERNATIONAL JOURNAL OF ENGINEERING, (IJE) Volume (4): Issue (1) March 2011 pp.93–104.

Filho M. B. D. C., Souza J. C. S. de, Oliveira F. M. F. de and Schilling M. Th., "Identifying Critical Measurements & Sets for Power System State Estimation", 2001 IEEE Porto Power Tech Conference, Porto, Portugal, 0-7803-7139-9/01 © 2001 IEEE,

Fitiwi D.Z. and Rao K.S.R., "Assessment of ANN-Based Auto-Reclosing Scheme Developed on Single Machine-Infinite Bus Model with IEEE 14-Bus System Model Data", 978-1-4244-4547-9/09 © 2009 IEEE, pp.1–6

Gou B., “Optimal Placement of PMUs by Integer Linear Programming”, IEEE TRANSACTIONS ON POWER SYSTEMS, VOL. 23, NO. 3, AUGUST 2008, 0885-8950 © 2008 IEEE, pp.1525–1526

Huang G. M. and Lei J., “Measurement Design of Data Exchange for Distributed Multi-Utility Operation”, 0-7803-7322-7/02 © 2002 IEEE, pp.222–227

Iyambo P.K. and Tzoneva R., “Transient Stability Analysis of the IEEE 14-Bus Electric Power System”, 1-4244-0987-X/07 © 2007 IEEE, pp.1-9

Jiang W., *and* Vittal V., “Optimal Placement of Phasor Measurements for the Enhancement of State Estimation”, PSCE 2006, 1-4244-0178-X/06 © 2006 IEEE, pp.1550–1555

Jiang W., Vittal V. and Heydt G.T., “A Distributed State Estimator Utilizing Synchronized Phasor Measurements”, IEEE TRANSACTIONS ON POWER SYSTEMS, VOL. 22, NO. 2, MAY 2007, 0885-8950 © 2007 IEEE, pp.563–571

Kamwa I. and Grondin R., “PMU Configuration for System Dynamic Performance Measurement in Large Multiarea Power Systems”, IEEE TRANSACTIONS ON POWER SYSTEMS, VOL. 17, NO. 2, MAY 2002, 0885-8950/02 © 2002 IEEE, pp.385-394

Kezunovic M., Abur A., Huang G., Bose A. and Tomsovic K., “The Role of Digital Modeling and Simulation in Power Engineering Education”, IEEE TRANSACTIONS ON POWER SYSTEMS, VOL. 19, NO. 1, 2004, 0885-8950/04 © 2004 IEEE, pp.64-72

Klump R., Wilson R.E. and Martin K.E., “Visualizing Real-Time Security Threats Using Hybrid SCADA / PMU Measurement Displays”, Proceedings of the 38th Hawaii International Conference on System Sciences – 2005, 0-7695-2268-8/05 © 2005 IEEE, pp.1–9

Madtharad C., Premrudeepreechacharn S., Watson N.R. and Saeng-Udom R., “An Optimal Measurement Placement Method for Power System Harmonic State Estimation”, IEEE TRANSACTIONS ON POWER DELIVERY, VOL. 20, NO. 2, APRIL 2005, 0885-8977 © 2005 IEEE, pp.1514-1521

Madtharad C., Premrudeepreechacham *S.*, Watson N. *R.* and Saenrak D., "Measurement Placement Method for Power System State Estimation: Part I", 0-7803-7989-6/03 ©2003 IEEE, pp.1629–1632

Magnago F. H. and Abur A., "A Unified Approach to Robust Meter Placement Against Loss of Measurements and Branch Outages", IEEE TRANSACTIONS ON POWER SYSTEMS, VOL. 15, NO. 3, AUGUST 2000, 0885–8950/00 © 2000 IEEE, pp.945–949

Meshram S. and Sahu O.P., "Application of ANN in economic generation scheduling in IEEE 6-Bus System", INTERNATIONAL JOURNAL OF ENGINEERING SCIENCE AND TECHNOLOGY (IJEST), ISSN : 0975-5462 Vol. 3 No. 3, 2011, pp.2461–2466

Milosevic B. and Begovic M., "Nondominated Sorting Genetic Algorithm for Optimal Phasor Measurement Placement", IEEE TRANSACTIONS ON POWER SYSTEMS, VOL. 18, NO. 1, FEBRUARY 2003, 0885-8950/03 © 2003 IEEE, pp.69–75

Nuqui R.F. and Phadke A. G., "Phasor Measurement Unit Placement Techniques for Complete and Incomplete Observability", IEEE TRANSACTIONS ON POWER DELIVERY, VOL. 20, NO. 4, 2005, 0885-8977 © 2005 IEEE, pp.2381-2388

Nwohu M.N., "Estimation of bifurcation point in multi-bus system using generator reactive power limit approach", JOURNAL OF ELECTRICAL AND ELECTRONICS ENGINEERING RESEARCH, March 2010, Vol. 2(2), pp.048-056,

Ota Y., Ukai H., Nakainura K. and Fujita H., "PMU based Midterm Stability Evaluation of Wide-area Power System", 0-7803-7525-4/02 ©2002 IEEE, pp.1676–1680.

Phadke A.G, Thorp J.S., Nuqui R.F. and Zhou M., "Recent Developments in State Estimation with Phasor Measurements", 978-1-4244-3811-2/09 ©2009 IEEE, pp.1-7

Phadke A.G., "SYNCHRONIZED PHASOR MEASUREMENTS – A HISTORICAL OVERVIEW", 0-7803-7525-4/02 © 2002 IEEE, pp.476–479

Rahman K. A., Mili L., Phadke A., Ree J. D. L. & Liu Y., "Internet Based Wide Area Information Sharing and Its Roles in Power System State Estimation", 0-7803-6672-7/01 © 2001 IEEE, pp.470–475

Rakpenthai C., Premrudeepreechacham S., Uatrongjit S. and Watson N. R., "Measurement Placement for Power System State Estimation by Decomposition Technique", 2004 11TH INTERNATIONAL CONFERENCE ON HARMONICS AND QUALITY OF POWER, 0-7803-8746-5/04 ©2004 IEEE, pp.414–418.

Sangrody H. A., Ameli M.T. and Meshkatoddini M.R., "The Effect of Phasor Measurement Units on the Accuracy of the Network Estimated Variables" , 2009 SECOND INTERNATIONAL CONFERENCE ON DEVELOPMENTS IN ESYSTEMS ENGINEERING, 978-0-7695-3912-6/09 © 2009 IEEE, pp.66–71

Tanti D.K., Singh B., Verma M.K., Mehrotra O. N., "An ANN based approach for optimal placement of DSTATCOM for voltage sag mitigation", INTERNATIONAL JOURNAL OF ENGINEERING SCIENCE AND TECHNOLOGY (IJEST), ISSN : 0975-5462 Vol. 3 No. 2 Feb 2011 pp.827–835

Weekes M.A., Hydro Manitoba and Hydro Kerry Walker Manitoba, "PMU Challenges and Performance Issues", 1-4244-1298-6/07 ©2007 IEEE, pp.1 – 4

Xu B. and Abur A., "Observability Analysis and Measurement Placement for Systems with PMUs", 0-7803-8718-X/04 © 2004 IEEE, pp.1–4

Zhao L. and Abur A., "Multiarea State Estimation Using Synchronized Phasor Measurements", IEEE TRANSACTIONS ON POWER SYSTEMS, VOL. 20, NO. 2, 2005, 0885-8950 © 2005 IEEE, pp.611–617

Zhou M., Centeno V. A., Thorp J.S., and Phadke A. G., "An Alternative for Including Phasor Measurements in State Estimators", IEEE TRANSACTIONS ON POWER SYSTEMS, VOL. 21, NO. 4, NOVEMBER 2006, 0885-8950 © 2006 IEEE, pp.1930–1937

- Real time dynamics monitoring system [Online]. Available: http://www.phasor rtdms.com.
- http://en.wikipedia.org

APPENDIX A
(Park Transform)

A.1 The Park Transform and Non-sinusoidal Waveforms

The Park transformation function [Angelo Baggini] converts the time-dependent three-phase, three-wire voltage vector $\mathbf{v}(t)_{abc}$ and the time-dependent three-phase line current vector $\mathbf{i}(t)_{abc}$ to time dependent Park voltage vector $\mathbf{v}(t)_{Park}$ and Park current vectors $\mathbf{i}(t)_{Park}$, respectively. The Park transform is a unique case of the Clarke transform. The d–q axis is stationary and also known as the p–q theory. It is a linear orthogonal transformation which makes use of an orthogonal matrix $\boldsymbol{T}_{Park}$:

$$T_{Park} = \begin{bmatrix} \sqrt{2/3} & -\sqrt{1/6} & -\sqrt{1/6} \\ 0 & \sqrt{1/2} & -\sqrt{1/2} \\ \sqrt{1/3} & \sqrt{1/3} & \sqrt{1/3} \end{bmatrix} \qquad \left| T_{Park} \right| = 1 \tag{A.1}$$

The Park transformation of the voltage phase-domain vector is defined as

$$\begin{bmatrix} v_d(t) \\ v_q(t) \\ v_0(t) \end{bmatrix} = \begin{bmatrix} \sqrt{2/3} & -\sqrt{1/6} & -\sqrt{1/6} \\ 0 & \sqrt{1/2} & -\sqrt{1/2} \\ \sqrt{1/3} & \sqrt{1/3} & \sqrt{1/3} \end{bmatrix} . \begin{bmatrix} v_a(t) \\ v_b(t) \\ v_c(t) \end{bmatrix} \tag{A.2}$$

with $v_a(t) = \sum_{h=1}^{N} v_d(t)_h$, and similarly for phases b and c, where $v_a(t)_h$ is the phase a time-dependent voltage at harmonic frequency $h\omega_1$ (referenced to earth plane), and similarly for phases b and c; and

$$v_d(t) = \sum_{h=1}^{N} v_d(t)_h, \; v_q(t) = \sum_{h=1}^{N} v_q(t)_h, \; v_0(t) = \sum_{h=1}^{N} v_0(t)_h \tag{A.3}$$

where $v_d(t)_h$ is the Park direct-axis time-dependent voltage at harmonic frequency $h\omega_1$, $v_q(t)_h$ the quadrature-axis component and $v_0(t)_h$ the additional zero-sequence component but not part of the Park voltage vector $\mathbf{v}(t)_{Park}$.

The compact notation of the above is

$$\boldsymbol{v}(t)_{Park} = \boldsymbol{T}_{Park} \, . \, \boldsymbol{v}(t)_{abc} \tag{A.4}$$

The Park transformation of the current phase-domain vector is defined as

$$\begin{bmatrix} i_d(t) \\ i_q(t) \\ i_0(t) \end{bmatrix} = \begin{bmatrix} \sqrt{2/3} & -\sqrt{1/6} & -\sqrt{1/6} \\ 0 & \sqrt{1/2} & -\sqrt{1/2} \\ \sqrt{1/3} & \sqrt{1/3} & \sqrt{1/3} \end{bmatrix} . \begin{bmatrix} i_a(t) \\ i_b(t) \\ i_c(t) \end{bmatrix} \quad \text{(A.5)}$$

with $i_a(t) = \sum_{h=1}^{N} i_d(t)_h$, and similarly for phases b and c, where $i_a(t)_h$ is the phase a time-dependent current at harmonic frequency hω$_1$ (referenced to earth plane), and similarly for phases b and c; and

$$i_d(t) = \sum_{h=1}^{N} i_d(t)_h,\ i_q(t) = \sum_{h=1}^{N} i_q(t)_h,\ i_0(t) = \sum_{h=1}^{N} i_0(t)_h \quad \text{(A.6)}$$

where $i_d(t)_h$ is the Park direct-axis time-dependent voltage at harmonic frequency hω$_1$, $i_q(t)_h$ the quadrature-axis component and $i_0(t)_h$ the additional zero-sequence component but not part of the Park current vector $\boldsymbol{i}(t)_{Park}$.

The compressed notation of the above is

$$\boldsymbol{i}(t)_{Park} = \boldsymbol{T}_{Park} . \boldsymbol{i}(t)_{abc} \quad \text{(A.7)}$$

The time-dependent Park voltage $\boldsymbol{v}(t)_{Park}$ and current $\boldsymbol{i}(t)_{Park}$ vectors are complex and contain two orthogonal quantities:

$$\begin{aligned} v(t)_{Park} &= v(t)_d + j\, v(t)_q \\ i(t)_{Park} &= i(t)_d + j\, i(t)_q \end{aligned} \quad \text{(A.8)}$$

The multi-frequency Park transformation also yields zero-sequence components $v_0(t)_h$ and $i_0(t)_h$ that are similar to the zero-sequence components yielded by its single-frequency counterpart. As in the single-frequency case, no zero-sequence components exist when the phase-domain voltage vectors have a common reference and current vectors do not have a common return (neutral).

The inverse multi-frequency Park transform for voltage is given by

$$\begin{bmatrix} v_a(t) \\ v_b(t) \\ v_c(t) \end{bmatrix} = \begin{bmatrix} \sqrt{2/3} & -\sqrt{1/6} & -\sqrt{1/6} \\ 0 & \sqrt{1/2} & -\sqrt{1/2} \\ \sqrt{1/3} & \sqrt{1/3} & \sqrt{1/3} \end{bmatrix}^{-1} . \begin{bmatrix} v_d(t) \\ v_q(t) \\ v_0(t) \end{bmatrix} \quad \text{(A.9)}$$

and

$$\begin{bmatrix} i_a(t) \\ i_b(t) \\ i_c(t) \end{bmatrix} = \begin{bmatrix} \sqrt{2/3} & -\sqrt{1/6} & -\sqrt{1/6} \\ 0 & \sqrt{1/2} & -\sqrt{1/2} \\ \sqrt{1/3} & \sqrt{1/3} & \sqrt{1/3} \end{bmatrix}^{-1} . \begin{bmatrix} i_d(t) \\ i_q(t) \\ i_0(t) \end{bmatrix} \quad \text{(A.10)}$$

Because $\boldsymbol{T}_{Park}$ is an orthogonal matrix, $\boldsymbol{T}^{-1}{}_{Park} = \boldsymbol{T}^{T}{}_{Park}$.

A.2 Power Definitions in the Park Domain

Time-dependent power $\boldsymbol{p}(t)_{Park}$ can be defined based on the Park vectors of voltages and currents, $\boldsymbol{v}(t)_{Park}$ and $\boldsymbol{i}(t)_{Park}$, respectively. This power is numerically the exact same quantity as the three-phase time-dependent power $p(t)_{3\phi}$ because the Park transform is a linear orthogonal transform:

$$\begin{aligned} p(t)_{Park} &= v(t)_{Park}.i(t)_{Park} = [\, v_d(t) \quad v_q(t) \quad v_0(t)] \begin{bmatrix} i_d(t) \\ i_q(t) \\ i_0(t) \end{bmatrix} \\ &= v(t)_{3\phi}.i(t)_{3\phi} \\ &= [\, v_a(t) \quad v_b(t) \quad v_c(t)\,] \begin{bmatrix} i_a(t) \\ i_b(t) \\ i_c(t) \end{bmatrix} \\ &= p(t)_{3\phi} \end{aligned} \tag{A.11}$$

The Park time-dependent complex power $\boldsymbol{a}(t)_{Park}$ is defined from the product of the Park time-dependent complex voltage and current:

$$a(t)_{Park} = v(t)_{Park}.\, i(t)^{*}_{Park} \tag{A.12}$$

The Park time-dependent real power $\boldsymbol{p}(t)_{Park}$ and the Park time-dependent non-active imaginary power $\boldsymbol{q}(t)_{Park}$ is defined as

$$\boldsymbol{a}(t)_{Park} = \boldsymbol{p}(t)_{Park} + j\,\boldsymbol{q}(t)_{Park} \tag{A.13}$$

$$= \mathrm{Re}\,[\,\boldsymbol{a}(t)_{Park}] + j\,\mathrm{Im}[\,\boldsymbol{a}(t)_{Park}] \tag{A.14}$$

$$= [v_d(t).i_q(t) + v_q(t).i_q(t)] + j[v_q(t).i_d(t) - v_d(t).i_q(t)] \tag{A.15}$$

The three-phase time-dependent power $p_{3\phi}(t)$ relates to the Park time-dependent real power $p_{Park}(t)$ and the zero-sequence power $p_0(t)$:-

$$p_{3\phi}(t) = p_{Park}(t) + p_0(t) \tag{A.16}$$

$$p_0(t) = v_0(t).i_0(t) \tag{A.17}$$

The average values of the Park time-dependent complex power are

$$A_{Park} = P_{Park} + jQ_{Park} = \frac{1}{T}\int_T v_{Park}(t).i_{Park}{}^{*}(t)\,dt \tag{A.18}$$

$\boldsymbol{P}_{\text{Park}}$ is equal to the average value of the Park real / active power when the zero-sequence time dependent power $p_0(t)$ is zero. $\boldsymbol{Q}_{\text{Park}}$ is the average value of the Park imaginary / reactive power.

The following characteristics of the Park power quantities $\boldsymbol{a}(\,t\,)_{\text{Park}}$, $\boldsymbol{p}(\,t\,)_{\text{Park}}$, $\boldsymbol{P}_{\text{Park}}$, $\boldsymbol{q}(\,t\,)_{\text{Park}}$, $\boldsymbol{Q}_{\text{Park}}$ and $p_0(t)$ are important:

- The Park powers are defines quantities that can be regarded as actual powers and not apparent powers because their sign depends on the reference directions chosen for the voltages and currents.
- These powers satisfy the energy conservation principle: that is, the algebraic sum of powers associated with each element of an isolated network will sum to zero.

APPENDIX B
(Specification)

Data for IEEE - 6 Bus System

Table B1:- Generator Data for IEEE - 6 Bus System

Generator Bus No.	1	2	C
MVA	300	60	30
x_1 (p.u.)	0.01	0.2	0.48
r_a (p.u.)	0	0.003	0.073
x_d (p.u.)	1.05	0.898	0.42
X'_d (p.u.)	0.185	0.3	0.26
X''_d(p.u.)	0.13	0.23	0.012
T'_{do}	6.1	7.4	12.4
T''_{do}	0.04	0.03	0.032
x_q (p.u.)	0.98	0.646	0.232
x'_q (p.u.)	0.36	0.646	0.232
x''_q (p.u.)	0.13	0.4	0.4
T'_{qo}	0.3	0.4	0.5
T''_{qo}	0.099	0.033	0.003
H	6.54	5.148	5.482
F	2	2	2
P	32	32	32

Table B2:- Bus Data of IEEE – 6 Bus Test System:

Bus No.	*Bus Type	P_g	Q_g	P_d	Q_d
1	1	0	0	0	0
2	2	0.45	0.24	0	0
3	3	0	0	-0.275	-0.065
4	3	0	0	-0.15	-0.09
5	3	0	0	-0.15	-0.09
6	3	0	0	-0.275	-0.065

*Bus Type: (1) swing bus, (2) generator bus (PV bus) and (3) load bus (PQ bus)

Table B3:- Line Data of IEEE – 6 Bus Test System:

From Bus	To Bus	R (pu)	X (pu)	B (pu)
1	6	0.123	0.518	0.03
1	4	0.08	0.37	0.01
2	3	0.0723	1.05	0.022
2	5	0.282	0.064	0.12
3	4	0	0.133	0.33
4	6	0.097	0.407	0.01
5	6	0	0.3	0.025

Data for IEEE – 9 Bus System

Table B4:- Generator Data for IEEE – 9 Bus System

Generator Bus No.	1	2	3	C
MVA	300	60	60	30
x_1 (p.u.)	0.01	0.2	0.2	0.48
r_a (p.u.)	0	0.003	0.003	0.073
x_d (p.u.)	1.05	0.898	0.898	0.42
X'_d (p.u.)	0.185	0.3	0.3	0.26
X''_d(p.u.)	0.13	0.23	0.23	0.012
T'_{do}	6.1	7.4	7.4	12.4
T''_{do}	0.04	0.03	0.03	0.032
x_q (p.u.)	0.98	0.646	0.646	0.232
x'_q (p.u.)	0.36	0.646	0.646	0.232
x''_q (p.u.)	0.13	0.4	0.4	0.4
T'_{qo}	0.3	0.1	0.1	0.5
T''_{qo}	0.099	0.033	0.033	0.003
H	6.54	5.148	5.148	5.482
F	2	2	2	2
P	32	32	32	32

Table B5:- Bus Data of IEEE – 9 Bus Test System

Bus No.	*Bus Type	P_g	Q_g	P_d	Q_d
1	1	0	0	0	0
2	2	0.3	0.25	0	0
3	2	0.3	0.25	0	0
4	3	0	0	0	0
5	3	0	0	-0.3	-0.1
6	3	0	0	0	0
7	3	0	0	-0.33	-0.11
8	3	0	0	0	0
9	3	0	0	-0.42	-0.16

*Bus Type: (1) swing bus, (2) generator bus (PV bus) and (3) load bus (PQ bus)

Table B6:- Line Data of IEEE – 9 Bus Test System

From Bus	To Bus	R (pu)	X (pu)	B (pu)
1	4	0	0.0576	0.25
2	8	0	0.0625	0
3	6	0	0.0586	0
4	5	0.017	0.092	0.158
4	9	0.01	0.085	0.176
5	6	0.039	0.17	0.358
6	7	0.0119	0.1008	0.209
7	8	0.0085	0.072	0.149
8	9	0.032	0.161	0.306

Data for IEEE - 14 Bus System

Table B7:- Generator Data for 14 Bus System

Generator Bus No.	1	2	3	4	5	C
MVA	500	60	60	45	45	30
x_1 (p.u.)	0.134	0.2	0.2	0.24	0.24	0.48
r_a (p.u.)	0	0.003	0.003	0.035	0.035	0.073
x_d (p.u.)	1.25	0.898	0.898	0.693	0.693	0.42
X'_d (p.u.)	0.232	0.3	0.3	0.296	0.296	0.26
X''_d(p.u.)	0.12	0.23	0.23	0.122	0.122	0.012
T'_{do}	4.75	7.4	7.4	12.4	12.4	12.4
T''_{do}	0.06	0.03	0.03	0.013	0.013	0.032
x_q (p.u.)	1.22	0.646	0.646	0.462	0.462	0.232
x'_q (p.u.)	0.715	0.646	0.646	0.462	0.462	0.232
x''_q (p.u.)	0.12	0.4	0.4	0.4	0.4	0.4
T'_{qo}	1.5	0	0	0.1	0.1	0.5
T''_{qo}	0.21	0.033	0.033	0.013	0.013	0.003
H	5.06	5.148	5.148	5.342	5.342	5.482
F	2	2	2	2	2	2
P	32	32	32	32	32	32

Table B8:- Bus Data of IEEE – 14 Bus Test System:

Bus No.	*Bus Type	P_g	Q_g	P_d	Q_d	Susceptance
1	1	2.32	0	0	0	0
2	2	0.375	0.18	0.217	0.127	0
3	2	0.375	0.18	0.942	0.19	0
4	3	0	0	0.478	0	0
5	3	0	0	0.076	0.016	0
6	2	0.375	0.18	0.112	0.075	0
7	3	0	0	0	0	0
8	2	0.375	0.18	0	0	0
9	3	0	0	0.295	0.166	0.19
10	3	0	0	0.09	0.058	0
11	3	0	0	0.035	0.018	0
12	3	0	0	0.061	0.016	0
13	3	0	0	0.135	0.058	0
14	3	0	0	0.149	0.05	0

*Bus Type: (1) swing bus, (2) generator bus (PV bus) and (3) load bus (PQ bus)

Table B9:- Line Data of IEEE – 14 Bus Test System

From Bus	To Bus	R (pu)	X (pu)	B (pu)
1	2	0.0194	0.05917	0.053
1	5	0.054	0.22304	0.049
2	3	0.047	0.19797	0.044
2	4	0.0581	0.17632	0.037
2	5	0.057	0.17388	0.034
3	4	0.067	0.17103	0.346
4	5	0.0134	0.04211	0.013
4	7	0	0.20912	0
4	9	0	0.55618	0
5	6	0	0.25202	0
6	11	0.095	0.1989	0
6	12	0.1229	0.25581	0
6	13	0.0662	0.13027	0
7	8	0	0.17615	0
7	9	0	0.11001	0
9	10	0.0318	0.0845	0
9	14	0.1271	0.27038	0
10	11	0.0821	0.19207	0
12	13	0.2209	0.19988	0
13	14	0.1709	0.34802	0

Data for IEEE - 30 Bus System

Table B10:- Generator Data for IEEE - 30 Bus System

Generator Bus No.	1	2	3	4	5	6	C
MVA	750	60	60	60	45	45	30
x_1 (p.u.)	0.134	0.2	0.2	0.2	0.24	0.24	0.48
r_a (p.u.)	0	0.003	0.003	0.003	0.035	0.035	0.073
x_d (p.u.)	1.35	0.898	0.898	0.898	0.693	0.693	0.42
X'_d (p.u.)	0.232	0.3	0.3	0.3	0.296	0.296	0.26
X''_d(p.u.)	0.12	0.23	0.23	0.23	0.122	0.122	0.012
T'_{do}	4.75	7.4	7.4	7.4	12.4	12.4	12.4
T''_{do}	0.06	0.03	0.03	0.03	0.013	0.013	0.032
x_q (p.u.)	1.22	0.646	0.646	0.646	0.462	0.462	0.232
x'_q (p.u.)	0.715	0.646	0.646	0.646	0.462	0.462	0.232
x''_q (p.u.)	0.12	0.4	0.4	0.4	0.4	0.4	0.4
T'_{qo}	1.5	0	0	0	0.1	0.1	0.5
T''_{qo}	0.21	0.033	0.033	0.033	0.013	0.013	0.003
H	5.06	5.148	5.148	5.148	5.342	5.342	5.482
F	2	2	2	2	2	2	2
P	32	32	32	32	32	32	32

Table B11:- Bus Data of IEEE – 30 Bus Test System:

Bus No.	*Bus Type	P_g	Q_g	P_d	Q_d	Susceptance
1	1	2	1.1.	0	0	0
2	2	1	0.5	0.21	0.12	0
3	3	0	0	0.024	0.012	0
4	3	0	0	0.076	0.016	0
5	2	0.5	0.24	0.94	0.19	0
6	3	0	0	0	0	0
7	3	0	0	0.22	0.1	0
8	2	0.5	0.24	0.3	0.3	0
9	3	0	0	0	0	0
10	3	0	0	0.058	0.02	0.19
11	2	0.5	0.24	0	0	0
12	3	0	0	0.11	0.07	0
13	2	0.5	0.24	0	0	0
14	Bus 14	0	0	0.062	0.016	0
15	Bus 15	0	0	0.08	0.025	0
16	Bus 16	0	0	0.035	0.018	0
17	Bus 17	0	0	0.09	0.058	0
18	Bus 18	0	0	0.032	0.09	0
19	Bus 19	0	0	0.095	0.034	0
20	Bus 20	0	0	0.022	0.07	0
21	Bus 21	0	0	0.17	0.11	0
22	Bus 22	0	0	0	0	0
23	Bus 23	0	0	0.032	0.016	0

24	**Bus 24**	**0**	**0**	**0.087**	**0.067**	**0.04**
25	**Bus 25**	**0**	**0**	**0**	**0**	**0**
26	**Bus 26**	**0**	**0**	**0.035**	**0.023**	**0**
27	**3**	**0**	**0**	**0**	**0**	**0**
28	**3**	**0**	**0**	**0**	**0**	**0**
29	**Bus 29**	**0**	**0**	**0.024**	**0.09**	**0**
30	**Bus 30**	**0**	**0**	**0.11**	**0.019**	**0**

*Bus Type: (1) swing bus, (2) generator bus (PV bus) and (3) load bus (PQ bus)

Table – B12:- Line Data of IEEE – 30 Bus Test System

From Bus	To Bus	R (pu)	X (pu)	B (pu)	From Bus	To Bus	R (pu)	X (pu)	B (pu)
1	**2**	**0.0192**	**0.0575**	**0.0528**	**12**	**13**	**0**	**0.14**	**0**
1	**3**	**0.0452**	**0.1652**	**0.0408**	**12**	**14**	**0.1231**	**0.2559**	**0**
2	**4**	**0.057**	**0.1737**	**0.0368**	**12**	**15**	**0.0662**	**0.1304**	**0**
2	**5**	**0.0472**	**0.1983**	**0.0418**	**12**	**16**	**0.0945**	**0.1987**	**0**
2	**6**	**0.0581**	**0.1763**	**0.0374**	**14**	**15**	**0.221**	**0.1997**	**0**
3	**4**	**0.0132**	**0.0379**	**0.0084**	**15**	**18**	**0.1073**	**0.2185**	**0**
4	**6**	**0.0119**	**0.0414**	**0.009**	**15**	**23**	**0.1**	**0.202**	**0**
4	**12**	**0**	**0.256**	**0**	**16**	**17**	**0.0524**	**0.1923**	**0**
5	**7**	**0.046**	**0.116**	**0.0204**	**18**	**19**	**0.0639**	**0.1292**	**0**
6	**7**	**0.0267**	**0.082**	**0.017**	**19**	**20**	**0.034**	**0.068**	**0**
6	**8**	**0.012**	**0.042**	**0.009**	**21**	**22**	**0.0116**	**0.0236**	**0**
6	**9**	**0**	**0.208**	**0**	**22**	**24**	**0.115**	**0.179**	**0**
6	**10**	**0**	**0.556**	**0**	**23**	**24**	**0.132**	**0.27**	**0**
6	**28**	**0.0169**	**0.0599**	**0.013**	**24**	**25**	**0.1885**	**0.3292**	**0**
8	**28**	**0.0636**	**0.2**	**0.0428**	**25**	**26**	**0.2544**	**0.38**	**0**
9	**10**	**0**	**0.11**	**0**	**25**	**27**	**0.1093**	**0.2087**	**0**
9	**11**	**0**	**0.208**	**0**	**27**	**28**	**0**	**0.396**	**0**
10	**17**	**0.0324**	**0.0845**	**0**	**27**	**29**	**0.2198**	**0.4153**	**0**
10	**20**	**0.0936**	**0.209**	**0**	**27**	**30**	**0.3202**	**0.6027**	**0**
10	**21**	**0.0348**	**0.0749**	**0**	**29**	**30**	**0.2399**	**0.4533**	**0**
10	**22**	**0.0727**	**0.1499**	**0**					